MARCH 2018 Ph.D. in Civil Engineering MUHAMD DAFER AL YAHYA BAG

**UNIVERSITY OF GAZİANTEP**

**GRADUATE SCHOOL OF**

**NATURAL & APPLIED SCIENCES**

# USE OF CONSTRUCTION AND DEMOLITION MATERIALS TO IMPROVE GEOTECHNICAL PROPERTIES OF A CLAY

**Ph.D. THESIS**

**IN**

**CIVIL ENGINEERING**

**BY**

**MUHAMD DAFER AL YAHYA BAG**

**MARCH 2018**

**Use of Construction and Demolition Materials to Improve Geotechnical Properties of a Clay**

**Ph.D. Thesis**

**in**

**Civil Engineering**

**Supervisor**

**Prof. Dr. Ali Fırat ÇABALAR**

**by**

**Muhamd Dafer AL YAHYA BAG**

**March 2018**

REPUBLIC OF TURKEY
UNIVERSITY OF GAZİANTEP
GRADUATE SCHOOL OF NATURAL & APPLIED SCIENCES
CIVIL ENGINEERING DEPARTMENT

Name of the thesis: Use of Construction and Demolition Materials to Improve Geotechnical Properties of a Clay

Name of the student: Muhamd Dafer AL YAHYA BAG

Exam date: 29.03.2018

Approval of the Graduate School of Natural and Applied Sciences

Prof. Dr. A. Necmeddin YAZICI
Director

I certify that this thesis satisfies all the requirements as a thesis for the degree of Doctor of Philosophy.

Prof. Dr. Hanifi ÇANAKCI
Head of Department

This is to certify that we have read this thesis and that in our consensus opinion it is fully adequate, in scope and quality, as a thesis for the degree of Doctor of Philosophy.

Prof. Dr. Ali Fırat ÇABALAR
Supervisor

| Examining Committee Members | Signature |
|---|---|
| Prof. Dr. Mehmet KARPUZCU | ..................... |
| Prof. Dr. Mustafa ÖZAKÇA | ..................... |
| Assoc. Prof. Dr. Murat ÖRNEK | ..................... |
| Assist. Prof. Dr. Volkan İŞBUĞA | ..................... |
| Prof. Dr. Ali Fırat ÇABALAR | ..................... |

**I hereby declare that all information in this document has been obtained and presented in accordance with academic rules and ethical conduct. I also declare that, as required by these rules and conduct, I have fully cited and referenced all material and results that are not original to this work.**

**Muhamd Dafer AL YAHYA BAG**

**ABSTRACT**

**USE OF CONSTRUCTION AND DEMOLITION MATERIALS TO IMPROVE GEOTECHNICAL PROPERTIES OF A CLAY**

**AL YAHYA BAG, Muhamd Dafer**
**Ph.D. in Civil Engineering**
**Supervisor: Prof. Dr. Ali Fırat ÇABALAR**
**March 2018**
**160 pages**

A study was conducted to explore the various effects of construction and demolition materials (CDMs), which are considered to be solid waste materials (SWMs), on the geotechnical properties of clay. The properties of the mixed samples were investigated by adding crushed brick pieces (CBPs), dumped asphalt pieces (DAPs), and crushed concrete pieces (CCPs) into clay. The laboratory tests included the testing of consistency limits, California bearing ratio (CBR), unconfined compressive strength (UCS), swelling, consolidation, and direct shear. A series of plate loading tests on clay with 10% CDMs was also carried out in a specially-designed model box made of reinforced concrete with a dimension of 2.0m diameter and depth of 1.5m to gain a deep understanding of the samples. The results show that when the CDMs percentages were 20%, there were decreases of about 15% and 25% in liquid limit and plasticity index of clay, respectively. Small increases of about 3% in $\gamma_{drymax}$ for the clay were noticed when the DAPs and CCPs content was increased from 5% to 20%. A reduction of about 35% of $w_{opt}$ for clay was shown by increasing the DAP percentage to 20%. The CBR and UCS strength values of the clay were increases by around 25% by increasing the CDMs percentage from 5% to 20%. In the direct shear test, 10% of all CDMs additions gave out the maximum angle of internal friction. In the plate load test, the addition of 10% CDMs increased the ultimate bearing capacity of clay by about 50% to 75%. The oedometer characteristics, including the swelling and consolidation of CDMs-clay mixtures, were controlled mainly by the type and content of CDMs in the clay. Using Plaxis 2D for program, a remarkable matching of the results of the numerical simulation and the plate load test was observed ($R^2$=0.97).

**Keywords:** Clay, solid waste materials, geotechnical properties.

# ÖZET

## BİR KİLİN GEOTEKNİK ÖZELLİKLERİNİ İYİLEŞTİRMEK İÇİN İNŞAAT YIKINTI ATIKLARININ KULLANIMI

**AL YAHYA BAG, Muhamd Dafer**
**Doktora Tezi, İnşaat Mühendisliği Bölümü**
**Tez Yöneticisi: Prof. Dr. Ali Fırat ÇABALAR**
**Mart 2018**
**160 sayfa**

Bu çalışmada çeşitli inşaat yıkıntı atıklarının, bir kilin bazı geoteknik özellikleri üzerindeki etkilerini araştırmak için deneysel bir araştırma yapılmıştır. Zemin karışım numunelerine ait özellikler tuğla, atık asfalt ve kırılmış beton parçaları eklenerek incelenmiştir. Laboratuvarda kıvam limit, kaliforniya taşıma oranı, serbest basınç dayanımı, şişme potansiyeli, konsolidasyon ve kesme kutusu deneyleri yapıldı. Zemin davranışını daha iyi anlamak için, 2m çapında ve 1.5m derinliğindeki betonarme bir kuyuda %10 inşaat yıkıntı atıklarıyla bir dizi plaka yükleme deneyleri gerçekleştirildi. Deney sonuçları, inşaat yıkıntı atıklarının yüzdeleri 20'ye arttırıldığında, kilin likit limitlerinde %15 azalma ve plastisite indeksinde de yaklaşık %25 azalma olduğunu gösterdi. Atık asfalt parçaları ve parçalanmış atık beton yüzdeleri 5'den 20'ye arttırıldığında, kilin $\gamma_{kurumax}$'ında yaklaşık %3'lük, küçük bir artış olduğu görülmüştür. Atık asfalt parçalarının yüzdeleri 20'ye çıkarıldığında kil için optimum su oranı yaklaşık %35'lik bir azalma göstermiştir. İnşaat yıkıntı atıklarının yüzdeleri 5'den %20'ye arttırıldığında ise kaliforniya taşıma oranı ve serbest basınç değerleri ile temsil edilen kilin dayanımı %25'e yakın bir oranda artmıştır. Kesme kutusu deneylerinin %10'luk inşaat yıkıntı atıkları karışımları maksimum içsel sürtünme açısını vermiştir. İnşaat yıkıntı atığının eklenmesiyle, plaka yükleme deneylerinde maksimum taşıma kapasitesi yaklaşık %50 ila %75 oranında artmıştır. Plaka yükleme deney sonuçları ile, Plaxis 2D kullanarak yapılan nümerik sonuçlar büyük ölçude benzerlik göstermiştir ($R^2$=0.97)



**Anahtar Kelimeler:** Kil, katı atık malzemeler, geoteknik özellikler.

To My Family

## ACKNOWLEDGEMENTS

I would like to express my deepest gratitude to my supervisor, Prof. Dr. Ali Fırat Çabalar, for his unlimited supervision, patience and support during this research. Without his supervision and advice, this thesis would not have been possible.

I gratefully acknowledge Mosul University and the Ministry of Higher Education and Scientific Research in Iraq for the Ph.D. scholarship provided by them.

I would also like to express my gratitude to all my colleagues at the department of civil engineering, Gaziantep University.

I would like to sincerely and gratefully thank my parents, father and mother, brother, sisters, aunts and the spirits of my granny for their endless support and encouragement during my study period.

Finally, I would like to thank my wife for her endless support and sacrifice, and my wonderful kids for their endless energy, without their encouragement, I would not have finished this thesis.

# TABLE OF CONTENTS

**Page**

## LIST OF TABLES

**Page**

## LIST OF FIGURES

**Page**

## LIST OF SYMBOLS AND ABBREVIATIONS

## SYMBOLS

| | |
|---|---|
| $c'$ | Effective cohesion ($kN/m^2$) |
| $C_c$ | Compressibility index |
| $C_s$ | Swelling index |
| $C_v$ | Coefficient of consolidation ($cm^2/s$) |
| $e_o$ | Initial void ratio |
| $e_f$ | Final void ratio (at end of loading stage) |
| $E_{ref}$ | Modulus of elasticity ($kN/m^2$) |
| $k$ | Hydraulic conductivity (cm/s) |
| $m_v$ | Coefficient of volume change ($cm^2/gm$) |
| $P_{max}$ | Swelling pressure ($kN/m^2$) |
| $q_u$ | Terzaghi's ultimate bearing capacity ($kN/m^2$) |
| S | Swell percentage (%) |
| $\gamma_w$ | Unit weight of water ($kN/m^3$) |
| $\gamma_{unsat}$ | Unsaturated field density ($kN/m^3$) |
| $\gamma_{sat}$ | Saturated field density ($kN/m^3$) |
| $\gamma_{drymax}$ | Maximum dry unit weight ($kN/m^3$) |
| $\nu$ | Poisson's ratio |
| $\phi$ | Angle of internal friction (°) |
| $\phi'$ | Effective angle of internal friction (°) |
| $w_{opt}$ | Optimum water content (%) |

## ABBREVIATIONS

| | |
|---|---|
| AASHTO | American Association of State Highway and Transportation Officials |
| ASTM | American Society for Testing and Materials |
| CDMs | Construction and Demolition Materials |
| CBR | California Bearing Ratio |
| CB | Crushed Brick |
| CBPs | Crushed Bricks Pieces |
| CCPs | Crushed Concrete Pieces |
| CSA | Crushed Stone Aggregate |
| DAPs | Dumped Asphalt Pieces |
| EDX | Energy Dispersive X-Ray |
| GTM | Gyratory Testing Machine |
| FA | Fly Ash |
| PI | Plasticity Index |
| Plaxis 2D | Plaxis Two Dimensions |
| RAP | Reclaimed Asphalt Pavement |
| RAS | Reclaimed Asphalt Shingle |
| RCA | Recycle concrete Aggregate |
| SWMs | Solid Waste Materials |
| SEM | Scanning Electron Micrograph |
| UCS | Unconfined Compressive Strength |
| USCS | Unified Soil Classification System |
| XRD | X-Ray Diffraction |

# CHAPTER 1

# INTRODUCTION

## 1.1 General

Most of clays have one or more of the following three geotechnical problems: low strength, high compressibility, and swelling. Most clay shows volumetric changes when its water content changes. Clay is considered as one a type of difficult soils that is especially problematic and requires extra effort on the part of geotechnical engineers (Coduto, 1999). Clay swells when its moisture content increases and it shrinks when its moisture content decreases. It has been recognized that expansive clays cause huge amounts of money to be lost every year in the United States, more than all natural disasters combined (Jones and Holtz, 1973; Day, 1999; Chen, 2012). The consolidation of soft clay is considered to be the biggest and the oldest problem with such types of soils. The dissipation of the excess pore water pressure that is generated by the stress increase in a saturated compressible clay layer is known as consolidation (Das and Sobhan, 2014). Most of the structures built on clays are exposed to different amounts of settlement due to the consolidation of under-foundation clay. Meanwhile, many researchers have attempted to describe and deal with this issue. Terzaghi (1925) developed the theory of consolidation for clay. Today, researchers continue studying this problem (Fan et al., 2014; Soleimanbeigi and Edil, 2015). The strength of clay is considered to be the foremost problem in the clay type of soil (Coduto, 1999) and plays a significant role in the analysis of clay stability problems (Das and Sobhan, 2014).

Increasing urbanization, population explosion, and improving standards of living due to technological innovations have contributed to increases in the quantity of a variety of SWMs generated by industrial, domestic, mining, and agricultural activities. As a result of the land using growth in the construction in the world, clay is mixed with different types of SWMs from various sources. Recent re-construction activities for the urban transformation of cities have resulted in environmental impacts because waste materials are left behind after large-scale Transformation projects and accumulated in tremendous amounts that force geo-environmental engineers to look for every opportunity to make use of this bulk material in environmentally friendly manners. Most SWMs are produced by CDMs sectors.

Use of the CDMs has environmental benefits, such as reducing greenhouse gas emissions, water savings, the conservation of energy and natural resources, and the prevention of pollution. While many researchers focus on using recycled asphalt shingles, crushed concrete aggregates, and crushed bricks in various geotechnical applications, the performances of these CDMs, when mixed with clay at different mixture proportions, has not been previously reported. Recycling and reusing CDMs as a soil improvement technique is an alternative in which many waste materials can be utilized at once. This is because one of the main principles of high quality waste management is finding methods to safely reuse waste materials. Hence, studies to identify the potential to use these materials in road stabilization have been undertaken (Arulrajah et al., 2012). Conventional road stabilization methods are used to develop the quality of road subgrade and pavement layers. These methods enable people to improve the current material properties on project sites and reach required specifications. Likewise, these methods enhance the filling layers, and the use of high-quality pavement decreases the entire thickness of pavement and leads to a reduction in administrative costs (Modarres and Nosoudy, 2015).Three types of SWMs that are generated by CDMs activities were mixed with clay: crushed bricks from rubble, asphaltic material removed from old pavement, and crushed concrete materials from paving debris. Many of such SWMs are available in the municipal in any city or any blank area. According to Sus Vic (2010), CDMs account for about half of all SWMs. Also, within this half, the concrete material occupies 58%, brick rubble occupies 16%, and dumped asphalt occupies 7.0%. As stated before, 80% of these three materials are generated by CDMS activity. In most unused land, exposed clays are accidentally or deliberately mixed with these types of SWMs that come from different sources.

## 1.2 Aims and Objectives of the Thesis

The author of this study aimed to experimentally investigate the effects of three types of CDMs (crushed bricks pieces, dumped asphalt pieces, and crushed concrete pieces) on some geotechnical properties of clay (index properties, shear strength, and oedometer set). The effects of solid waste resources and their potential to stabilize clay were studied. One of the study targets was to investigate the behavior of clay mixed with a specific percentage of CDMs in a cylindrical box under plate load pressure. Measuring the stress distribution within the soil before, during, and after applying the load in the plate test was one of the objectives of this study.

The two theoretical objectives of the study are (1) to estimate the ultimate bearing capacity of clay and clay-CDMs mixtures by using direct shear tests and plate load tests and comparing the results and (2) to compare the settlements of footing obtained by plate load tests and settlements calculated using geotechnical software (Plaxis 2D) for clay and clay-CDMs mixtures.

### 1.3 Organization of the Thesis

The main body of this thesis contains six chapters. The first chapter includes general information about the soil and SWMs used in the study. In addition, information about the aim of this study and the organization the thesis content is included in this chapter. The second chapter includes a literature review with a focus on the definition of SWMs and CDMs problems, the reuse of SWMs for different purposes, the effects of the use of SWMs on the geotechnical properties of soil, and the box model used for soil testing. The third chapter covers experimental work. It is divided into three parts about materials used for the study, sample preparation, and testing method and equipment used. The fourth chapter includes descriptions of the fundamental rules and the method of calculation of bearing capacity and settlement for clay and clay-CDMs mixture. The input parameters used in Plaxis 2D to calculate the load-settlement curve for clay and clay-CDMs mixture are also described in the fourth chapter. The fifth chapter deals with the results obtained from all experimental and numerical work and include scientific discussions of these results. Finally, the sixth chapter includes conclusions and relevant recommendations based on the study results. The main body is preceded by a suitable abstract that briefly describes the study and followed by references to all past studies used in the thesis.

# CHAPTER 2

# LITERATURE REVIEW

## 2.1 Introduction

This chapter presents a review of studies that deal with SWMs, particularly CDMs. Firstly, some information is given about the types and sources of the SWMs and CDMs materials and the potential use of these materials in construction sectors. Secondly, some data is given in this chapter about the problem of growing CDMs materials in Turkey. Thirdly, in another part of this chapter, a detailed review is given about the reuse of SWMs as construction materials. Finally, the author highlights the effects of SWMs, especially CDMs, on the geotechnical properties of soils. The studies in literature deal with main problems of soil-SWM mixtures, like swelling, consolidation, and strength are taken extensively. The studies about the effects of the use of SWMs on soil strength can be divided into two categories: those in which normal or traditional laboratory tests are conducted and those in which field or box models are used for the tests. A big part of the literature review is focused on the properties of CDMs as base or sub-base filling materials. The last part of this chapter addresses the use of box models as containers in which to conduct various studies on the materials in question.

## 2.2 Solid Waste Materials

The modern world creates large amounts of different types of waste, which imposes much pressure on the environment. SWMs are considered to be the central part of all waste. The recycling and reuse of solid waste in civil engineering applications has been the topic of a significant number of investigations over a relatively long time. Different types and sources of solid waste and their recycling and utilization possibilities as construction materials are shown in Table 2.1. Recently, many SWMs have started to be used in the production of construction materials, as shown by Safiuddin et al., (2010) in Table 2.2.

**Table 2.1** Different types and sources of solid wastes and their recycling and reusing potentials for construction materials (Pappu et al., 2007)

| S/No. | Type of solid wastes | Source details | Recycling and utilization potentials |
|---|---|---|---|
| 1 | Agro-waste (organic) | Rice and wheat straw and husk, ground nut shell, jute, sisal, saw mill waste, cotton stalk, vegetable residues, baggage | Cement board, insulation boards, particle boards, wall panels, binder, roof sheets, fibrous building panel, bricks, coir fiber, acid-proof cement, reinforced composites, and polymer composites |
| 2 | Industrial waste (inorganic) | residues, steel slag, bauxite red mud, building debris, coal combustion | Bricks, blocks, cement, tiles, paint, fine and coarse aggregates, concrete, ceramic products, wood substitute products |
| 3 | Mining/Mineral waste | Coal washers waste; mining waste tailing from iron, zinc, copper, gold ,and aluminum industries | Fine and coarse lightweight aggregates, Bricks, and tiles |
| 4 | Non-hazardous waste | Lime sludge, limestone waste, waste gypsum, broken glass and ceramics, marble processing residues, kiln dust | Bricks, blocks, cement clinker, hydraulic binder, gypsum plaster, fibrous gypsum boards, and super-sulfated cement |
| 5 | Hazardous waste | Galvanizing waste, contaminated blasting materials, metallurgical residues, tannery waste, sludge from wastewater and waste treatment plants | Bricks, cement, Boards, ceramics, and tiles |

**Table 2.2** Major solid wastes and their uses in the production of construction materials (Safiuddin et al., 2010)

| S/No. | Solid waste name | Solid waste type | Use in construction materials |
|---|---|---|---|
| 1 | Construction and demolition debris (concrete rubble, waste bricks, tiles, etc.) | Industrial | Coarse and fine aggregates, concrete, blocks, bricks, sub-base pavement materials |
| 2 | Phosphogypsum, waste glass, granulated blast-furnace slag, waste steel slag, rubber tire. | Industrial | Coarse and fine aggregates, concrete, blocks, bricks, tiles, ceramic products, blended cement. |
| 3 | Bottom ash, Fly ash, rice husk ash, palm oil fuel ash, organic fiber | Agro-industrial | Aggregate, concrete, blended cement, additional cementing materials, cement boards, bricks, tiles, blocks, particle boards, insulation boards, wall panels, roof sheets, reinforced polymer composites. |
| 4 | Quarry dust | Mining/mineral | Coarse and fine aggregates, concrete, tiles, bricks, blocks, surface finishing materials. |

### 2.3 Construction and Demolition Materials

Waste from the construction, remodeling, and repairing of individual houses and commercial buildings and other civil engineering activities is classified as construction waste. Waste from destroyed buildings is usually defined as demolition waste (Oglesby et al., 1989; Spencer, 1989, 1990; Apotheker, 1990; Gavilan and Bernold, 1994; Huang, 2002). Demolition waste is also produced by environmental disasters, such as earthquakes, tornadoes, hurricanes, and floods (Outwater and Tansel, 1994; Huang, 2002). In the recent decades, CDMs have been a major attractive research subjects due to the significant increases of these materials around the world. According to a study by Anik et al., (1996) the construction sector consumes about half of the raw materials from nature and produces more than half of total waste. Donovan (1990) defined CDMs materials as solid waste, which is generated by many construction and demolition activities, as shown in Table 2.3. Most of these materials, like crushed brick, recycled concrete aggregate, dumped asphalt pavement, plastics, steel, and timber, cause economic and environmental problems. Urban and industry transformation projects, which produce a significant amount of CDMs waste materials, have been growing fast in developing countries, including Turkey.

**Table 2.3** Construction and demolition types and contents (Donovan, 1990)

| Waste type | Contents |
|---|---|
| Asphalt | Roads, bridges, parking lots |
| Rubble | Dirt, bricks, cinder blocks, concrete |
| Plaster | Sheetrock, gypsum, drywall |
| Glass | Doors, windows |
| Plastic | Vinyl siding, doors, windows |
| Tar-based materials | Tar paper, Shingles |
| Ferrous metal | Pipes, flashing, roofing, steel |
| Non-ferrous metal | Aluminum, copper, brass, stainless steel |
| Harvested wood | Limbs, tops, stumps |
| Untreated wood | Framing, scraps |
| Treated wood | Plywood, pressure-treated, creosote-treated, laminates |
| White goods | Appliances |
| Contaminants | Lead-based paint, fiberglass, asbestos, fuel tanks |

SWMs, especially from CDMs projects, are considered to be a growing problem with economic and environmental effects in Turkey. A government report in 2005 indicated that the amount of solid waste produced yearly in Turkey is nearly 38 million tons (Öztürk, 2005). The growth of this problem is connected to increases in the amounts of CDMs for several reasons. First, the construction sector in Turkey can be considered as the main engine of economic activities in the country. Recently, the role of the construction sector has significantly increased due to new housing and infrastructure investments countrywide (Arslan et al., 2012). Second, due to the high risk of earthquakes, concentrated work, such as redesigning, reinforcement, and demolition work have continued in areas that are at serious risk. Due to the 1999 Marmara earthquake, a massive amount of debris (approximately 13 million tons) was produced (State Planning Organization, 2001). Another side effect of earthquake danger is that most housing constructions must be transformed through demolition and redesigning activities in the short term (Arslan et al., 2012). Third, because of the regular demolition of illegal constructions, the continuous generation of waste occurs. Lastly, during the period of the construction of residences in Turkey, for many reasons, frequent modifications were made to building materials and components, causing the accumulation of construction waste. Such accumulation leads to not only economic and industry losses but also adverse influences on the environment (Esin and Cosgun, 2007).

### 2.4 Reuse of Solid Waste Materials

During the past 25 years, much more information has become available on the use of SWMs as construction materials and for improving the properties of different types of soil. SWMs have been used for many constructions purposes. For example, McMahon (1997) presented information about the use of CDMs to develop a manufactured soil product. The chemical analysis of the material was discussed, as well as the procedure used to produce the soil. Meanwhile, the manufactured soil product is currently used as a daily landfill cover and temporary road fill material at construction sites in Northeast Florida. Miller et al., (1997) observed the problem of the wetting-induced collapse potential of compacted soil and shale and the use of kiln dust to condense or fix this problem. The paper presents the results of a study project concentrated on the cement kiln dust produced during the manufacturing of Portland cement. Results about the treated samples showed that when the humidity was greater than the optimum moisture content, the collapse potential was significantly reduced and disregarded when compared to untreated conditions. Furthermore, Lee and Nicholson (1997) investigated the possibility of using a mixture of municipal solid waste ash and quarry tailings in final landfill covers and for road sub-base material. Because there were limited resources in places like Hawaii and some small countries, the burning of municipal solid waste to reduce volume was a common solution in the past. Waste materials can be used to help to conserve valuable landfill space. Tests have been conducted on waste ash and quarry tailings to determine grain size, compaction, Atterberg limits, permeability, direct shear, and one-dimensional swell. Results of the study shows that a mixture of 90% solid waste ash and 10% Ameron tailings, seemed to be the best material for the final landfill cover when compared to the clay.

In a different study, Maher et al., (1997) focused on using SWMs as a base or sub-base for road construction. The use of recycled asphalt pavement (RAP) in construction as base and sub-base material in paving systems was investigated. The geotechnical characterization of the RAP involves looking at gradation, determining the engineering classification, and determining moisture-density relationships. The resilient properties of RAP were determined using an advanced soil machine under different load cycles to look at fragmentation and separation and develop a rutting index. The field test results indicated higher modulus and stiffness for RAP than the dense graded aggregate base that is typically used in the state of New Jersey.

McManis and Nataraj (1997) listed three possibilities for the use of diatomaceous earth filter cake as an additive for petroleum products, a lightweight fine aggregate in landfills, road base and sub-base, and free construction fill. Other potential uses were also offered. Complete physical and chemical descriptions of the ash and its scrubber mud were given. The testing program for this study shows that the ash is promising as a lightweight fine aggregate for use as an earth fill material.

Some researchers consider the possibility of using CDMs materials as a filling for gabions, which are metal cages filled with materials and used for different construction purposes, like retaining walls. Lima (1999) gave the pioneering reference to the potential reuse of CDMs materials in retaining structures. The author identified that CDMs materials have the necessary strength and dimensions to be used as gabion filling materials. Molenaar and van Niekerk (2002) researched the effects of composition, particle size, and the degree of compaction of the CDMs (recycled concrete and masonry rubble) when they were reused. The study was done in the Netherlands. The findings of this study were that the degree of compaction has the greatest significance effect in the results. Also, the others analyzed parameters (particle size, composition, and degree of compaction) have strong effects on the mechanical properties of the recycled materials. This conclusion is significant for construction practice because the degree of compaction is easier to control in the field than other factors, such as gradation and composition. The results revealed that recycled concrete and masonry rubble can be used to produce respectable-quality road bases.

Tam and Tam (2007) attempted to classify recycled aggregates by applying some international standards. Aggregates were collected from 11 sources and compared to the 12th sample (ordinary virgin aggregate). Samples 1–10 were collected from demolition sites, and Sample 11 was collected from the Tuen Mun Area 38 centralized recycling plants in Hong Kong. According to the test results, Sample 6 was found to be appropriate for all types of construction requests because it was similar to Sample 12 (natural aggregate). However, Samples 2 and 9 were completely unsuitable as recycled concrete aggregates for any use grade. Sample 11 was found to only be appropriate for non-structural applications, such as base course and fill. It was concluded that recycled aggregate should be classified on the bases its sources and crushed separately rather than being treated in a combined form, which will lower its general quality and limit its application.

Del Río Merino et al. (2009) conducted a study about the different applications that are currently used to optimize the recovery and/or use of CDMs waste for reuse. The authors discuss the challenges and strategies for various proposed measures and improve the processing of this waste. The authors give a clear example of waste processing in a plane in Spain. A typical approach used in the industry for producing aggregate from masonry waste as a substitute for virgin aggregate in new construction is to start with the classification of the waste in two different sizes. Pieces that are smaller than 40 mm are excluded because they frequently contain a lot of contaminants (gypsum, coal wood, steel, and glass). The acceptable size is a difference of 40-50 mm by the regulations for recycled aggregates established by the Madrid municipal standards. After this classification has taken place, the next step is to crush the waste using an impact crusher or hammer crusher, followed by additional grinding. After this, the elimination of impurities takes place using either the thermal method or the dry method. In Spain, nevertheless, the dry method, involving manually separating the large impurities in the first phase and crushing them to separate the small-sized units, is the most widely used method.

In some studies, such as the work of Saeed et al., (2011), the researchers selected recycled materials used in pavement foundations (base/sub-base layers) and provide recommendations for performance-related tests. In the work of Saeed et al., (2011), the test procedures were modified to account for the recycled materials in the aggregates mixture and further evaluated based on mechanical performance, accuracy, complexity, practicality, precision, and test cost. The adapted test procedures were originally designed for usual aggregates. This study showed that some parameters affect the performance of the unbound aggregate layers, as represented by shear strength, abrasion, toughness, durability, and frost susceptibility. However, the statistical analysis of the data revealed that the most effect parameters on the fulfillment of the unbound systems consisting of recycled materials were shear strength.

Nawagamuwa et al., (2013) considered different types of CDMs materials (concrete, bricks, pebbles, plaster, and bricks with mortar) to verify the probability of being recycled as gabion filling material. The authors considered the compressive strength and durability of the five selected CDMs materials and showed that only concrete could be considered as appropriate for use in gabions. All four other materials were not successful as gabion filling materials from the aspects of durability and compressive strength.

Rahman et al., (2015) used three-common recycled CDMs to evaluate their suitability as filter materials in permeable pavements. The investigators used recycled concrete aggregate (RCA), crushed brick (CB), and reclaimed asphalt pavement (RAP) in combination with nonwoven geotextile. Permeable pavement systems enable storm water to infiltrate through the pavement surface into the filter layer. Permeable pavements are progressively being used as urban storm water management systems. The researchers found that despite the increased pollutant removal efficiency of the CDMs materials by the geotextile layer, it has a potential to cause clogging due to continuous buildups of sediments over time. Regarding usage in permeable pavement filter layers, CDMs materials were found to have hydraulic and geotechnical properties equivalent or superior to those of typical granular quarry materials.

Other potential uses of recycled CDMs materials were also studied, such as applications in sea-wall foundations (Yeung et al., 2006), landfill cover layers (Harnas et al., 2013), and alternative pipe backfilling material (Rahman et al., 2014).

Vieira and Pereira (2015) provided a total review of the use of recycled CDMs materials in different geotechnical applications based on the results of many previous studies. They provide the criteria and specifications for fills used in geosynthetic-reinforced structures and the standards related to aggregates for the base layers of roadways.

### 2.5 Stabilization of Expansive Soil by Solid Waste Materials

Most clay exhibits volumetric changes when its water content changes. Clay swells when its moisture content increases and shrinks when its moisture content decreases. According to Mitchell and Soga (2005), both compositional and environmental factors affect the volumetric changes of expansive soil, including the physical and physicochemical interactions among particles, chemical and organic environment, mineralogical detail, fabric and structure, pore water chemistry, and stress path.

Extensive studies have been focused on the improvement of expansive soils using industrial waste products (Zaman et al., 1992; Chu and Kao, 1993; Miller and Azad, 2000). Nicholson and Ding (1997) investigated the improvement of tropical soils, which frequently have poor engineering properties, including high swelling potential and high plasticity with waste ash and lime admixtures. The study was shown to rapidly improve the workability of soil mixtures through reductions of moisture (i.e., the drying effect) and decreases of plasticity. Al-Rawas et al., (2002) conducted a comparative evaluation of various additives used to stabilize expansive soil. The researchers used four additives to reduce the swelling potential and plasticity of expansive soils. The additives used were cement by-pass dust, granulated blast furnace slag, copper slag, and slag cement. The soil used in this study was taken from Al-Khod (a town located in northern Oman). The study indicated that copper slag was unsuitable and caused a weighty increase in the swelling potential of the treated samples.

Yeşilbaş (2004) studied the effects of using rock powder and aggregate waste with lime on reducing the swelling potential of clay. The expansive soil used in this study was prepared in the laboratory by mixing kaolinite and bentonite. Rock powder and aggregate waste were added to the soil at 0 to 25% by weight. Lime was added to the soil at 0 to 9% by weight. The author concluded that these materials caused a reduction in the swelling potential and that the reduction was increased with increasing percentages of added stabilizers. Other stabilizers reduced the plasticity and swelling potential at variable grades. The author further specified that the amounts of sodium and calcium cations, as well as the cation exchange capacity, are effective indicators of the efficiency of chemical stabilizers used in soil stabilization. Al-Rawas et al. (2005) investigated the stabilization of the same soil (from Al-Khod) using cement, lime, a mixture of lime and cement, Sarooj (artificial pozzolan), and heat curing. It was established that due to the addition of 6% lime, both the swell pressure and swell percentage were reduced to zero. All stabilizers produced decreases in both swell percentage and swelling pressure, except Sarooj, which demonstrated in an increase in the swelling pressure with the addition of 6 and 9% lime.

Okagbue and Ene (2009) investigated the influence of pyroclastic rock dust addition on the geotechnical properties of expansive soil. In this study, expansive clay was mixed with varying amounts of pyroclastic rock dust. The researchers concluded that the pyroclastic rock dust coats the clay particles, binds them together, and fills the voids in the clay. This treatment improves the swelling properties and the workability of the soil by increasing soil aggregation, reducing water absorption, and changing the effects of clay minerals.

Başer (2009) studied the stabilization of expansive soils using waste dolomitic marble dust, waste limestone dust, and by-products from the marble industry. Expansive soil with predetermined percentages of stabilizers, ranging from 0 to 30%, was used. The rate of swell and swelling percentage was determined for the samples. The degree of swell increased and swelling percentage decreased with increasing stabilizer percentages. In the same field, Firat et al., (2012) mixed construction waste with soil in various applications, including road sub-base filling. The investigator studied the geotechnical properties of two types of clay mixed with three different types of waste, namely fly ash (FA), marble dust (MD), and waste sand (WS). It was concluded that the ratio of 15% is the optimal stabilization percentage for the three additives and that the mixture can be used as a road sub-base filling material. This conclusion was drawn according to the swelling percentages and the results of the saturated CBR tests.

Kalkan (2011) used silica fume waste material to stabilize expansive clay. The effects of wetting and drying cycles on the swelling behavior of stabilized expansive clay were been examined under laboratory conditions. The results showed that silica fume decreases the progressive distortion of modified expansive clays that are subjected to cyclic drying and wetting. Mirzababaei et al., (2013) studied the improvement of the swelling characteristics of compacted cohesive soils using household carpet waste. In this study, two different clays with noticeably different plasticity indexes (i.e., 17.0 % and 31.5 %) were cured with two different types of carpet waste fiber. It was concluded that the swelling pressure drops quickly as the percentage of fiber increases in samples prepared at the optimum moisture content and maximum dry unit weight. Modarres and Nosoudy (2015) studied the use of coal waste in its natural state and the ash of the coal after ignition at 750°C for the stabilization of medium plastic clay. Hydrated lime powder was applied as a traditional stabilizer in this study for comparison. The authors of the study concluded that the coal waste and its ash only had slight effects on plastic behavior compared to hydrated lime. However, the combined effect of coal and lime waste on the stabilization of clay was considerable. Likewise, for saturated specimens, hydrated lime had significantly the greatest effects on improving the swelling properties of the studied soil.

## 2.6 Effect of Solid Waste Materials on the Clay Compressibility

Consolidation leads to settlement in most of the structures built on clays. Sometimes, these soils contain different types of SWMs. These materials were added to the soil accidentally or deliberately as stabilizers. Numerous researchers have attempted to explain the compression behavior of municipal solid waste (Kavazanjian et al., 1999; Hossain, 2002; Durmusoglu et al., 2006; Reddy et al., 2009; Bareither et al., 2012).

The compressibility of solid residue byproducts produced by coal-burning electric utilities was investigated by Kim et al., (2005). The researchers used Class F fly and bottom ash in highway embankments. The researchers concluded that the compressibility values of compacted ash mixtures were similar to those of typical compacted sands. Saride et al., (2010) assessed the use of recycled or secondary materials in pavement construction. Two types of recycled materials, namely cement-stabilized quarry fines and reclaimed asphalt pavement were utilized as pavement base materials for a highway extension project in Arlington, Texas, United States. These materials showed small compression index ($C_c$) values compared to the natural subgrade soils. Wei et al., (2012) studied the compression behavior of zinc contaminated clays hardened with cement. The investigators found that with the increase of zinc concentration for specific cement content, the yield stress and compression index were decreased. Soleimanbeigi and Edil (2015) investigated the compressibility of different types of SWMs compared to glacial outwash sand. The compressibility parameters of five types of SWMs mixed with glacial outwash sand were estimated using one-dimensional (1D) compression tests. These SWMs included foundry slag, foundry sand, bottom ash, recycled pavement material, recycled asphalt pavement, recycled concrete aggregate, and recycled asphalt shingles. The results showed that the compressibility values of all the compacted recycled materials, except recycled concrete aggregate, were higher than that of the compacted glacial outwash sand.

There is a large volume of published studies that include descriptions of the compressibility and hydraulic conductivity of clay, especially bentonite when used as vertical cut-off walls. Soil–bentonite vertical cut-off walls installed with the slurry trenching technology are extensively used as in situ barriers to control the subsurface movement of contaminated groundwater in many countries in the world (Evans et al., 1995; Sharma and Reddy, 2004). Fan et al., (2014) studied the hydraulic conductivity and the compressibility of clay mixed with calcium bentonite for slurry wall backfill.

## 2.7 Effect of Solid Waste Materials on the Strength of Soil

### 2.7.1 Soil strength characteristics using laboratory tests

Nunes (1997) used repeated load triaxial and indirect tensile tests to examine a wide range of alternative materials, including CDMs, and offered a practical framework for their evaluation. The author's aim was to enable pavement engineers to cope with most applications in road construction. In triaxial testing, models used to study the resilient behavior of granular materials were found to provide good results for unbound but not for lightly treated secondary materials. Furthermore, Taha et al., (2002) performed experimental investigations to evaluate the use of cement to stabilize reclaimed asphalt pavement (RAP) and RAP-virgin aggregate mixtures as base materials. Compaction and UCS tests were performed on the following

RAP/virgin aggregate mixtures: 100/0, 90/10, 80/20, 70/30, and 0/100%. Samples were modified using 0, 3, 5, and 7% Portland cement, and they were cured for 0, 3, 7, and 28 days, respectively, in plastic bags at room temperature. Results showed that the addition of cement and virgin aggregate would increase the maximum dry density, optimum moisture content, and strength of RAP. Longer curing periods will produce higher strength results. Cement-stabilized RAP-virgin aggregate mixtures seem to be a practical alternative to the dense graded aggregate used in road base construction. The capability of RAP aggregate to operate as a structural component of the pavement is more marked when it is stabilized with cement rather than when mixing with only natural aggregate. However, 100% RAP aggregate should not be recommended for use as a base material unless it is stabilized with cement.

Park (2003) verified the compaction and physical properties of two recycled aggregates that were obtained from a concrete pavement rehabilitation project and a housing redevelopment site. The behavior of these recycled materials was compared to that of natural materials (crushed stone aggregate and gravel). The author evaluated the stability of recycled concrete aggregate (RCA) and shear resistance using the gyratory shear factor determined by the gyratory testing machine (GTM), which was available in the U.S. Army Corps of Engineers. Gyratory shear represents the resistance of the material to shear stress, and it is used in the evaluation of the stability of soils, asphalt mixtures, and aggregates. An aggregate with a high gyratory shear factor is more stable than an aggregate with a low gyratory shear factor. Figure 2.1 shows a comparison of the gyratory shear factor achieved for the RCA, the crushed stone aggregate (CSA), and gravel in dry conditions and after 48h of soaking (wet conditions). The results showed that the gravel was less stable after 300 GTM, but, RCA and CSA are very stable with increasing GTM revolutions. Nevertheless, under wet conditions (48h soaking) the gyratory shear factor decreases. The author concluded that the stability and the shear resistance of the recycled aggregates (in dry conditions) were higher than those of the gravel, and they were very similar to, or even better than, the values reached for the CSA. The RCA could be utilized as alternative material to CSAs in the bases and sub-bases of roadways. As expected, in misty conditions, the shear resistance and stability of RCA and CSA were lower than in dry conditions. However, the reduction rate is similar to the one observed in natural aggregates.

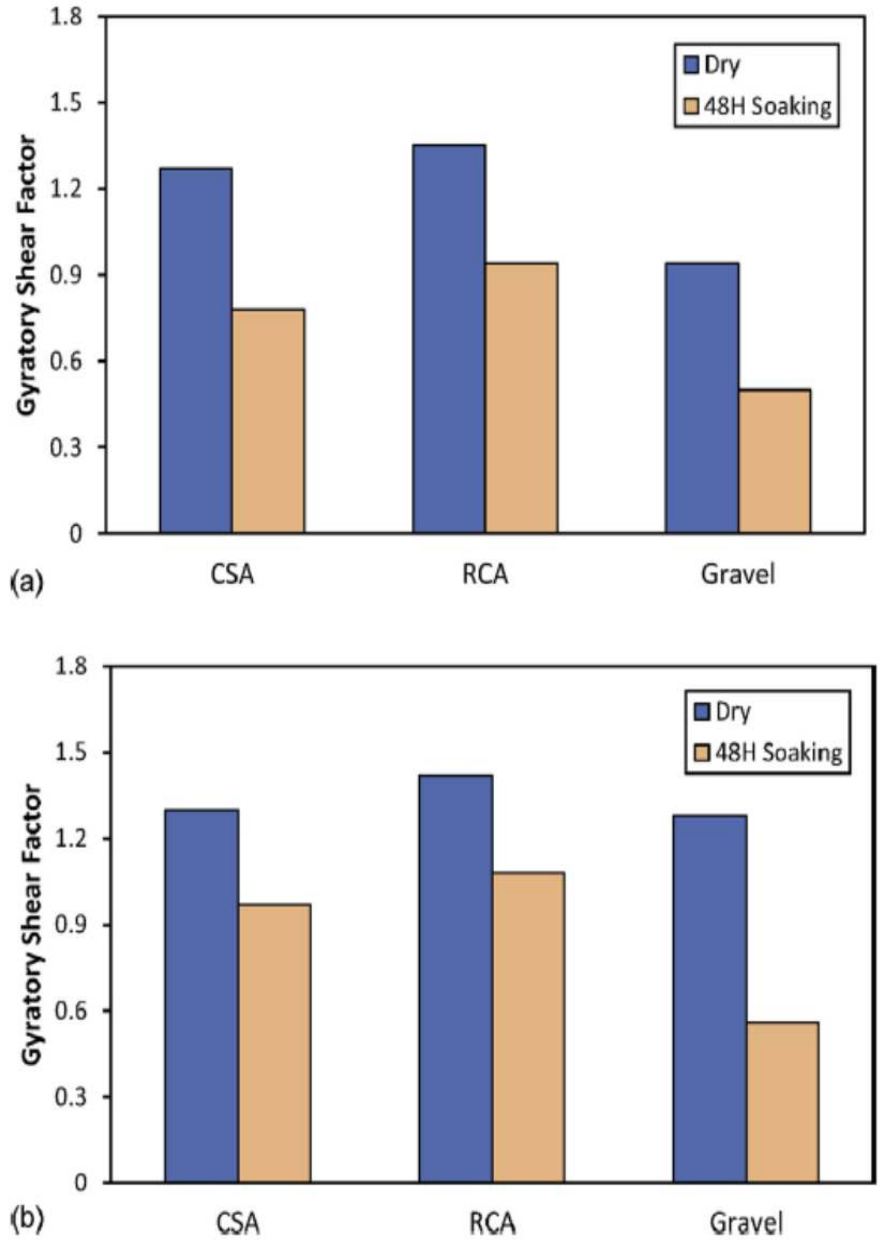


**Figure 2.1** Comparison of the gyratory shear factor for different aggregates (a) GTM150 revolutions (b) GTM300 revolutions (Park, 2003)

Sivakumar et al., (2004) conducted repeated loading tests in a large direct shear apparatus on building debris, crushed concrete, and crushed basalt (for comparison purposes). The primary target of the study was to check whether a possible drawback of the use of recycled CDMs is the risk of crushing during repeated loading. The results displayed that the recycled CDMs were more susceptible to particle crushing concerning the amount of crushing influenced by both the number of loading cycles and vertical pressure, despite the fact that the shear strength of the recycled materials is not meaningfully dissimilar to that of crushed basalt.

Leite et al., (2011) identified the importance of the composition of CDMs and the degree of compaction on their mechanical behaviors. A laboratory program was conducted by testing the geotechnical characterization of CDMs, repeated load triaxial tests, and bearing capacity. The results illustrated the influence of composition and compaction effort on the physical properties of the CDMs aggregate. The compaction process promoted the partial crushing of CDMs particles, increasing the percentage of cubic grains, and changing the grain size distribution. This physical change contributes to a better densification of the CDMs aggregate and, consequently, an improvement in bearing capacity.

Behiry (2013) takes the UCS as a central quality indicator of strength. The investigator uses this test to study the possibility of mixing traditional limestone aggregate with RCA. Traditional limestone aggregate is currently being used in base or sub-base applications in Egypt. Furthermore, the effect of mixture percentages on the mechanical properties of cement-treated recycled aggregate was investigated. Samples were prepared to determine tensile and compressive strengths based on mixing parameters. The results showed that adding RCA improves the mechanical properties of the blend. The other factors, such as cement content, dry density, and curing time, play significant roles in the determination of the performance of cement-treated recycled aggregate.

Mohammadinia et al., (2014) studied the strength of the same materials used in this thesis, but the investigators added cement as a curing material to enhance the strength. The CDMs investigated were reclaimed asphalt pavement (RAP) brick (CB), and RCA. The geotechnical properties of cement-treated CDMs were tested to evaluate their performance in pavement base/sub-base applications. The effect of curing time on the strength of the CDMs was examined by conducting repeated load triaxial and UCS tests. The results of the RAP showed the highest strength in all cases with the same cement content and curing time, followed by RCA and CB. RAP requires 2% cement (by weight) and either 7 or 28 days of curing to reach the local road-authority requirements. The RCA and CB require 4% cement and 28 days of curing. The increasing of cement content, curing time, and confining pressure increase the resilient moduli of CDMs. Humidity curing was found to have a significant effect on the strength development of cement-treated CDMs. The authors of this study showed that cement-treated CDMs were workable construction materials for pavement base/sub-base applications.

Disfani et al., (2014) carried out an experimental study to estimate the performance of cement-stabilized RCAs mixed with CB as a complementary material. An extensive suite of tests were undertaken on the RCA blends stabilized with 3% cement and CB. The experimental assessment included the index properties, a set of strength tests, like CBR, UCS, and repeated load triaxial, and flexural beam. The mixtures that had the physical properties that fulfilled the local state road-authority requirements were found to be the cement-stabilized blends with 3% cement and up to 50% CB content. The results of repeated load triaxial tests showed that the RCA/CB blends performed well with 50% CB content just on the borderline of bound pavement material criteria. UCS met the minimum requirements after seven days of curing for all blends while the 28-day strength of the blends was considerably enhanced. The above findings are consistent with the study by Mohammadinia et al., (2015). The authors examined the engineering characteristics of various cement-treated recycled CDMs obtained from extensive laboratory testing. The results of UCS tests used in this study illustrated that cement-treated recycled material can be considered acceptable as a pavement base or sub-base material in the field. The laboratory results showed that humidity, curing, and temperature conditions play vital roles in strength development in cement-treated materials. The durability of these materials was represented using the Los Angeles abrasion loss tests. Cement-treated recycled materials are durable.

Hoy et al., (2016) explored the strength development of RAP-FA geo-polymer for use as a road construction material. A mixture of sodium silicate solution ($Na_2SiO_3$) and sodium hydroxide solution (NaOH) was used as a liquid alkaline activator (L). To measure the strength development of RAP-FA blend (without L) and RAP-FA geo-polymer, UCS was used as an indicator. The UCS development was examined through SEM and XRD analyses. Test results displayed that the UCS values of the compacted RAP-FA blend met the specified strength requirements and might be used as a base course material. Also, the same material, RAP, was employed by Suebsuk et al., (2014) to study the effects of cement-treated soil-RAP mixture on compaction behavior and UCS. The porosity was implemented as an indicator for evaluating the strength of the mixed materials. The results illustrated that with an increase in RAP content, the $w_{opt}$ tends to decrease, up to the optimum soil-RAP ratio of 50:50. The authors used a particular point for asphalt content to display the effect of RAP on the strength. Asphalt fixation point is designated as a transitional point where the small change in strength turns to a considerable change. The decrease in strength is minimal when the asphalt content is lower than the asphalt fixation point of asphalt content of 3.5% (50:50 soil-RAP ratio), which is found to be the asphalt fixation point.

Many researchers have investigated the use of CDMs as backfill materials in geosynthetic-reinforced structures. To characterize the behavior of geo-grid/CDMs interfaces, Santos and Vilar (2008) made pull-out tests and direct shear tests, in their study of using CDMs as backfill in geosynthetic-reinforced structures. The potential for using alternative materials, such as recycled CDMs in geosynthetic-reinforced walls, was subsequently explored by Santos et al. (2010; 2013; 2014). Arulrajah et al., (2013b) investigated the interface shear strength of geogrid-reinforced recycled CDMs to evaluate the practicality of their use as alternative construction materials. The CDMs used in the research were CB, RCA, and RAP.

### 2.7.2 Strength characteristics using field or large scale tests

The field or models container to conducted soil tests were used by many investigators to study the strength characteristics of clay (Consoli et al., 1998; Rojas et al., 2007). The strength of clay stabilized by cement or geosynthetic reinforcement was also studied conducting plate load tests on soil models (Otani et al., 1998; Dalla et al., 2008; Consoli et al., 2009).

Consoli et al. (2003) used plate load tests (300 mm diameter, 25.4 mm thick) to investigate the load-settlement behavior of homogeneous residual soil stratum. The layered system is formed by two different top layers (300 mm thick). The upper layers were sand-cement and sand-cement fiber, which overlayed the residual soil stratum. The residual soil stratum had 3.5 m depth of homogeneous sandy-silty red clay, which is classified as low plasticity clay according to the USCS. To construct the sand-cement and the sand-cement fiber top layers, a 1.2m thick layer of the upper residual soil, was removed in the testing area. After removal, two improved soil layers, 300 mm thick and 2.25 $m^2$ each (1.5 m by 1.5 m), were built over the residual soil in three consecutive layers, each 100-mm thick. To reach the specified relative density, a vibratory plate was used. The results showed an increase in bearing capacity, reduction in displacement at failure, and changes in soil behavior to a visible brittle behavior due to the use of a cemented top layer. The addition of fiber to the cemented top layer made it maintain approximately the same bearing capacity but changed the post-failure behavior to ductile behavior (plastic behavior). After the maximum load was applied, the bearing capacity dropped toward nearly the same value found in the plate test carried out directly on the residual soil.

Arm (2003) researched the mechanical properties of individually-selected residues for the improved design of pavements. One of these materials was the crushed concrete. The deformation of loading, the resistance to mechanical and climatic action, and the potential strength development over time were studied in the laboratory and the field. The results were compared to those of the virgin aggregates they could possibly replace, such as crushed rock sand and gravel. Some of the tests used in the laboratory were cyclic load triaxial, freeze-thaw, and Los Angeles tests. In the field, test sections with residues and reference sections with conventional aggregates in the unbound layers were observed by means of falling weight deflectometer (FWD) measurements. Both laboratory and field results displayed several years' growth in stiffness for unbound layers of crushed concrete; this stiffness is not currently in unbound layers with natural aggregates.

Ornek et al., (2012) carried out a numerical and experimental study to predict the bearing capacity of shallow circular footings supported by layers of compacted granular fill over clay. Overall, of 28-field plate load tests were conducted in the Adana Metropolitan Municipality's water treatment facility center located in the western part of Adana, Turkey. Seven different sizes of footing models with diameters of 0.06, 0.09, 0.12, 0.30, 0.45, 0.60 and 0.90m were used in this study. The general design of the test arrangement is given in Figure 2.2. The theoretical work included the use of a multi-linear regression model and artificial neural networks to predict the bearing capacity of shallow circular footings. The results show that the use of granular fill layers over clay has a significant effect on bearing capacity characteristics.

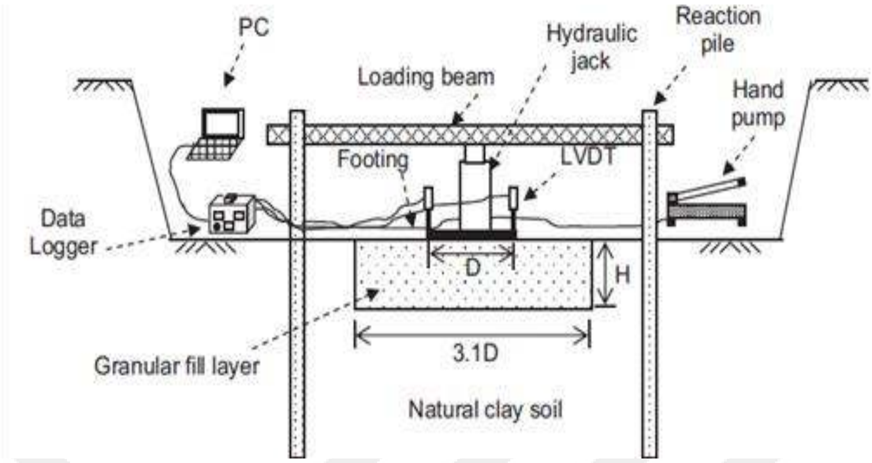


**Figure 2.2** Schematic view of test setup, loading, and reaction system and typical design of instrumentation (Ornek et al., 2012)

Khanal (2013) made a comparison in his thesis between the plate loading test results of three case studies of soil selected from Sweden, Portugal, and the United States and the load-settlement responses using the finite element method (FEM). The numerical analysis was completed using PLAXIS 2D. The parameters and soil profiles used in the analysis were based on either laboratory tests or in situ tests. The study targets to back-calculate the load tests using advanced soil models in PLAXIS 2D to gather data on soil behavior and constitutive models. The first case study was on clay fill at Tornhill, Sweden. The back-calculated load-settlement curves were numerically compared to measured load-settlement curves for three full-scale shallow foundations of different sizes. From the result, there was a reasonable agreement between the numerical curves obtained using finite element analysis and the measured results.

Neves et al., (2013) performed experimental investigations on the structural evaluation of the recycled materials used in unbound granular layers of bituminous pavements. The authors conducted the study on experimental pavements, where recycled materials were used in granular layers of sub-bases and bases. The experimental pavements were instrumented during the construction and acquiesced to loading tests. The aggregates used in the experimental work were CDMs (crushed concrete and ceramic mixtures) and reclaimed asphalt material (crushed asphalt and milled material). Natural limestone was used as the reference material for comparison. Four sections were instrumented with load cells and strain gauges placed in pavement layers and subgrade soil. The experimental tests included in situ loading test series performed by the falling weight deflectometer, for deflection measurements of the instrumented pavements with different recycled and natural materials. The results of the load tests confirmed the acceptable performance of the layers made with recycled materials.

## 2.8. Properties of Construction and Demolition Materials as a Base or Sub-Base

### 2.8.1 Bricks solid waste material

CB, which is a type of CDMs, is a by-product of demolition activities. While there are a considerable number of studies focused on using reclaimed asphalt shingles and crushed concrete aggregates in various geotechnical applications, limited research has been carried out on using CB. Chidiroglou et al., (2008) performed experimental investigations on the physical properties of demolition waste materials to reuse them as engineering fill. They present the physical features of three types of commercially crushed concrete and brick materials. The first material was CB, and the other two were similar crushed concrete materials with different degrees of processing. Geotechnical properties, such as particle size distribution, particle shape, aggregate impact, resistance to freeze-thaw, and crushing values, were established. The results showed that the two crushed-concrete-based materials that had been processed to different degrees had identical properties that depend on their composition, such as water absorption and particle density. Besides, the materials that had not been further processed had more angular/flaky particles, and the flakiness of particles reduces with reducing particle sizes. Moreover, materials with similar particle densities and water absorption behave similarly during large-scale compaction tests.

Aatheesan et al., (2010) presented the geotechnical properties of CB and proposed its use in sub-base applications. The materials for the experimental works were collected from a recycling facility in Victoria, Australia. The engineering characteristics of various proportions of crushed rock with CB blends obtained from wide-ranging experimental tests were shown in this study. To determine the potential use of CB blends, the engineering properties obtained were compared to current local road-authority specifications for pavement sub-base or light-duty base material for drainage systems. The laboratory test results indicated that up to 30% CB could be safely added to crush rock combinations for pavement sub-base applications.

Arulrajah et al., (2011) investigated the findings of a laboratory program on the characterization of recycled CB and a valuation of its performance as a pavement sub-base material. To assess its performance as a pavement sub-base material, the properties of the recycled CB were compared to the local state road-authority specifications in Australia. The experimental program was extensive and included tests such as particle size distribution, particle density, modified Proctor compaction, water absorption, CBR, Los Angeles abrasion loss, static triaxial, repeated load triaxial tests, pH, and organic content. CBR values were found to fulfill the local state road-authority requirements for a low strength sub-base material. The value of Los Angeles abrasion loss was just above the maximum limits specified for pavement sub-base materials. The geotechnical testing results shows that CB might have to be mixed with other durable recycled aggregates to enhance its performance in pavement sub-base applications and to improve its durability. The shear strength of the CB was found to be reduced beyond the acceptable limits, especially, at higher moisture ratio levels. The repeated load triaxial testing established that CB would perform satisfactorily at a 65% moisture ratio level. The results of the repeated load triaxial testing indicate that only recycled CB with water content of around 65% is a viable material for usage in pavement sub-base applications.

Arulrajah et al., (2012) analyzed the laboratory investigation to examine the use of recycled CB when mixed with crushed rock and RCA for pavement sub-base applications. The experimental work involved particle size distribution, particle density, modified Proctor compaction, water absorption, CBR, Los Angeles abrasion, repeated load triaxial tests, pH, and organic content testing. Laboratory tests were applied on mixtures of 10%, 15%, 20%, 25%, 30%, 40%, and 50% CB mixed with crushed rock or RCA. The results revealed that recycles concrete aggregate and crushed rock blends could be safely mixed with up to 25% CB in pavement sub-base applications. The repeated load triaxial test result indicate that the effects of CB content on the mechanical properties regarding permanent deformation and resilient modulus were minimal compared to the effects on dry density and moisture content.

### 2.8.2 Asphalt-concrete solid waste material

Certain laboratory evaluations of the geotechnical and geo-environmental properties of asphalt-concrete solid waste material have been undertaken in the literature. Most of these materials were found after removing old paved roads. Cooley (2005) investigated the possibility of reusing of reclaimed asphalt pavement (RAP) in full-depth recycling. The tests used to study the effect of RAP on the mechanical properties of recycled base materials from Northern Utah were the free-free resonant column test to measure stiffness and CBR test to measure strength. In another study, Sirigiripet (2007) made an inclusive experimental program to study two recycled materials, cemented quarry fines (CQFs) and RAP, which were used as a pavement base material. Results from the experimental tests, along with field monitoring data, displayed that these recycled materials were appropriate for use as pavement base materials.

Warner (2007) presented the evaluation of reclaimed asphalt shingles for reuse in roadway construction. He concluded that the reclaimed asphalt shingles (RAS) were not suitable as a base material while they could be used as a sub-base material. However, the RAS with aggregates were found to be suitable for use as sub-base while the mixtures exhibited a decrease in resilient modulus with an increase in reclaimed asphalt shingle content. Also, Soleimanbeigi et al., (2011) published a report on the evaluation of RAS as structural fill. The report included three individual self-contained technical articles published in ASTM journal. The study outlined in this proposal addresses the following suggestions. First, RAS, as a granular material, has sufficient drainage capacity and shear strength to qualify as structural fill material. RAS might show higher compressibility compared to traditional fill material because the material contains asphalt cement and cellulose felt. Second, the stabilization of RAS by less compressible materials can reduce the compressibility and increase the drainage capacity and shear strength of RAS. Third, because RAS contains asphalt cement, temperature variations affect its engineering properties. Fourth, because RAS includes asphalt cement, volumetric strain, or time-dependent shear under sustained deviator stress may be significant.

Warner and Edil (2011) used the same materials to study RAS for valuable reuse in roadway construction. The use of RAS as an additive or substitute for the earth materials typically employed in the aggregate base and aggregate sub-base layers of roadway pavements was considered in this paper. The aim of this study was to evaluate the practicality of the widespread application of RAS in the aggregate base and aggregate sub-base layers of roadway pavements. Also, the technical specifications of RAS, including the effects of FA stabilization on RAS strength, were determined. RAS, FA-stabilized RAS (S-RAS), RAS-silt mixtures and, RAS aggregate mixtures were evaluated for particle size characteristics, compaction properties, CBR, UCS, and resilient modulus. According to the results of the tests, pure RAS was found to be unsuitable as base material, even though RAS could potentially be used as a sub-base or general fill material. FA and S-RAS mixture was less susceptible to penetrative deformation than non-stabilized RASs. However, FA and S-RAS mixture was still very vulnerable to penetrative deformation when unpaved. RAS aggregate mixtures were suitable for use as sub-bases and possibly base course, yet RAS aggregate mixtures showed decreasing resilient modulus with increasing RAS content.

Hoyos et al., (2011) conducted laboratory and field assessments of the use of cement-treated reclaimed asphalt pavement blends as roadway base materials. Mixes containing 100%, 75%, and 50% RAP and treated with Portland cement of different amounts were used in an inclusive laboratory testing program. A mix design model based on granular base materials and typical RAP in Texas was proposed, and the parameters that affect the properties of cement-treated RAP mixes were identified. The design model was verified by the information from the initial field experiment on actual construction projects. In this study, it was suggested that cement-fiber-treated reclaimed asphalt shingles can be used as an environmentally- and structurally-sound material in the sub-base layers of road pavements.

Zhu et al., (2012) performed experimental investigations of the use of earthquake-damaged building waste as recycled aggregate in asphalt mixtures. Waste materials were processed into recycled aggregate and used in asphalt mixtures with natural limestone aggregate. A liquid silicone resin was used to pre-treat the recycled aggregate because of the high absorption and the low strength of the recycled aggregate. Various tests, including physical properties tests, surface morphology tests of both pre-treated untreated recycled aggregate, moisture susceptibility tests, three-point bending beam tests, and permanent deformation tests of asphalt mixtures, were carried out. The study concluded that fine recycled aggregates without treatment are not suitable for use in asphalt mixtures due to its high absorption capacity. Nevertheless, the pre-treatment of coarse recycled aggregate using used liquid silicone resin improves the absorption, strength, adhesion with asphalt, and surface morphology of coarse recycled aggregate because of its great hydrophobicity, permeability, and adhesion with both asphalt of solidified silicone resin and inorganic base materials.

Arulrajah et al., (2013) conducted a comprehensive laboratory investigation of the geotechnical behaviors of various CDMs, including reclaimed asphalt shingles, crushed concrete aggregate and, CBs in possible sub-base applications. The researchers concluded that crushed concrete aggregates have more strength than granular sub-base materials, whereas others needed some curing with additives to be used as sub-base materials. Table 2.4 summarizes the results of the comparison between the materials used in the study.

Hoppe et al., (2013) published a report about their investigation of the feasibility of RAP use as road base and sub-base material. The results showed that the use of RAP in road base and sub-base materials is possible and has been employed by some transportation agencies. The results also revealed that there are potentially weighty economic advantages if RAP can be used in base and sub-base applications. Approximately 30% of material costs could be saved with a 50/50 blend of RAP and natural aggregate.

Recently, Thakur and Han (2015) presented a comprehensive review of several new experimental studies on treated RAP bases (blended RAP aggregates, cement and FA S-RAP, and geocell-confined RAP). The authors discussed the key findings of these studies, including the proportion of RAP to natural aggregate. The percentage of stabilizing agent, modulus, strength, creep deformation of treated RAP under static loading, and permanent deformation of processed RAP under cyclic loading were discussed in the review too.

### 2.8.3 Crushed-concrete solid waste material

Many researchers have studied the use of crushed concrete produced from different CDMs activities for geotechnical purposes.

O'Mahony and Milligan (1991) first identified the potential to use demolition debris and crushed concrete as sub-base recycled aggregate. Their laboratory study is mainly a comparison of the performance of recycled materials and limestone aggregates using CBR tests. The demolition debris showed reduced CBR values when compared to the natural aggregate. In contrast, the CBR values showed similarity between crushed concrete and the natural aggregates.

**Table 2.4** Various geotechnical properties of CDMs materials (Arulrajah et al., 2013)

| Type of test or geotechnical properties | RCA[1] | CB[2] | WR[3] | RAP[4] | FRG[5] | Regular Quarry Material |
|---|---|---|---|---|---|---|
| Gravel (%) | 50.7 | 53.6 | 44.7 | 48.0 | 0.0 | |
| Sand (%) | 45.7 | 39.8 | 45.1 | 46.0 | 94.6 | |
| Fines (%) | 3.6 | 6.6 | 10.2 | 6.0 | 5.4 | Less than 10 |
| USCS classification | GW | GW | SW | GW | SW | |
| $C_u$ | 31.2 | 44.4 | 74.7 | 25.6 | 7.5 | |
| $C_c$ | 0.9 | 2.0 | 5.4 | 2.5 | 1.5 | |
| Los Angeles abrasion (%) | 28 | 36 | 21 | 42 | 25 | Less than 40 |
| CBR (%) | 118-160 | 123-138 | 121-204 | 30-35 | 42-46 | Larger than 80 |
| Maximum dry density (kN/m$^3$) | 19.13 | 19.73 | 21.71 | 19.98 | 17.40 | Larger than 17.5 |
| Optimum moisture content (%) | 11.0 | 11.25 | 9.25 | 8.0 | 10.5 | 8-15 |
| Organic content (%) | 2.3 | 2.5 | 1 | 5.1 | 1.3 | Less than 5 |
| pH | 11.5 | 9.1 | 10.9 | 7.6 | 9.9 | 7-12 |
| Hydraulic conductivity (m/s) | $3.3\times10^{-8}$ | $3.3\times10^{-9}$ | $3.3\times10^{-7}$ | $3.3\times10^{-7}$ | $3.3\times10^{-5}$ | Larger than $3.3\times10^{-9}$ |
| Flakiness index | 11 | 14 | 19 | 23 | | Less than 35 |
| Cohesion (kPa) | 44 | 41 | 46 | 53 | 0 | Larger than 35 |
| Friction angle (°) | 49 | 48 | 51 | 37 | 37 | Larger than 35 |
| Resilient modulus 70% of the OMC | 575-769 | 280-519 | 127-233 | | | 175-400 |
| Resilient modulus 80% of the OMC | 487-729 | 303-361 | 202-274 | | | 150-300 |
| Resilient modulus 90% of the OMC | 239-357 | 301-319 | 121-218 | | | 125-300 |

1-Recycled concrete aggregate 2- Crushed brick 3- Waste rock 4- Reclaimed asphalt pavement 5- Fine recycled glass

Bakoss and Ravindrarajah (1999) have demonstrated that it is common in Australia to blend small amounts of CBs and soil with RCA to gain a recycled product suitable for use in pavements.

Bennert et al., (2000) evaluated the behavior of RCA in road base and sub-base applications. The investigators determined that the optimal mixture was 75% natural aggregate and 25% RCA. This mixture was able to reach the same permanent deformation and resilient response properties of a dense graded aggregate base course that is frequently used in base and sub-base layers. Chini et al., (2001) explored the effects of using RCA produced from destroyed concrete pavement in Santa Rosa County, FL on the properties of road base samples. The results exposed that the properties of the RCA used in the study was suitable when compared to those of natural aggregate. Besides, the results are within the limits established by most highway agencies for concrete aggregates. The gradation of RCA and the results of the soundness test using sodium sulfate were the exceptions of tests out the limits. To fix these two problems, the authors suggested that the cement mortar that adhered to the recycled aggregate was sensitive to sodium sulfate and contributed to an increased loss in the soundness test.

To investigate the possibility of using crushed clay bricks and RCAs as aggregates in unbound sub-base materials, Poon and Chan (2006) conducted a study at University of Hong Kong Polytechnic. The results displayed a decrease in the $\gamma_{drymax}$ and an increase in the $w_{opt}$ of the 100% RCA sub-base materials compared to those of natural sub-base materials. Furthermore, the replacement of RCAs with crushed clay brick further increased the $w_{opt}$ and decreased the $\gamma_{drymax}$. These reasons were mainly attributed to the higher water absorption and lower particle density of crushed clay brick compared to those of RCAs. The CBR values (with and without soaking) of the 100% RCA sub-base materials were lower than those of natural sub-base materials.

The CBR values further decreased as the replacement level of RCAs by crushed clay brick increased. As highlighted by Tam and Tam (2007), the influences of the size and shape of crushed concrete aggregates were pointed in a series of experimental studies. This influence revealed the significance of such physical characteristics of crushed concrete aggregates on the behavior of pavements, embankments, roads, and bridges.

Melbouci (2009) studied the compaction and shearing behavior of recycled aggregates. To examine their mechanical response and determine their geotechnical characteristics CBR, Proctor test, and shearing tests were carried out. The researcher stated that the compaction and shear behavior of geo-materials used in roadways in high traffic could be improved by mixing crushed concrete aggregates, sand, cement, and brick elements at certain ratios.

Melton et al., (2012) presented a comprehensive review of the construction of highways using building-derived concrete debris. Building-derived concrete (BDC) was used, and the gradation, unit weight, $w_{opt}$, and resilient modulus were measured for the control materials and the BDC. The sand and crushed stone were used as control materials for comparison. The resilient modulus was measured using both a light falling weight deflectometer (LWD) and a laboratory triaxial cell in a trial pit. The resilient modulus of the BDC exceeded that of the control materials, as measured using the LWD and in the laboratory. Besides, the laboratory resilient modulus had a notable correlation with the LWD stiffness. These results suggest that BDC would perform like natural aggregates in base course applications.

Pasandín (2013) conducted a laboratory study of hot-mix asphalt (HMA) use for base courses in pavements. The study included the use of RCA from CDMs in the HMA. The mixes contained 0%, 5%, 10%, 20%, and 30% RCA instead of natural aggregate. The Marshall mix design procedure was used to improve the mixes. The mixes were cured in an oven for 4 hours to improve the moisture sensitivity of the mixes. The results showed that the mixes comply with Spanish moisture damage specifications. Correspondingly, the results showed that asphalt absorption is an important parameter that affects the volumetric properties of HMA made with RCA.

Herrador et al., (2011) highlights the need to confirm the technical practicability of the base pavement layers of road surfaces using construction waste material. A field study was done with this aim. It involved testing the performance of pavement composed of asphalt mix, concrete, and ceramic waste aggregate. The experimental program was done by investigating the features of the recycled material on a segment of an actual road under real vehicle traffic conditions. It was concluded that the load-bearing capacity of the recycled artificial CDMs aggregate was satisfactory. Azam and Cameron (2013) published a paper about the engineering characteristics of mixtures of RCA with recycled clay masonry (RCM) from two material producers from South Australia. The percentage of the dry mass of RCM was 20% of the total mass. Samples were tested at a constant dry density ratio and between 60 and 100% of $w_{opt}$. Results were reported for static and repeated loading triaxial tests and standard engineering classification tests. To study the effect of suction on strength and identify soil water characteristic curves, matric suctions were measured using the filter paper method. Triaxial testing showed that varied cohesion values between 9 and 89 kPa were dependent on molding matric suction, humidity content, and material source. Permanent strain and resilient modulus were also affected by suction. Based on the laboratory testing database, the RCM blends seemed to be suitable for application as sub-base.

## 2.9 Large Models of Field Tests

Many researchers have tried to use models to obtain soil properties to simulate field conditions. These studies can be separated into three types. The first category encompasses studies that deal with theoretical models only, using some software or analytical solutions. The second type involves the use of real models and soil tests using different types of material for models. The final type involves the use of composite models of theoretical and experimental work to obtain results.

The following review was focused on the studies used practical models to find useful information about box design. A box was used to create a realistic field condition for soil in the laboratory environment. The model employed by Park et al. (2000) is shown in Figure 2.3. They studied the liquefaction of embankments on sandy soil and the optimum countermeasure against such liquefaction. The shaking table tests for 12 different cases were performed to investigate the behavior of embankments resting on liquefiable sand grounds in a model box. The dimensions of the transparent model box were 194cm in length, 44cm in width, and 60cm in depth. The test box was made of Plexiglas.

**Figure 2.3** Picture for Liquefaction of embankments box model
(Park et al., 2000)

Gupta and Trivedi (2009) studied the behavior of model circular footing on silty soil with cellular support. They made six series of laboratory model tests in a test box with a frame. The soil beds were set in a test tank with inside dimensions of (0.60m by 0.60m by 0.60m). This tank was placed in a big box. The dimensions of all apparatus are shown in Figure 2.4. Kumar and Prasada (2009) studied the use of lime and cement to stabilize pavement in road construction. The tests were carried out on a flexible pavement model in a circular steel tank with a diameter of 60cm, as shown in Figure 2.5. The load was applied using a circular metal plate with diameter of 10cm, which was placed on top of the pavement layer. The steel tank was put on the pedestal of the compression-testing machine.

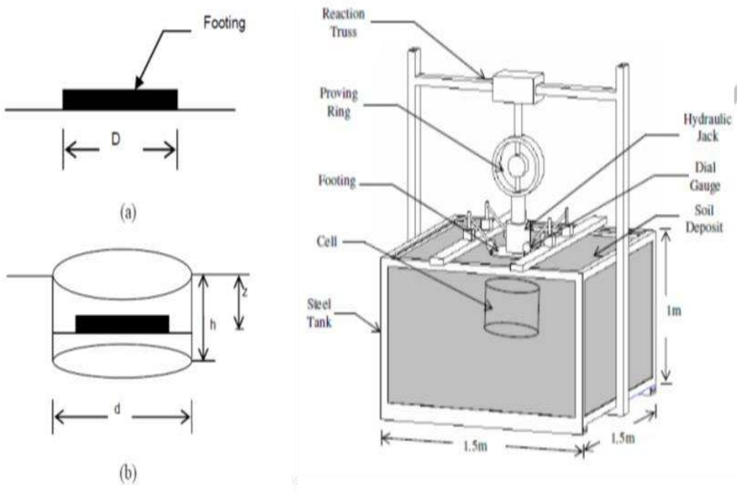


**Figure 2.4** Circular footing box model (Gupta and Trivedi, 2009)

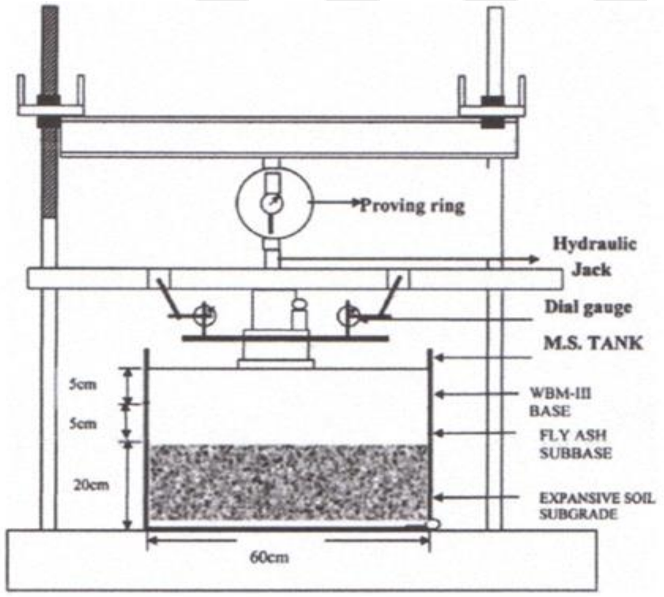


**Figure 2.5** Pavement stabilization by lime and cement using circular model box (Kumar and Prasada, 2009)

Wilson (2009) used a rigid vertical concrete wall inside a large soil container in his Ph.D. study, as shown in Figure 2.6. A dense, well-graded silty sand backfill (2.15m high, 5.6m long and 2.9m wide) was constructed behind a concrete wall. This large soil container was used to study large-scale passive force-displacement and dynamic earth pressure. Cell pressures and different transducers were used in different locations, as shown in Figures 2.7 and 2.8.

**Figure 2.6** Restrained laminar soil container on shake table used to study Dynamic Earth Pressure (Wilson, 2009)

**Figure 2.7** Cells pressure fixed on the wall to study dynamic earth pressure (Wilson, 2009)

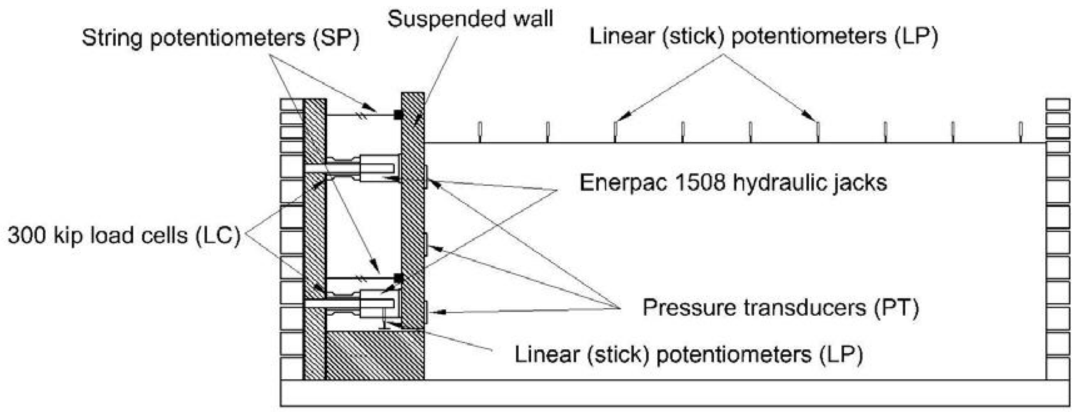


**Figure 2.8** Elevation view sketch showing instrumentation labels used to study Dynamic Earth Pressure (Wilson, 2009)

Kolay et al., (2013) published a paper about their investigation of the improvement of the bearing capacity of shallow foundations on geogrid-reinforced silty clay and sand. They used a model test tank with the dimensions of 762.0mm in length, 304.8mm in width, and 749.3mm in depth. The tank was fabricated to perform the test, with stiff vertical and horizontal sides and steel angle sections at the bottom, top, and middle of the tank. The stiffeners helped prevent lateral yielding when the load was applied at the model footing, and the compaction of the soil in the tank through the experiment. Two sidewalls of the reservoir were made of 25.4mm-thick Plexiglas plates. The other two sidewalls of the tank were made of 19.05mm wooden plates as supports and12.7mm-thick Plexiglas plates. The inside walls of the reservoir were smooth to reduce side friction, as shown in Figure 2.9.

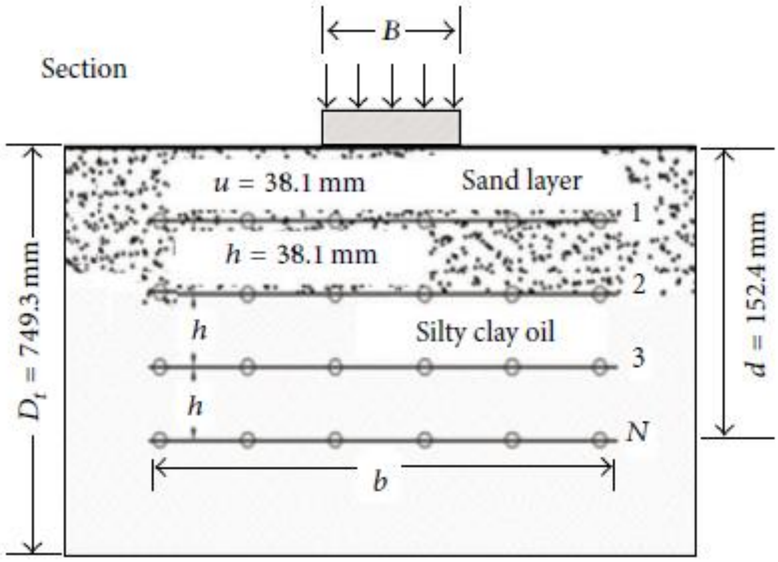


**Figure 2.9** Shallow foundation model on geo-grid reinforced soil (Kolay et al., 2013)

Sanjeev et al., (2013) observed the use of plate load tests to predict the bearing capacity of granular layered soils. In this study, the observation of the load-settlement behavior of plates of different sizes resting on layered coarse soils was arranged in a large test tank. Using square mild steel plates, tests were carried out on two layers of soils, a fine gravel layer on top of a sand layer. The effect of the thickness of the top layer on the bearing capacity and settlement characteristics of the footing was studied in this paper. The large test reservoir, shown in Figure 2.10, had inside dimensions of 2.0m by 2.0m and 1.50m in depth. The tank was made from steel plates and supported directly on 50mm by 50mm steel angle sections. Cast iron angles and plates were used at the corners, top, and bottom of the tank to strengthen it. The entire reservoir was rested on a solid concrete base. To support the loading device, A cross beam was fixed on vertical posts. A horizontal crossbeam (channel section) was placed across the middle of the tank. An overall view of the test arrangement is illustrated in Figure 2.10.

**Figure 2.10** Pictures of plate load test on granular layered soils (Sanjeev et al., 2013)

Abd Elsamee (2013) studied the effects of foundation depth and shape in addition to the size on the the modulus subgrade reaction (ks) of cohesionless soils. A plate load test was placed in an open square box, as shown in Figure 2.11. Different soil layers were used to fill the box with compaction to different density percentages that were determined using sand cone tests. Nine rigid steel plates were used in the tests and divided into three groups. First to third plate had rigid circular-shaped. Fourth to sixth plates were similar to the first group, but they had square-shaped. The seventh and eighth plates had equivalent diameters of 455mm and 610mm. The ninth one is a rigid rectangular plate having the same areas as the first group.

**Figure 2.11** Effect of foundation dimensions and shape using box model with a frame (Abd elsamee, 2013)

# CHAPTER 3

# EXPERIMENTAL STUDY

Firstly, a plan for experimental work was presented to determine all the tests conducted for the clay and clay-CDMs mixtures, as well as test durations. After that, the characteristics of the clay and CDMs used in this study were given. The previous part is followed by a description of the testing apparatus and experimental techniques for each test. The instrumentation set-up and calibration were also illustrated.

## 3.1 Schedule of the Work

The experimental program of tests is shown in Table 3.1. Furthermore, the table shows the start time, end time, and duration time of each test. After the plate load test, which was the last experimental test, the simulation of that test using Plaxis 2D was conducted with the final analysis for all tests.

## 3.2 Materials of Experımental Work

### 3.2.1. Clay

The soil used in the study was clay. According to the unified soil classification system (USCS), when 50% or more of a soil passes through a No. 200 sieve, the soil is considered to be a fine-grained soil. This fine soil is classified as silt or clay and can be further categorized as organic or inorganic soil. Fine-grained inorganic soil is classified as clay if its plasticity index (PI) is higher than 7, which is the type of soil used in this study. Clay is defined as having particles smaller than 0.002mm and developing plasticity when mixed with a limited amount of water (Grim, 1953). The plasticity of clay is the putty-like property of clays that contain a certain quantity of water (Das and Sobhan, 2014). The control mixture used in the tests consisted of potable water and clay. The clay used for the study was excavated from Gaziantep University campus. The plastic limit and liquid limit values were 24.5% and 42.5%, respectively (ASTM D4318). The specific gravity of the clay grains was 2.7. The grain size distribution of the clay used is shown in Figure 3.1. The clay was classified as CL according to USCS and A-7-6 with group index 19 according to AASHTO.

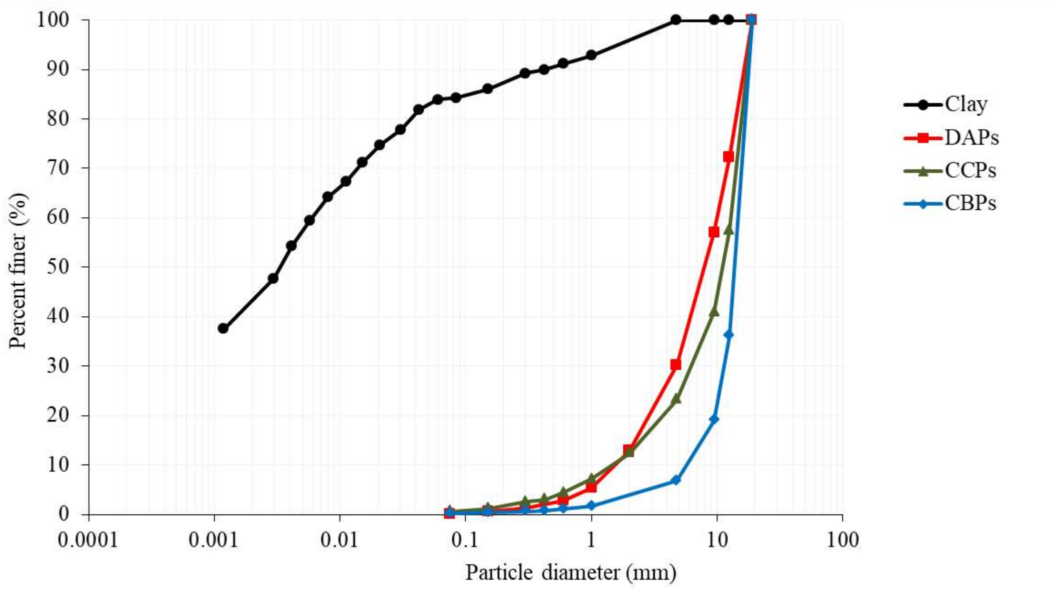


**Figure 3.1** Grain size distributions for clay and CDMs

**Table 3.1** Schedule of the progress of work

| Test | Materials or mixtures type | Date |
|---|---|---|
| Specific gravity | Clay and (5, 10, 15,and 20% CDMs-clay) | 1-4/10/2014 |
| grain size analysis (by the hydrometer) | Clay | 2-3/10/2014 |
| grain size analysis (by sieve) | Clay and (5, 10, 15,and 20% CDMs-clay ) | 11/12/2014 |
| CBR test | Clay ,(5, 10, 15,and 20% CDMs-clay), and 100% CDMs | 22/10/2014-18/12/2014 |
| Consistency limits (liquid limit and plastic limit) | Clay and (5, 10, 15,and 20% CDMs-clay ) | 10/02/2015-10/03/2015 |
| unconfined compression strength (UCS) | Clay and (5, 10, 15,and 20% CDMs-clay ) | 23/03/2015-28/03/2015 |
| **Oedometer tests set** | | |
| Free swelling test | Clay and (5, 10, 15,and 20% CDMs-clay ) | 4-9/04/2015 |
| Constant pressure test | Clay and (5, 10, 15,and 20% CDMs-clay ) | 09/04/2015-01/06/2015 |
| consolidation | Clay and (5, 10, 15,and 20% CDMs-clay ) | 09/04/2015-01/06/2015 |
| SEM pictures and EDX analysis | Clay and 100% CDMs | 02/11/2015 |
| direct shear test | Clay and (5, 10, 15,and 20% CDMs-clay ) | 24/07/2015-23/02/2016 |
| plate load test | Clay and (10% CDMs-clay) | 25/03/2016-01/05/2016 |
| Theoretical work , results analysis, and thesis writing | Clay and (10% CDMs-clay) | 1/05/2016-01/01/2018 |

### 3.2.2 Construction and demolition materials

Three different CDMs were used as additive materials, which were dumped asphalt, crushed brick pieces, and crushed concrete paving slab. Dumped asphalt pieces were obtained from the repaired and/or renewed roads and highways in Gaziantep City, Turkey. Crushed brick pieces were gained from the destroyed/repaired buildings in the city. The main material of the bricks is known to be clay. Crushed concrete aggregates were obtained from the paving slabs used in the city. The CDMs with a size of less than 19 mm were artificially sieved to provide uniform specimens for visual classification purposes. All these materials are obtainable on municipal of Gaziantep City-Turkey Figure as shown in 3.2 and 3.3.

**Figure 3.2** Picture of pile of crushed concrete and bricks

**Figure 3.3** Picture of pile of old pavement asphalt

## 3.3 Testing Apparatus and Experimental Techniques

### 3.3.1 Sample preparation

All the clay used in the laboratory tests was oven dried and then mixed with clean, dry, and crushed CDMs. The selected contents of the CDMs were 5%, 10%, 15%, and 20% by dry weight of the complete sample. The mixtures of clay and CDMs were prepared in room conditions. The CDMs came in large plastic bags. Then they were clean, dried, and crushed until all materials passed through a 3/4" (19mm) sieve. This process was done to make the CDMs suitable for all tests, as illustrate in Figure 3.4. The grain size distribution of CDMs is shown in Figure 3.1.

### 3.3.2 Consistency limits test

The clay and CDMs was passed through a no. 40 (0.42 mm) sieve for a consistency test. The consistency limits were calculated for clay and clay-CDMs mixtures according to ASTM D 4318.

### 3.3.3 California bearing ratio test

The clay and CDMs were passed through a 3/4" (19mm) sieve for the CBR test, as shown in Figure 3.6. The mixtures were prepared with five or six different water content with suitable ranges. The prepared mixtures were compacted into the CBR mold with five layers according to ASTM D1557. After the surface of the specimen was trimmed out for leveling, two filter papers were put on the bottom and top of the sample in the mold to avoid the loss of fine particles during the soaking period (ASTM D1883). The maximum dry density and optimum moisture content was calculated for every mixture after compaction (ASTM D2216). After that, the samples soaked for four days to achieve full saturation. During the soaking period, the specimens in the mold were subjected to a 4.5kg surcharge load. A metal tripod was used to support the dial gage that was used to measure the amount of swell. The initial reading for swelling was taken before soaking. After the 96hr soaking period, the final reading of the swelling percentages was taken using the dial gage fixed on the top of the sample.

### 3.3.4 Unconfined compressive strength test

The UCS test was carried out using the same mixtures at the optimum water content for each specimen. The size of the CDMs employed in the UCS test was less than

4.75mm (sieve no. 4) according to (ASTM D2166) specifications. The specimens were prepared using a two-part split mold with a diameter of 4.2cm, and a height of 10.2cm. The samples were compacted in five layers with 31 blows using a specially designed hammer described previously by Cabalar et al., (2014).


(a)


(b)


(c)

**Figure 3.4** Pictures of CDMs used in CBR test (a) crushed brick pieces, (b) dump asphalt pieces, and (c) crushed concrete pieces

### 3.3.5 Free swell test and apparatus

This test was done according to ASTM D4546-14 method specifications. Swelling pressure tests were performed using an ELE consolidometer apparatus. Swell tests were conducted in samples 75mm in diameter (D) and 20mm in thickness (H). The clay and CDMs were sieved through a no. 10 (2mm) sieve, as shown in Figure 3.8. The samples were prepared at the particular maximum dry density and optimum moisture content obtained from the compaction curves of clay and clay-CDMs mixtures. The specimens were statically compressed in the ring of the oedometer at a constant rate (0.02 mm/sec or 0.5 inch/min). The specimen compaction was done using a CBR testing machine. Swell percentage (S %) and swelling pressure ($P_{max}$) were determined for clay and clay–CDMs mixtures.

Swelling pressure was defined as the maximum pressure, $P_{max}$ that was applied to the specimen to prevent deformation in the upward vertical position when the specimen is saturated with water and supported by side restraints. A seating pressure of 1kPa (20lb/ft$^2$) was applied to each unsaturated specimen, and the dial gage was set to zero or another specific initial reading. The seating pressure included the mass of the top porous stone and load plate. The specimen was located between two porous stones on its upper and lower surfaces and confined in a ring to prevent lateral side deformation. The piston of the cell was in contact with the loading arm, whose displacement can be accurately measured with a dial gage. The piston was attached to the upper porous stone. The initial reading of the dial gage was recorded, and the specimen was submerged in potable water. Weight was added to the loading ram once the specimen swelled after absorbing water until the dial gage returned to the initial reading. The maximum allowable soil strain was ±0.02mm. Using the previous procedures; the swelling pressure was achieved by the load applied for a corresponding time. The maximum swelling pressure ($P_{max}$) was obtained when the reading of the pointer was not altered for 24h. Swelling percentage was defined as the maximum swelling percentage (S %), which is the ratio of the specimen height after free swell, measured while the specimen is saturated, to the initial specimen height as shown in equation (3.1).

$$(S\ \%) = 100^{*}\ \Delta H/H_0 \qquad (3.1)$$

where $\Delta H$ is the difference between the initial dial gage reading before adding water and the final dial gage reading (after 24h), and $H_0$ is the initial specimen height at a seating pressure of 1kPa before water was added.

### 3.3.6 Consolidation test and apparatus

The specimens were compressed in the ring of oedometer statically at a constant rate (0.02mm/sec or 0.05inch/min). Specimen compaction was done by CBR testing machine. The tests were conducted in samples of 75mm in diameter and 20mm in thickness. The clay and CDMs were sieved on a no.10 (2mm) sieve, as shown in Figure 3.8. The specimens were prepared at the particular maximum dry densities and optimum moisture contents obtained from the compaction curves of clay and clay-CDMs mixtures. The tests were performed using an ELE consolidometer apparatus and consisted of two stages. The first stage was done to identify the consolidation parameters according to ASTM D 2435-2011a. The initial reading was then taken. The first load applied on the specimens was 25kPa. The final reading was obtained when the reading of the pointer stopped changing. The loading was then doubled for each incremental step up until a maximum loading of 800kPa was reached. The duration of each loading was determined according to when the reading on the dial gage stopped or after 24h of reading. Compressibility index $C_c$ was calculated in this stage using Equation 3.2.

$$C_c = \frac{\Delta e}{\Delta \log p} \tag{3.2}$$

The hydraulic conductivity values of the 400 kN/m$^2$ and 800 kN/m$^2$ loads were estimated following Terzaghi's one-dimensional consolidation theory using equation (3.3)

$$k = C_{v.}\, Mv.\, \gamma_w \tag{3.3}$$

Where, $M_v = \frac{a_v}{1+e_o}$ $\qquad a_v = \frac{\Delta e}{\Delta p}$

The k is the hydraulic conductivity (in cm/s), and the $C_v$ is the consolidation coefficient (in cm$^2$/s) determined through the Taylor method (square root of time). The coefficient $m_v$ is of volume change (in cm$^2$/gm), and $\gamma_w$ is the unit weight of water (in gm/cm$^3$). This method of determining k value is widely accepted (Chai et al., 2004; Horpibulsuk et al., 2007; Sivapullaiah et al., 2000; Yong et al., 2009; Watabe et al., 2011; Mishra et al., 2011). The method is likely to underestimate the k values of clays (Chapuis, 2012), but it is used in this study for the relative comparison of the hydraulic conductivity of clay and SWMs. The second stage is the unloading part, which is considered the inverse of the loading stage. It was done by taking the last reading of the last load, which is then considered the initial reading, removing the load and taking the final reading. In this stage, swelling index Cs was calculated in the rebound part of e-log p curve according to equation (3.4).

$$C_s = \frac{\Delta e}{\Delta \log p} \tag{3.4}$$

### 3.3.7 Direct shear test and apparatus

The specimens were prepared by compaction in the direct shear mold statically at a constant rate (0.02mm/sec or 0.05inch/min). The compaction was conducted in square 60mm samples that were 20mm in height. The clay and CDMs were sieved on a no. 10 sieve (2mm), as shown in Figure 3.5. The specimens were prepared at the particular maximum dry density and optimum moisture content obtained from the compaction curves of clay and clay-CDMs mixtures. After the compaction, the specimens were transformed into direct shear cells at the same constant rate (0.02mm/sec or 0.05inch/min). The specimen compaction levels were measured using a CBR testing machine. The tests were performed using an ELE direct shear apparatus and according to the consolidated drained (CD) type of direct shear test to ASTM D 3080-2011 specifications. Direct shear tests were performed to determine the drained shear strength parameters (cohesion and angle of internal friction) on clay and clay-CDMs mixtures using three matching samples for each test. The normal loads used in the three samples were 100kN/m$^2$ for Sample1, 200kN/m$^2$ for Sample 2 and 300kN/m$^2$ for Sample 3. The test consists of two stages. The first stage was the consolidation of each sample under the specific normal load for the sample for duration of 24h. After the first stage, the samples were sheared at a constant prolonged rate of 0.02mm/min. The slow rate was used to ensure a full dissipation of pore water pressure and complete drainage in the sample. The relations between the normal stress and shear stress were drawn for clay and clay-CDMSs mixtures by passing the best-fit line among the three points for each mixture. The slope of the fit line gives the effective angle of internal friction ($\phi'$), whereas its intersection with the y-axis gives the effective cohesion ($c'$) for this mixture.

(a)

(b)

(c)

**Figure 3.5** Pictures of CDMs size used in oedometer test and direct shear test (a) CBPs, (b) DAPs, and (c) CCPs

### 3.3. 8 Plate load test and apparatus

#### 3.3.8.1 Model of plate load test

Many types of soil research deal with theoretical, experimental, and composite models. Materials used for most empirical models include steel, glass, Plexiglas, and concrete to make box models for soil testing. These models were used as constant or temporary models for multi-purpose soil studies.

This study included the construction of a reinforced cylindrical concrete box in the ground that was used as a container for soil samples during the research. A big reinforced concrete structure (2.0m in diameter by 1.5m in depth) was used. This model was used for plate load tests for clay and clay-10% CDMs mixtures. Before the plate load tests started, a steel frame was installed above the box. Figure 3.6 shows the box and frame used for plate load testing. Walls and a rooftop were constructed for the box to ensure suitable separation from outside conditions.

**Figure 3.6** Box and frame used for plate load test

#### 3.3.8.2 Sample preparation

According to the results of the direct shear tests on the clay-CDMs mixtures, the plan was to carry out the test four times. The first stage was for clay, and the other three tests were mixtures of clay with 10% CBPs, DAPs, and CCPs. The soil used for the plate load test was brought on two trucks from Gaziantep University campus to the laboratory and sieved using a no. 4 sieve to separate the large gravel and rock from the homogeneous soil, as shown in Figure 3.7. The CDMs were sieved using no. 3/4" sieve (19mm), which represent the maximum particles size in the compaction and CBR test. All the clay and CDMs were stored in plastic packs in the laboratory before use in the plate test model, as shown in Figure 3.8.

#### 3.3.8.3 Filling of the box for plate load test

The amounts of clay and CDMs used in each plate load test were determined according to two limits: (1) the predetermined values of maximum dry density and optimum moisture content of the clay-10% CDMs mixtures and (2) the volume of the plate test model. The inner wall of box was 1.5m and was marked by painting each 10cm height (15 marked signs). These signs were considered as an indicator for the thickness of one layer of soil after compaction as shown in Figure 3.9. The first layer was filled with clay and compacted, and it was fixed in all the tests as a base layer for the two cells. After the installation of cell pressure transducers, another clay layer was compacted above the cells and fixed in the entire test as a protection for the pressure cell transducers.

The specific field density used in the plate test model was 90% of the maximum dry density of clay and the clay-10% CDMs mixtures. Due to the swelling potential of clay, the low percentage of field density (less than 95%) was recommended in many soil mechanics literature (Budhu, 2011; Chen, 2012; Das and Sobhan, 2014). Table 3.2 shows the amounts of clay, water, and CDMs used for each plate load test and the method of determination of materials used. The compaction was done in layers. Each layer was 10cm thick after compaction. The CDMs was added to each layer of clay-CDMs mixtures by spreading the dry CDMs with dry clay and mixing before adding the water, as shown in Figure 3.10. Each layer of dry clay or the dry clay-CDMs mixtures was leveled before adding water, as illustrated in Figure 3.11. The water was added homogeneously for each layer, as shown in Figure 3.12. Samples were taken from the mixtures to check the water content and to compare it to the required water content. After adding water, the mixtures (soil, CDMs, and water) were left at a convenient time as to cure until the mixture became homogeneous and ready for compaction, as shown in Figure 3.13. The compaction was done using a heavy concrete roller and a cylindrical concrete hammer connected to a long steel bar, as shown in Figure 3.14. The compaction process was continued until the layers reached 10cm. Figure 3.15 shows the box after it was filled and compacted.

**Figure 3.7** Picture of clay sieving for plate load test


**Figure 3.8** Picture of clay and CDMs sieved and stored for plate load test

**Figure 3.9** Picture of preparing of the box by painting for soil compaction

**Table 3.2** Materials filling calculation for clay and CDMs used in box model for plate load test

| Waste material type | Clay | CBPs | DAPs | CCPs |
|---|---|---|---|---|
| Waste material content (%) | 0 | 10 | 10 | 10 |
| Optimum moisture content (%) | 18.0 | 17.5 | 12.6 | 16.3 |
| Maximum dry unit weight (kN/m³) | 17.30 | 17.21 | 17.92 | 17.70 |
| Total weight of the dry mixture (clay and CDMs) used [a] (kg) | 6172 | 6140 | 6394 | 6315 |
| The weight of dry CDMs used (kg) | 0 | 614 | 639 | 632 |
| The net weight of dry soil used [b] (kg) | 6172 | 5526 | 5754 | 5684 |
| The weight of water used [c] (lt) | 1111 | 1075 | 806 | 1029 |
| The total weight of the moist mixture (soil + CDMs+ water) used [d] (kg) | 7283 | 7215 | 7199 | 7344 |

a= Field density (0.9 * Maximum dry unit weight) * volume filled of box
b= Total weight –CDMs weight (total weight *0.1)
c= Total weight of dry mixture* Optimum moisture content
d= Net weight of dry soil + weight of dry CDMs + weight of water

(a)

(b)

(c)

**Figure 3.10** Mixing of dry CDMs with dry clay for compaction in plate load box (a) CBPs, (b) DAPs, and (c) CCPs

**Figure 3.11** Leveling of dry mixtures layers for compaction in plate load box

**Figure 3.12** Spreading of water for compaction in plate load box

**Figure 3.13** Clay-CDMs mixtures just before compaction in plate load box

(a)

(b)

(c)

**Figure 3.14** Pictures of compaction tools and methods of compaction in plate load box model (a) compaction tools, (b) cylindrical concrete hammer using, (c) heavy concrete roller using

**Figure 3.15** Picture of the box after filling with clay-CDMs mixtures and compaction

### 3.3.8.4 Determination of stress variations in the samples

The total geostatic stresses (overburden pressure), which represents the weight of a column of soil above a point, and the induced stresses, which represent the effect of surface load on the point of soil, were studied on clay and clay-10% CDMs mixtures using plate load tests. The geostatic and induced stress was measured using two pressure cell transducers produced by Encardio-rite Electronics Pvt. Ltd., with a cell diameter of (200mm). The pressure cell transducers capacities were 0.5 and 1.0MPa, and the pressure transducer calibration data is shown in Table 3.3. The pressure cell transducers were installed at the bottom of the box, above one soil layer, and covered by another soil layer with the same thickness. These two layers were considered to be protection for the pressure cell transducers and were not removed for all plate load tests. The first cell transducer was installed at the center of the box and the second was installed at the center of one-quarter of the box, as shown in Figure 3.16. The two pressure cell transducers were connected to a data logger, as shown in Figure 3.17. The multichannel logger, DT2055 (6 channels and 12-bit data), produced by RST Instruments Lts., was used. The data logger used a specific Windows software program supplied by the producer (version1.1.6 with DT2055). It started at the beginning of the first layer filing for the first plate load test and ending with the completion of the final plate load test.

**Table 3.3** Pressure transducer calibration data used in box

| **Pressure transducer capacity 0.5 MPa** | | | | | | |
|---|---|---|---|---|---|---|
| **Input pressure (MPa)** | **Observed value** | | | **Average** | **End point fit (MPa)** | **Polynomial fit (MPa)** |
| | **Up1 (digit)** | **Down (digit)** | **Up2 (digit)** | **(digit)** | | |
| 0.000 | 6403.8 | 6403.5 | 6403.5 | 6403.7 | 0.000 | 0.0001 |
| 0.100 | 6163.1 | 6166.1 | 6163.3 | 6164.7 | 0.099 | 0.0999 |
| 0.200 | 5924.7 | 5924.5 | 5925.0 | 5924.9 | 0.199 | 0.1999 |
| 0.300 | 5682.8 | 5682.8 | 5683.2 | 5683.0 | 0.300 | 0.3005 |
| 0.400 | 5444.2 | 5444.9 | 5444.6 | 5444.4 | 0.399 | 0.3995 |
| 0.500 | 5201.6 | 5201.6 | 5201.5 | 5201.6 | 0.500 | 0.5001 |
| **Pressure transducer capacity 1.0 MPa** | | | | | | |
| 0.000 | 6232.3 | 6233.4 | 6233.4 | 6232.9 | 0.000 | 0.0000 |
| 0.200 | 5924.9 | 5926.6 | 5925.4 | 5925.1 | 0.201 | 0.1999 |
| 0.400 | 5618.1 | 5620.5 | 5617.9 | 5618.0 | 0.403 | 0.4001 |
| 0.600 | 5312.7 | 5315.1 | 5313.1 | 5312.9 | 0.602 | 0.5999 |
| 0.800 | 5008.3 | 5010.1 | 5008.2 | 5008.2 | 0.808 | 0.8001 |
| 1.00 | 4705.3 | 4705.3 | 4705.3 | 4705.3 | 1.000 | 1.0000 |

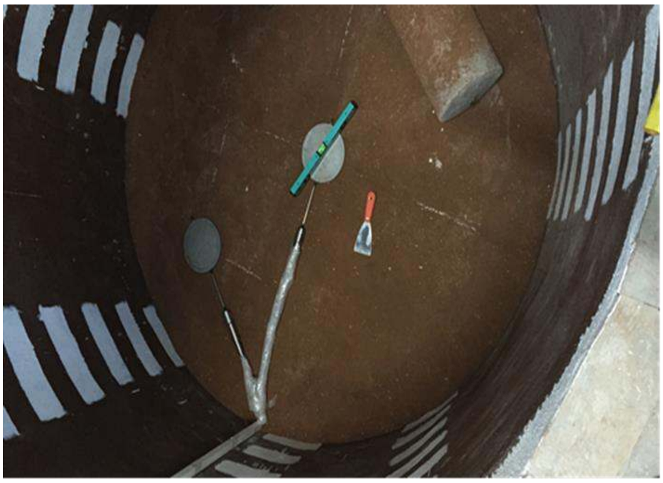

**Figure 3.16** Picture of installation of pressure cell transducers in the bottom of plate load test box

### 3.3.8.5 Plate load test apparatus and procedures

The box model used for the plate load test was used to do four plate load tests, one test of clay and three-test of clay-CDMs mixtures. The filling was compacted into 10cm soil layers. After each filling, one plate load test was done using a new plate load equipment model (UTS- 1200/1201 (200/500kN) from UTEST. Because new plate load equipment was used, calibration was done using a calibrated compression machine before the equipment was used, as shown in Figure 3.17. The tests were done according to ASTM D 1194-1994 specifications. A Schematic view is given in Figure 3.18 for the plate load test setup used in the model with the actual box model and plate load apparatus. All tests were done at the center of the surface of the box, using a bearing plate of 60cm in diameter and three strain gauges set as in the form of fan blades at approximately 120° apart, as shown in Figure 3.19. The load was applied to the soil in cumulative equal increments of no more than 1.0 ton/ft$^2$ (95kPa). The settlement measurements were taken before and after the application of each load increment as soon as possible and at equal time intervals while the load was being held constant. The tests were continued until a well-defined failure load was observed, as shown in Figure 3.20.

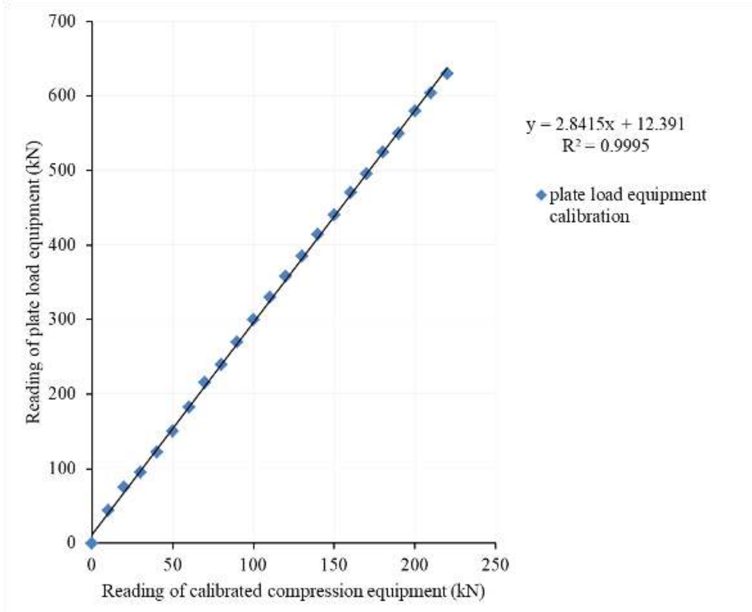


**Figure 3.17** Plate load test equipment calibration

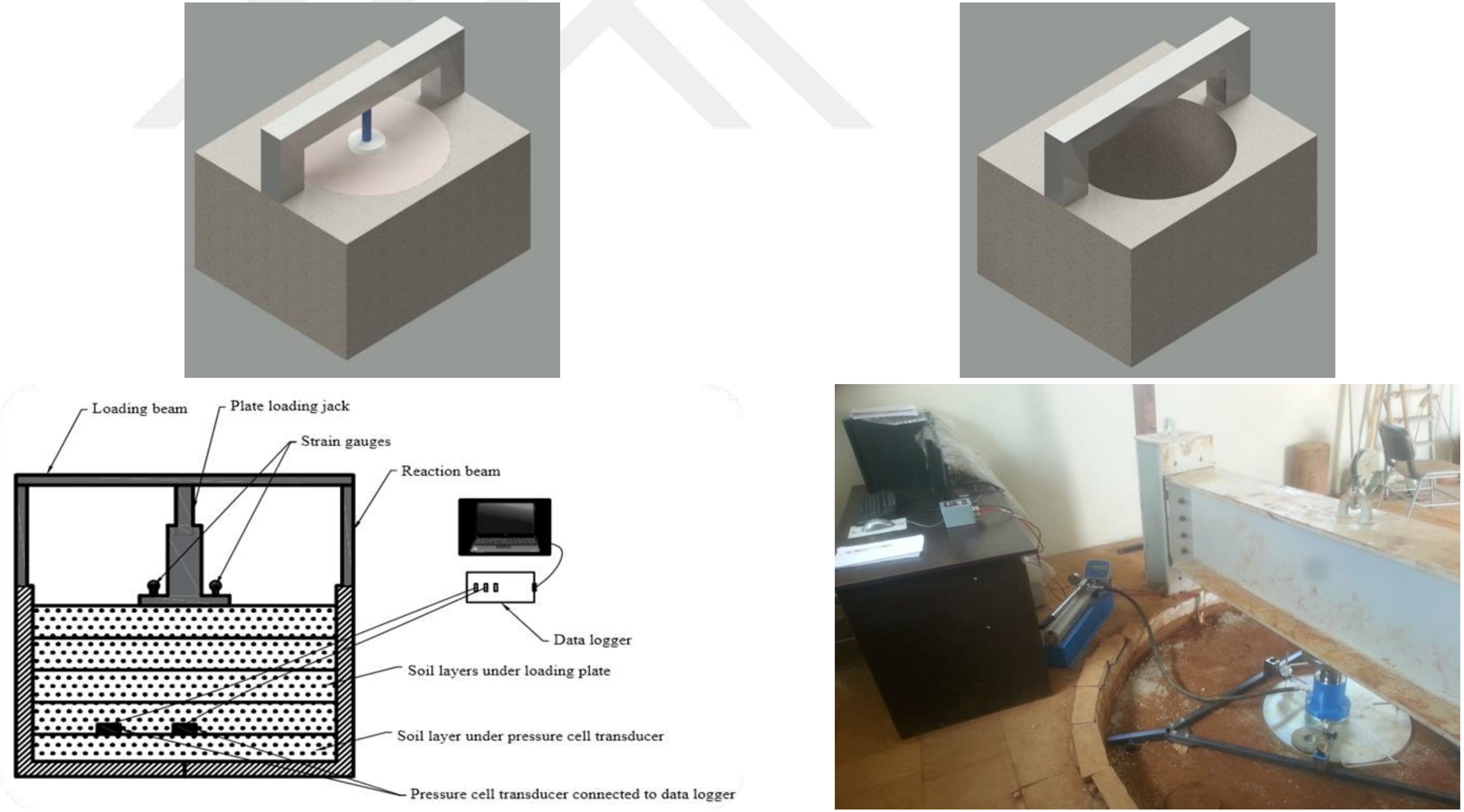


**Figure 3.18** Schematic view of the test setup, loading and sampling system with the actual box model and plate load apparatus

**Figure 3.19** Picture showing the location of the bearing plate and strain gauges used for plate load test

**Figure 3.20** Picture showing the failure at the end of test

# CHAPTER 4

# THEORETICAL STUDY

## 4.1 Theoretical Work Plan

The theoretical work was conducted using the practical results about the clay-CDMs mixtures. This work was done after collecting all the results of the experimental works and presenting them in an appropriate method. The study involved comparing the settlements of footing obtained by plate load tests and the settlements calculated using geotechnical software (Plaxis 2D) for clay and clay-CDMs mixtures. Besides, the ultimate bearing capacities of clay and clay-CDMs mixture were calculated using direct shear tests and plate load tests. The comparison between the two test results was done at the end.

## 4.2 Bearing Capacity Calculations

Two tests were used to obtain the ultimate bearing capacity of clay and clay-CDMs: the direct shear test and the plate load test.

### 4.2.1 Bearing capacity from direct shear test parameters

The shear strength parameters ($c'$ effective cohesion and $\phi'$ the effective angle of internal friction) obtained through the direct shear test, were used to calculate the bearing capacity of clay and clay-CDMs mixtures. Terzaghi's ultimate bearing capacity equation for circular footing, as given in Equation 4.1, was used to determine the bearing capacity of three footing have (0.6, 1.0, and 1.5m) diameter for 1.0m depth.

$$q_u = c' Nc + q N_q + 0.3\gamma B N_\gamma \tag{4.1}$$

Where, $q_u$ is Terzaghi's ultimate bearing capacity, ($N_c$, $N_q$, $N_\gamma$) is Terzaghi's ultimate bearing capacity factors (Das and Sobhan, 2014), $q=\gamma D$, where $\gamma$ is dry density in $kN/m^3$, D is the depth of the footing (m), and B is the diameter of the footing (m).

### 4.2.2 Bearing capacity from plate load test

The ultimate bearing capacity of the clay ($q_u$) was calculating using a plate load test and Equation 4.2, which was given by Das and Sobhan (2014).

$$q_{u\ (footing)} = q_{u\ (plate)} \tag{4.2}$$

## 4.3 Footing Settlement Calculations

Two methods were used to obtain the settlement values of actual footing setting on clay and clay-CDMs. The pressure-settlement curves from the plate load tests and the geotechnical software; (Plaxis 2D) were determined with the comparison between the results.

### 4.3.1 Footing settlement from plate load test

Das and Sobhan (2014) give an approximated equation (4.3) to calculate the footing settlement for clay using a plate load test.

$$S_{e\ (footing)} = S_{e\ (plate)} \left(B_{(footing)} / B_{(plate)}\right) \tag{4.3}$$

Where $B_{(footing)}$ = diameter of footing (m), $B_{(plate)}$ = diameter of plate (m), $S_{e\ (footing)}$ = settlement of footing (mm), $S_{e\ (plate)}$ = settlement of plate (mm), If the $B_{(footing)} = B_{(plate)}$, then $Se_{(footing)} = S_{e\ (plate)}$

In this case, the load-settlement curve from the plate load test will present the actual load-settlement curve for footing with the same diameter bearing plate used in the plate load test.

### 4.3.2 Footing settlement using geotechnical software Plaxis 2D

Geotechnical software (Plaxis 2D) was used to simulate the box model used for the plate load test. The simulation was used to get the pressure-settlement curves for footing with the same diameter bearing plate used in the plate load test. A comparison between the pressure-settlement curves from the plate load test and the load-settlement curve from the simulation in Plaxis 2D is discussed in the results.

#### 4.3.2.1 Soil parameters used in geotechnical software Plaxis 2D

The parameters used for the simulation in Plaxis 2D are shown in Table 4.1. As the table shows, the input parameters were divided into four groups according to the requirements of the Plaxis software. In the first set, the Mohr-Coulomb was chosen as the materials model, as recommended in the Plaxis manual for failure models for most types of soil. The undrained types of materials were selected because they represent the method of applying the loads in plate load test. The second and third groups were taken from the geotechnical properties of clay and clay-CDMs mixtures obtained from laboratory tests. In the fourth group, the $E_{ref}$ (modulus of elasticity) values of clay and clay-CDMs mixtures were estimated using suitable values from the literature review to get the best curve fittings for simulation.

**Table 4.1** Methods of calculations input data parameters used in the Plaxis 2D simulation of box.

| **Soil inputs for Plaxis model** | **Method of inputs computing** |
|---|---|
| Group 1 | Materials set |
| Materials model | Mohr-Coulomb |
| Materials type | Undrained |
| **Group 2** | **General geotechnical properties** |
| $\gamma_{unsat.}$ (unsaturated field density) | $\gamma_{unsat.}$ (unsaturated field density) =0.9* ($\gamma_{dry}$ *(1+o.m.c))<br>$\gamma_{dry}$: from compaction test |
| $\gamma_{sat.}$ (saturated field density) | $\gamma_{sat.}$ (saturated field density) = 0.9*($\gamma_w$(Gs+e)/(1+e))<br>Gs: specific gravity, e: initial void ratio from oedometer test |
| Horizontal permeability m/day | From oedometer test |
| Vertical permeability m/day | From oedometer test |
| **Group 3** | **General geotechnical properties Soil strength** |
| $C_{ref}$ (cohesion) kN/m$^2$ | From direct shear test |
| ffective angle of internal friction ($\phi'$) | From direct shear test |
| $\Psi$ (psi) | $\Psi$ (psi)=0.0 for $\phi' \leq 30$, and $\Psi$ (psi)=$\phi'$-30.0 for $\phi' \geq 30$ (Brinkgreve, 2002) |
| **Group 4** | **Soil stiffness** |
| $\nu$ (Poisson's ratio) | $\nu = k_o/(1+k_o)$ from elastic theory, $k_o = 1-\sin\phi'$ (Jaky,1944) |
| $E_{ref}$ (modulus of elasticity) kN/m$^2$ | suitable values from the literature review |

#### 4.3.2.2 Modulus of elasticity (E) estimation

The modulus of elasticity (E) or Young's modulus of soil is one of the input stiffness parameters required for the box simulation using Plaxis 2D. The estimation of the modulus of elasticity (E) in the laboratory required a series of specified tests, like the triaxial test, which demands large amounts of effort and time. Also, some empirical equations to estimate soil stiffness for different types of soil were given by many researchers (Hardin and Black, 1968; Marcuson and Wahls, 1972; Shibuya and Tanaka, 1996; Shibuya et al., 1997). Most of the empirical equations were adopted for a specific type of soil and depend on one of following tests: resonant column test, triaxial test, torsional shear test, bender element test, or seismic cone test. Hoque and Tatsuoka (1998) illustrated that the small strain Young's modulus $E_i$ in the i direction (e.g., vertical or horizontal) is a function of the effective stress in the coaxial direction (i direction) only. The increase in Young's modulus with stress in the coaxial direction is shown in Figure 4.1a, and no change in the modulus with the increase of stress in the orthogonal direction is shown in Figure 4.1b.

In light of the available data, the value of the modulus of elasticity (E) was estimated in the calculation at a reasonable value on the basis of experience and a review of the literature. Then the E values were chosen to obtain the best matching between the simulation of the pressure-settlement curve from Plaxis 2D and the actual pressure-settlement curve from the plate load test. For the estimation of E values, the (1.5m) depth of soil in the box model was divided into three equal parts (0.5m each part), and the average E values were used for each part. The E values were increased linearly with the depth increase for each part, as shown in Figure 4.2.

#### 4.3.2.3 Plaxis 2D model of plate load test box

The Plaxis 2D model used to simulate the cylindrical concrete box used in the plate load test is shown in Figure 4.3. Because the model was symmetrical in the vertical direction, the general model used in the simulation was asymmetrical, as illustrated in Figure 4.3(b), instead of the original box, which is shown in Figure 4.3(a). The model shown in Figure 4.3 was used for clay and clay-CDMs mixture, with input parameters as demonstrated in Table 4.1. After the program calculations had been done, the output was given as after loading failure shape, Figure 4.3(c) and 4.3(d), and load-settlement curves.

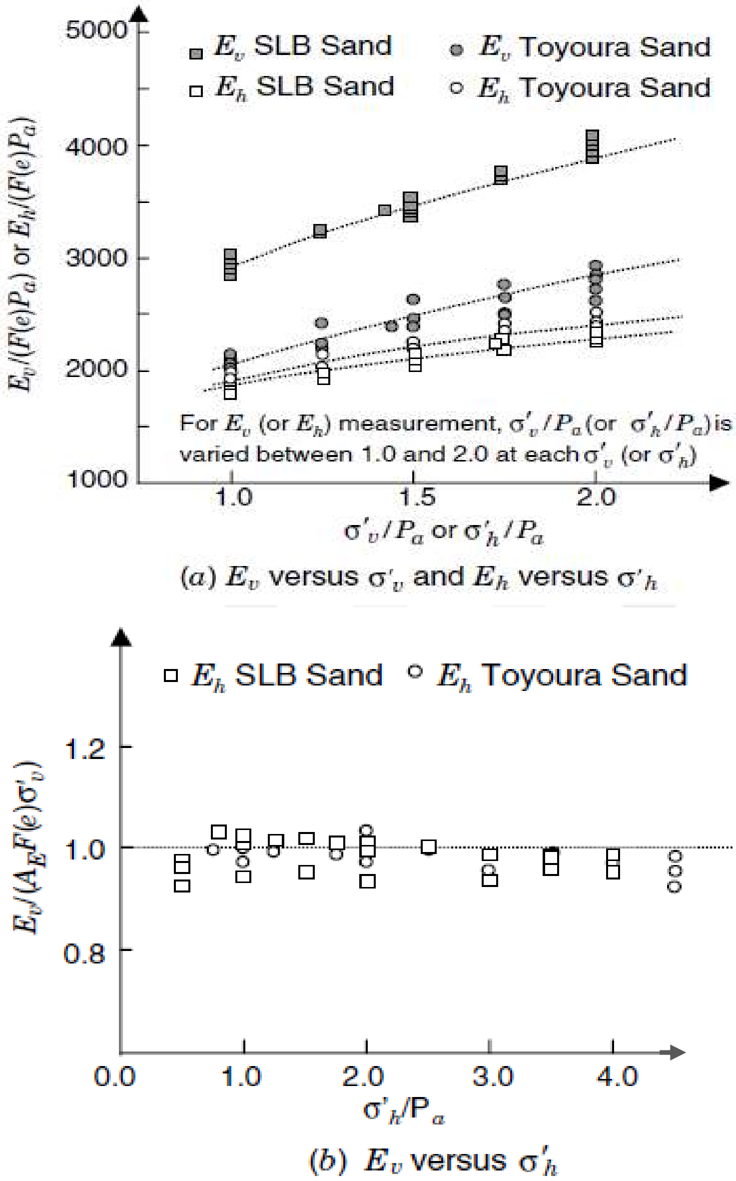


**Figure 4.1** Vertical and horizontal Young's modulus as a function of anisotropic stresses for Toyoura sand (Hoque and Tatsuoka, 1998)

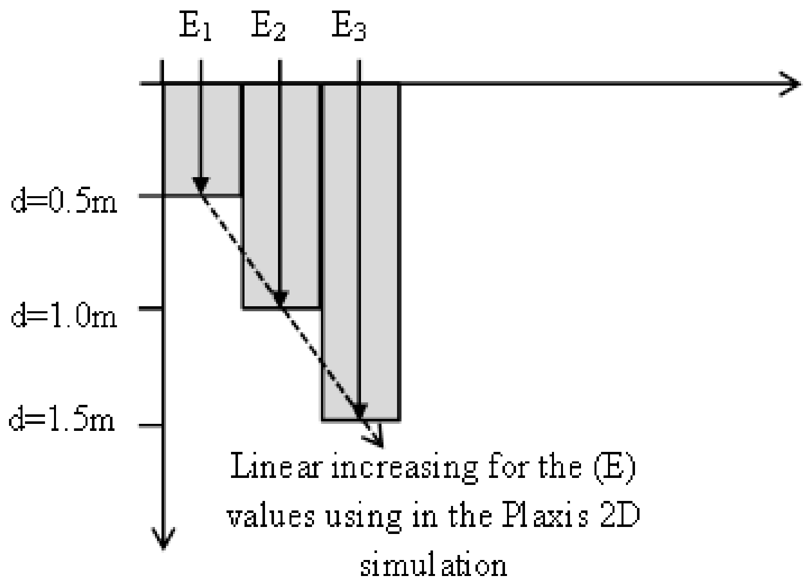


**Figure 4.2** Schematics view of the box model and the (E) values using in the Plaxis 2D simulation for the pressure-settlement curve in the plate load test

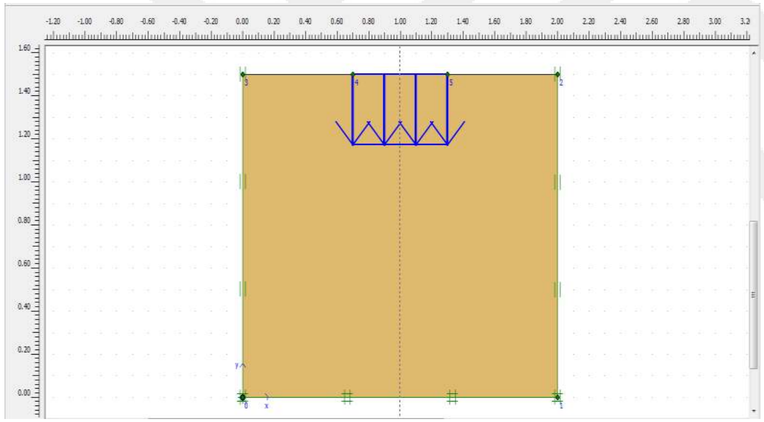

(a) Symmetrical cylindrical box model for plate load test

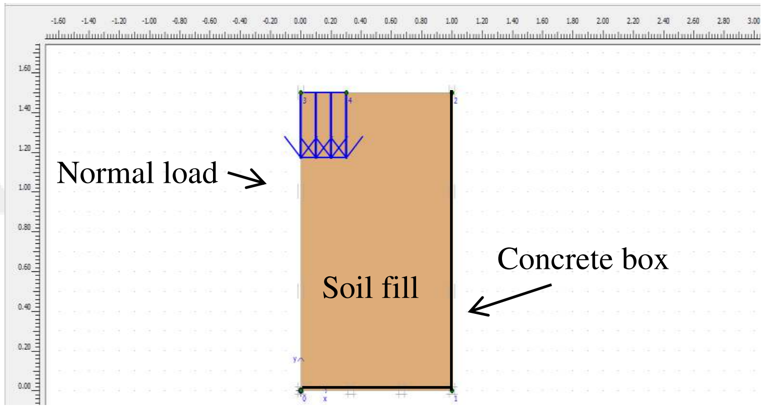


(b) Plate load test box model used in Plaxis 2D

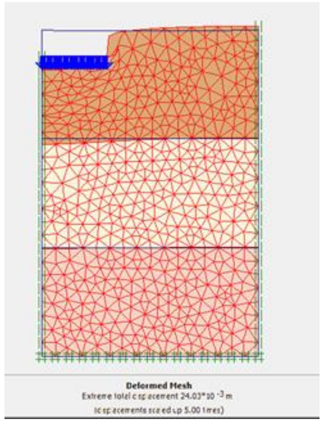


(c) Deform mesh after loading for plate load test box model

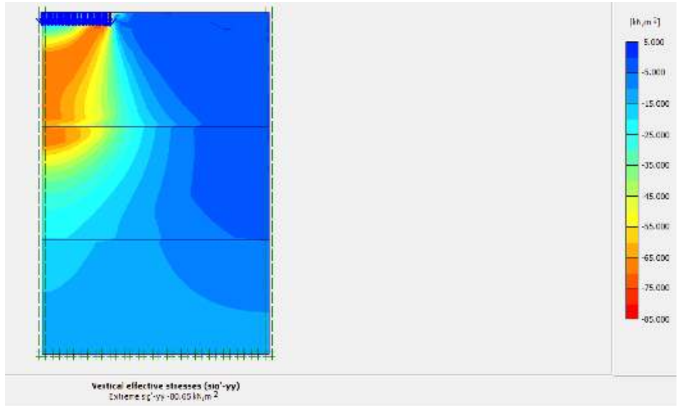


(d) Vertical effective stresses after loading for plate load test box

**Figure 4.3** Model used in Plaxis 2D simulation of plate load test box of clay and clay-CDMs mixtures

# CHAPTER 5

# RESULTS AND DISCUSSION

This study deals with the effects of CDMs on the main problems in the clay, high plasticity, consolidation, swelling, and low strength, especially when water content changes. Although there are many studies about the proper treatment of CDMs in geotechnical and pavement applications as aggregates, there are little-known efforts to explore the effects of these materials on the clay and the possibility of stabilizing clay with these materials. The results were divided into two parts, the experimental results of the plate load tests using the box model and the theoretical results of Plaxis 2D simulation.

## 5.1 Experimental Results

### 5.1.1 Scanning electron micrograph pictures and energy dispersive x-ray

Figure 5.1 gives the surface morphology of clay, CBPs, DAPs, and CCPs, as obtained by SEM. It was observed that the surface morphology of CBPs is similar to that of clay, which has a solid or dense surface. The resource material of the bricks is known to be clay. The surface morphologies of DAPs and CCPs are more porous than those of clay or CBPs. The porous structure causes high absorption in these waste materials. Zhu et al., (2012) was observed that the surface morphology of CBPs and CCPs was porous, and the porous structure causes high absorption which indicates the same results.

Figure 5.2 and Table 5.1 give the dispersive energy X-Ray analysis for clay and the three CDMs. The significant concentration of Si and Al with the O element in the clay and CBPs shows the similarities between these compound materials. The high concentration of C in the analysis of DAPs gives an indication about the organic nature of this material. Ca and O had the highest concentrations in the analysis of the CCP because of the presence of CaO, which is the elementary portion of the cement material in the crushed concrete.

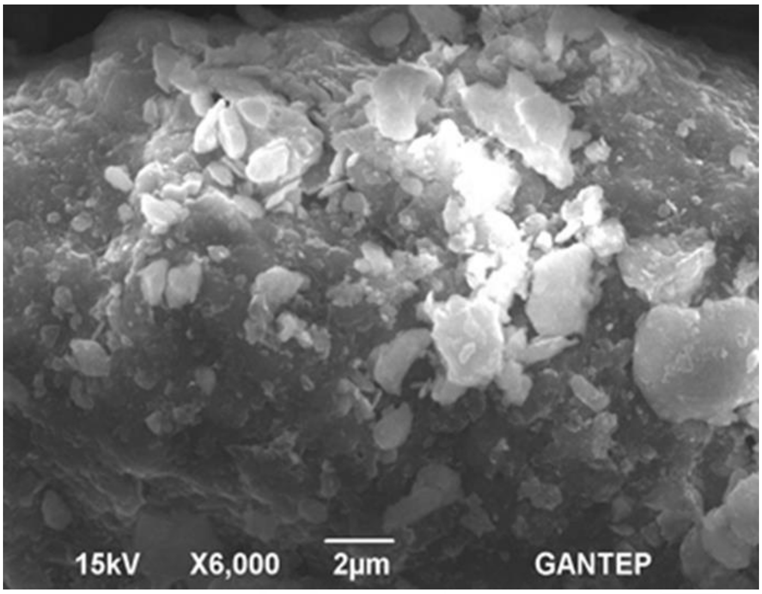


(a)

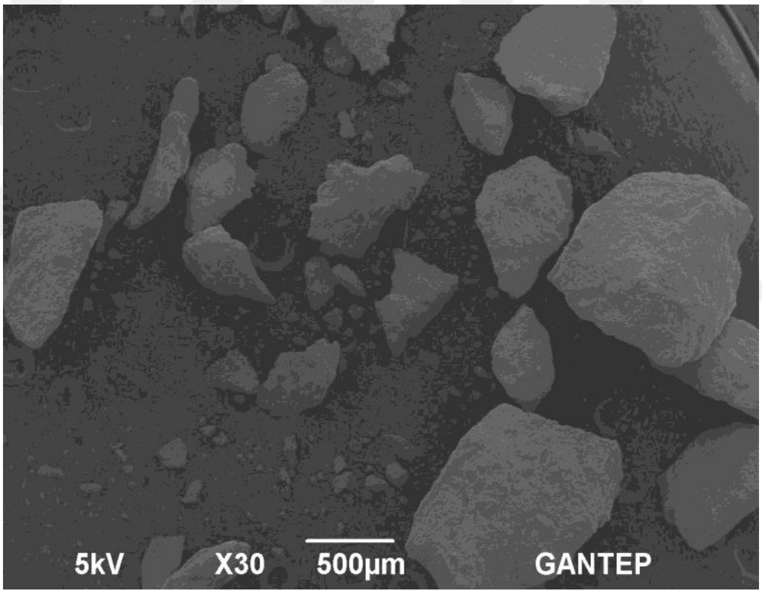


(b)

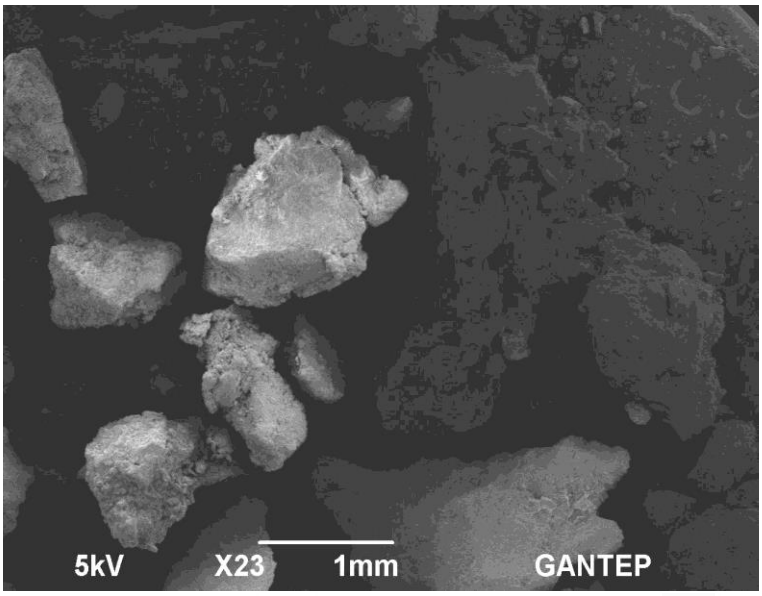


(c)

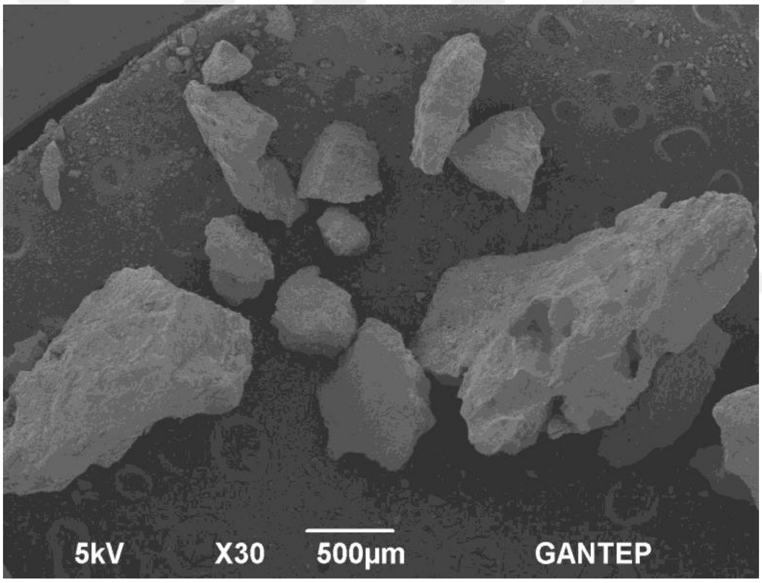


(d)

**Figure 5.1** SEM pictures for (a) clay (b) CBPs, (c) DAPs, and (d) CCPs.

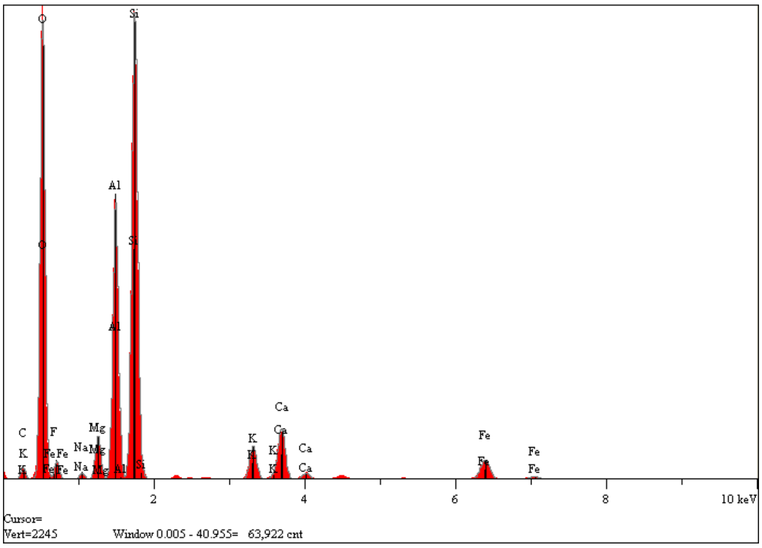
O
Si
Al
C
K
F
Fe
Na
Mg
Ca
2
4
6
8
10 keV
Cursor=
Vert=2245
Window 0.005 - 40.955= 63,922 cnt

(a)

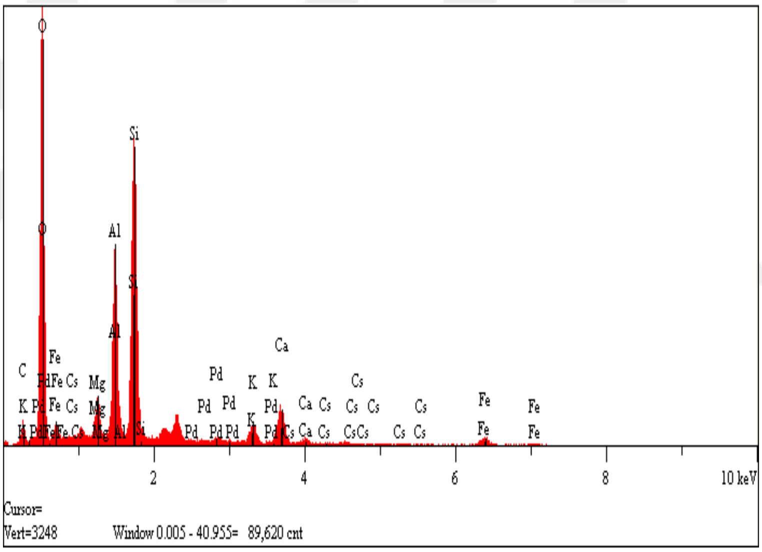
O
Si
Al
C
K
Pd
Fe
Cs
Mg
Ca
2
4
6
8
10 keV
Cursor=
Vert=3248
Window 0.005 - 40.955= 89,620 cnt

(b)

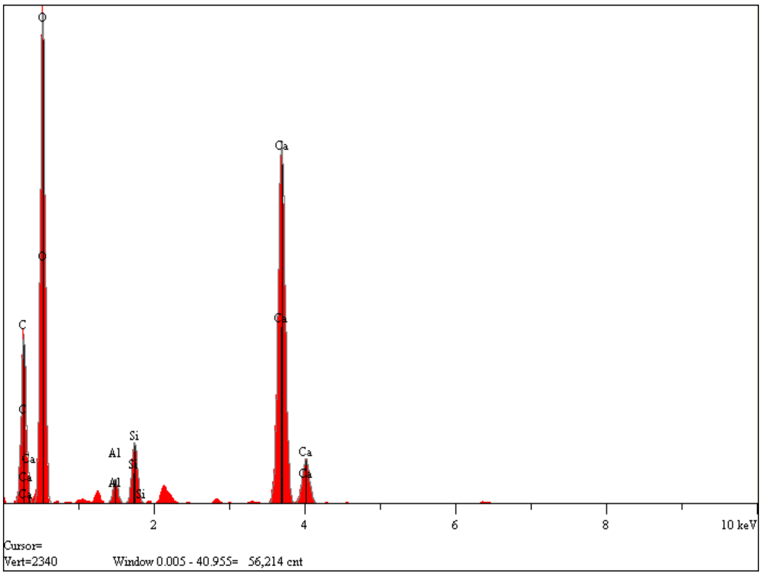


(c)

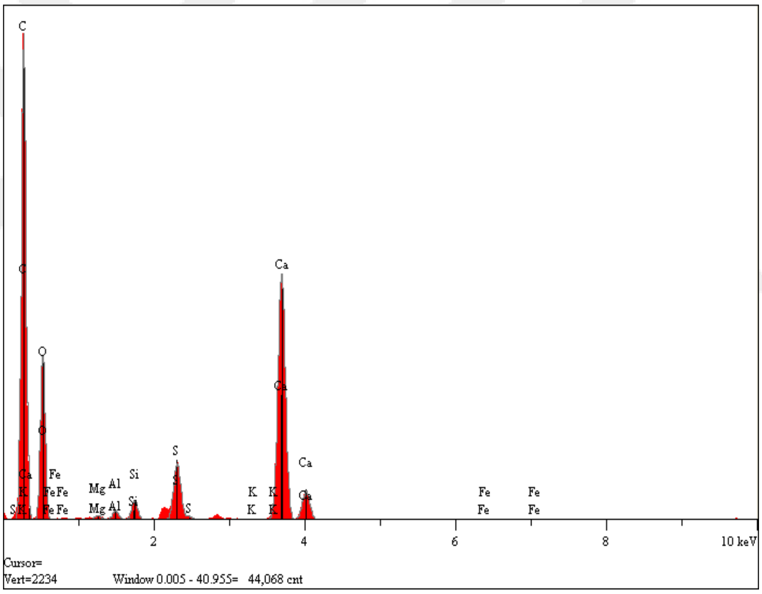


(d)

**Figure 5.2** Pictures of EDX analysis (a) clay (b) CBPs, (c) DAPs, and (d) CCPs

**Table 5.1** The EDX analysis for clay and CDMs

| | | Materials used in the study | | | |
|---|---|---|---|---|---|
| | | Clay | CBPs | DAPs | CCPs |
| Element | Unit | Concentration | Concentration | Concentration | Concentration |
| C | wt.% | 8.371 | 3.806 | 45.080 | 15.429 |
| O | wt.% | 54.308 | 46.599 | 32.036 | 59.233 |
| Al | wt.% | 11.292 | 12.706 | 0.434 | 0.930 |
| Si | wt.% | 19.677 | 23.189 | 0.811 | 2.268 |
| Ca | wt.% | 1.162 | 3.994 | 18.127 | 22.140 |
| Na | wt.% | 0.083 | 0.380 | --- | --- |
| Mg | wt.% | 1.014 | 2.127 | 0.279 | --- |
| K | wt.% | 1.038 | 2.418 | 0.058 | --- |
| Fe | wt.% | 3.055 | 4.782 | 0.262 | --- |
| S | wt.% | --- | --- | 2.913 | --- |
| | | Total =100.0 | Total =100.0 | Total =100.0 | Total =100.0 |

### 5.1.2 Consistency limits and classification

Table 5.2 presents the consistency limits (Atterberg limits) for clay and all the mixtures of clay and CDMs. Figure 5.3 illustrates the relation between the percentages of CBPs and the consistency limits. From the data in Figure 5.3 and Table 5.2, it is apparent that there are decreases in liquid limits with increases in plastic limits as the CBPs percentage increase in general. As a result, the PI decreased. Figure 5.4 shows the relationships between the percentages of DAPs and consistency limits. The reduction in all limits was noticeable as the DAPs percentage increased. Figure 5.5 shows the relationship between the CCPs percentages and the consistency limits. In this figure, a similar behavior of CBPs plasticity can be noticed. Generally, all CDMs produced decreases in liquid limits and PI. The plastic limits were increased except in relation to DAPs. This reduction in consistency limits can be explained by the addition of the fractions of CDMs for the Atterberg limit test (i.e. Particles smaller than 0.425 mm). These additives are like gravel or sand in nature and are considered to be non-plastic materials. However, the DAPs, which have a notable percentage of bituminous content, have some plasticity effects on the consistency limits, particularly the plastic limit. Also, the DAPs have some organic content. Table 5.2 also shows the classification according to the USCS of clay and CDMs mixtures. Because of the general reduction in liquid limits and PI of clay-CDMs mixtures, the geotechnical behavior of clay, with small to medium plasticity CL, changed to the behavior of silt with low plasticity ML. The case of DAPs mixtures did not show this behavior. Figure 5.6(a–c) gives a comparison of grain size distribution for clay, pure CDMs, and clay-CDMs mixtures. This data was used with Atterberg limit values to classify clay, pure CDMs, and clay-CDMs mixtures according to the American association of state highway and transportation officials (AASHTO) classification system. According to the AASHTO, Table 5.2 shows that the clay used in this study is classified as A-7-6. However, pure CDMs are classified as A-1-a. The clay-CDMs mixtures were classified as A-6. This change is the due to the physical replacement of a fraction of the fine clay with the CDMs and the geotechnical change in clay properties.

**Table 5.2** Consistency limits and classification for clay and clay-CDMs mixtures

| Mixtures type | CDMs content (%) | Liquid limit | Plastic limit | Plasticity index | Classification USCS | Classification AASHTO |
|---|---|---|---|---|---|---|
| Clay | 0 | 42.50 | 24.50 | 18.00 | CL | A-7-6 |
| CBP [a] | 5 | 38.50 | 25.50 | 13.00 | ML | A-6 |
| CBP | 10 | 39.00 | 27.00 | 12.00 | ML | A-6 |
| CBP | 15 | 38.50 | 27.00 | 11.50 | ML | A-6 |
| CBP | 20 | 38.00 | 25.50 | 12.50 | ML | A-6 |
| CBP | 100 | - | - | N. P | - | A-1-a |
| DAP [b] | 5 | 37.25 | 23.25 | 14.00 | CL | A-6 |
| DAP | 10 | 36.50 | 22.50 | 14.00 | CL | A-6 |
| DAP | 15 | 35.00 | 22.00 | 13.00 | CL | A-6 |
| DAP | 20 | 33.75 | 22.25 | 11.50 | CL | A-6 |
| DAP | 100 | - | - | N. P | - | A-1-a |
| CCP [c] | 5 | 38.00 | 26.50 | 11.50 | ML | A-6 |
| CCP | 10 | 37.50 | 27.00 | 10.50 | ML | A-6 |
| CCP | 15 | 36.75 | 25.00 | 11.75 | ML | A-6 |
| CCP | 20 | 36.75 | 26.00 | 10.75 | ML | A-6 |
| CCP | 100 | - | - | N. P | - | A-1-a |

a: Crushed bricks pieces (CBPs) b: Dumped asphalt pieces (DAPs) C: Crushed concrete pieces (CCPs)

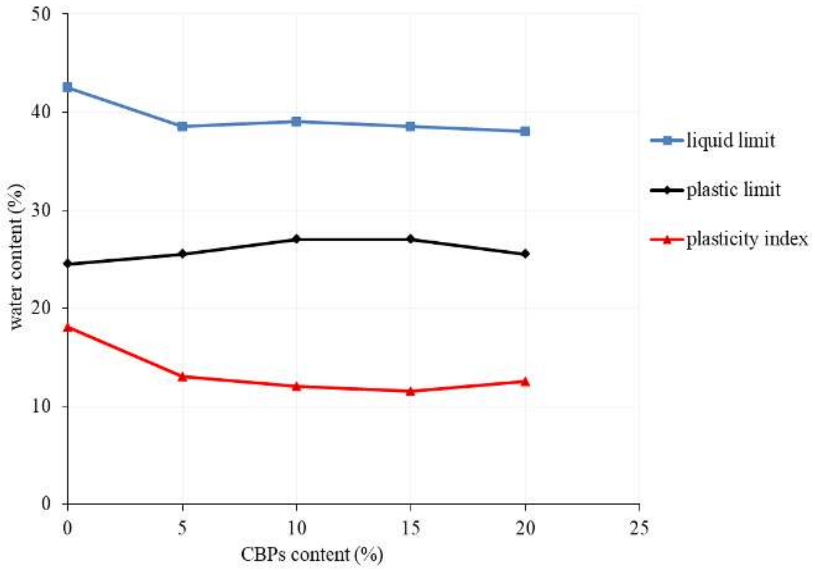


**Figure 5.3** Relationships between consistency limits and CBPs content

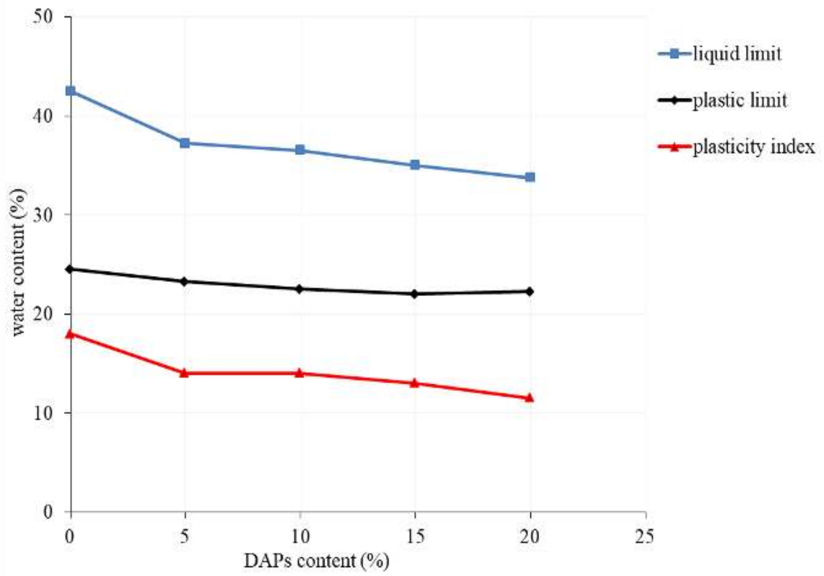


**Figure 5.4** Relationships between consistency limits and DAPs content

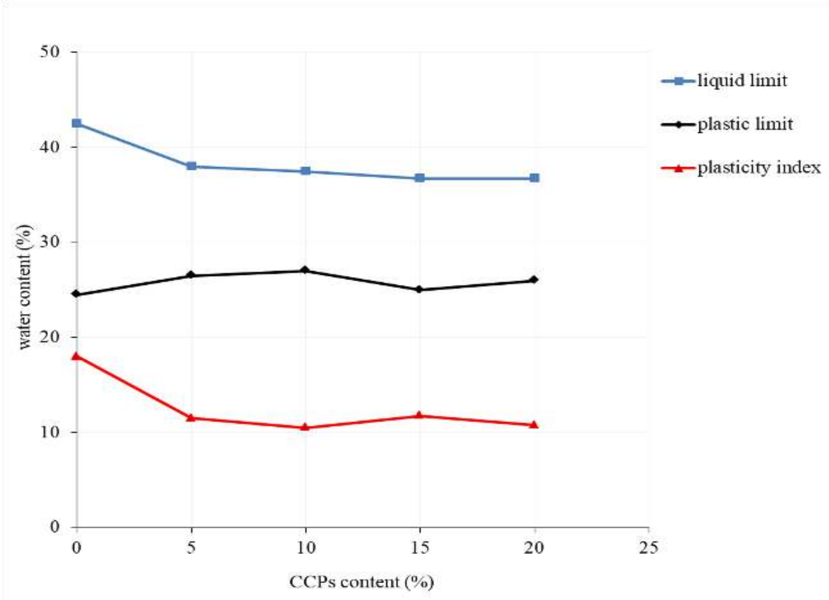


**Figure 5.5** Relationships between consistency limits and CCPs content

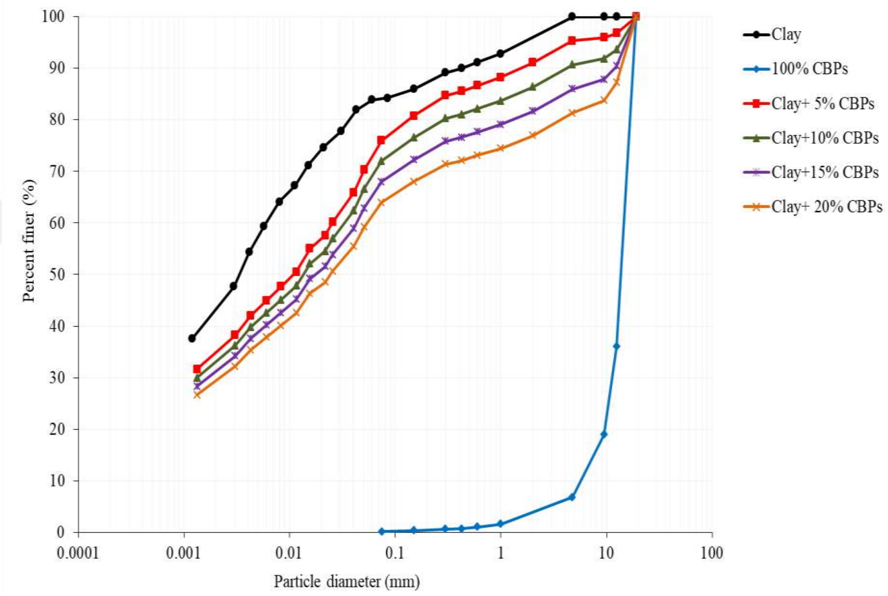


(a)

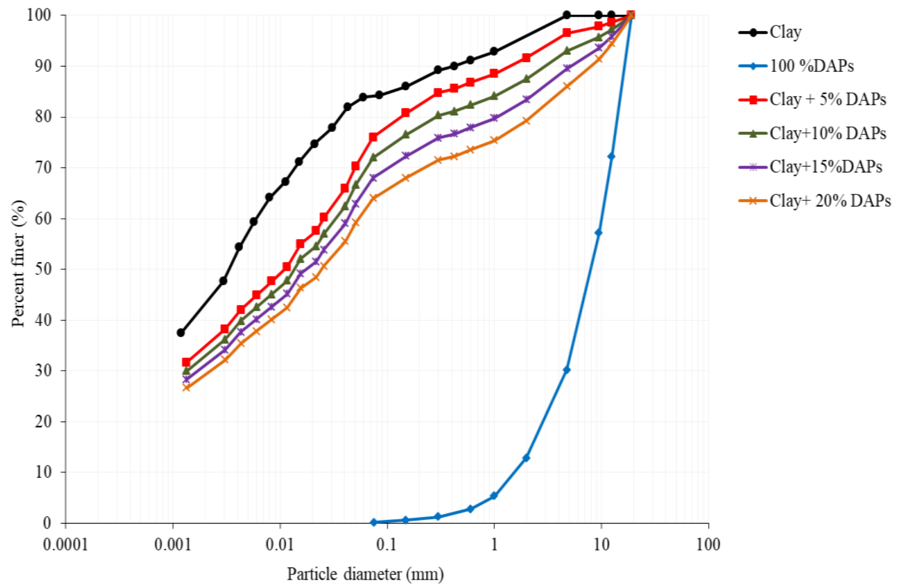


(b)

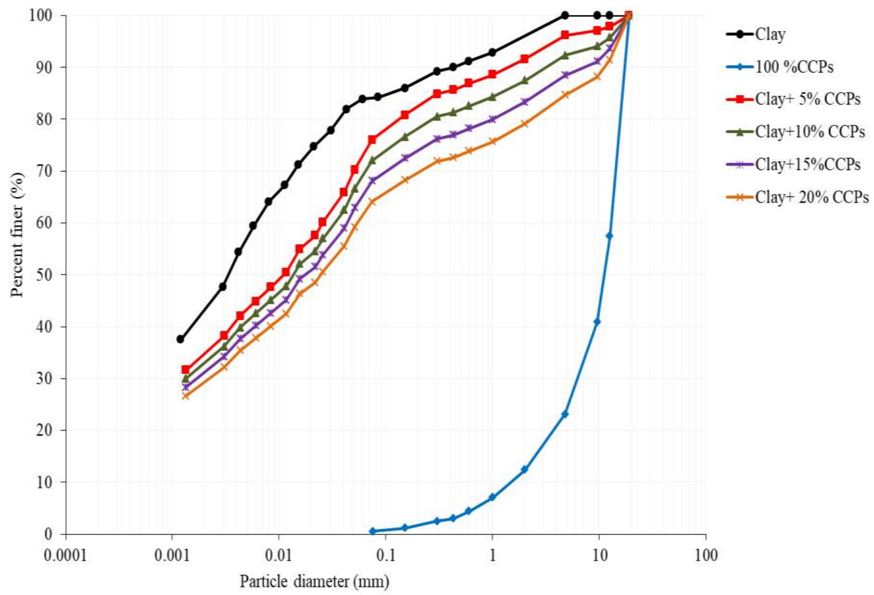


(c)

**Figure 5.6** The variation of the grain size distribution curves with the addition of the (a) CBPs, (b) DAPs, and (c) CCPs

### 5.1.3 Effects of construction and demolition materials on the strength of soil

#### 5.1.3.1 California bearing ratio test results

Table 5.3 gives a summary of the CBR experimental results reported here. The optimum water content values of the specimens decrease with increases in CDMs content. Specimens with CBPs only and CCPs had a much higher maximum value of CBR values than those with DAPs only.

Figure 5.7 shows the variation of dry unit weight (kN/m$^3$) and CBR value (percentage) as a function of water content (percentage) for the clay mixed with crushed brick particles at different contents (0%, 5%, 10%, 15%, 20%, and 100%). Decreases in maximum dry unit weight ($\gamma_{drymax}$) and optimum water content ($w_{opt}$) can be seen as the number of CBPs increases. This decreasing presumably occurs because the CBPs have a less value of specific gravity (Gs = 2.403) than the clay grains (2.7). It is also apparent that the clay grains have much greater water absorption capacity than CBPs. In addition, an increase in the maximum CBR values is seen as the amount of crushed brick particles increases in the mixture. These features suggest that a higher frictional resistance of the specimens reduces the penetration of the CBR piston, perhaps because of interlocking created by an increase in the amount of crushed brick particles in the specimens. These results are consistent with the results presented by Melton et al., (2012).

Figures 5.8 and 5.9 indicate the variation of dry unit weight (top) and CBR values (bottom) as a function of water content for the CDMs-clay mixtures (i.e., DAPs and CCPs) at various ratios (0%, 5%, 10%, 15%, 20%, and 100%). AS the percentages of the CDMs in the specimens were increased, the $\gamma_{drymax}$ increased while the $w_{opt}$ decreased. The dry unit weight and Gs values of the CDMs only were higher than those of the clay only. Therefore, the dry unit weight of the mixture increased. Replacing the clay with CDMs decreases $w_{opt}$ values of the specimens because the water absorption capacity of the DAPs and crushed concrete paving slab aggregates is less than that of the clay. A similar behavior was observed by Cabalar et al., (2014) and Cabalar and Karabash (2015). It is also realized that a certain amount of the CDMs mixed with clay results in a higher $\gamma_{drymax}$ than the clay alone and the CDMs alone. These percentages may be considered as the best mix ratios for each specimen.

It was also observed that the CBR performance of the mixtures increased as the amount of DAPs and crushed concrete paving slab aggregates increased. It is believed that the CDMs inclusions in the soil change the soil fabric and structure. In particular, such variations in the soil structure may affect the strength and stiffness of the soil (Burland, 1990). Decreases in the $\gamma_{drymax}$ values were observed as the amounts of CBPs increased. On the contrary, the $\gamma_{drymax}$ values in the clay-DAPs and clay-CCPs aggregates increased as the CDMs percentages were increased in the mixture. In general, the CBR values for all the clay-CDMs mixtures increase as the amount of waste in each specimen increases. Evidently, the CBR values of specimens with CDMs only have the maximum performance (Figures 5.10-5.12).

The thickness of sub-base pavement is controlled by the CBR value of subgrade soils. Figure 5.13 and 5.14 show the sub-base thickness capping design details. The thickness of the sub-base is 150mm for a subgrade with a CBR value higher than 15%. However, there are two options for subgrades with a CBR value between 2.5% and 15%: (1) 150mm thickness of sub-base with a different capping thickness and (2) a greater thickness of sub-base with no capping (Highway Agency, 1994). In the light of Figure 5.13 and Figure 5.14, the capping and sub-base thicknesses of each sand-clay mixture that depend on the CBR values are listed in Table 5.3.

Figures 5.15 to 5.18 present the variation of swelling percentages as a function of water content for the clay mixed with different CDMs at various contents. The swelling percentage of the clay only at $w_{opt}$ was found to be about 2.5%, and it was decreased by the addition of any waste material, except the DAPs materials, which diminished the swelling percentage at the end. It is postulated that this observed behavior could be due to low water absorption ability of the waste materials. A comparison of the results reveal that the swelling percentage of the clay with crushed concrete paving slab aggregates had a trend of decreasing much more sharply than the clay with other CDMs. The swelling percentages of the clay with dumped asphalt had a tendency to increase. This situation could be because of the high elastic properties of the dumped asphalt aggregates. It is also clearly seen that the swelling percentages decrease as the water content used for compaction increased

**Table 5.3** CBR and UCS test results with pavement thickness design alternative

| Mixtures type | CDMs (%) | Optimum moisture content (%) | Maximum dry unit weight ($kN/m^3$) | Maximum CBR value (%) | UCS at the OMC ($kN/m^2$) | Swelling percent at the OMC (%) | Pavement thickness design alternative by Highways Agency | | |
|---|---|---|---|---|---|---|---|---|---|
| | | | | | | | 1 | | 2 |
| | | | | | | | Sub- | Capping | Sub- |
| Clay | 0 | 18.0 | 17.30 | 4.50 | 494 | 2.5 | 150 | 300 | 260 |
| CBPs | 5 | 18.2 | 17.25 | 5.00 | 515 | 2.35 | 150 | 250 | 210 |
| CBPs | 10 | 17.5 | 17.21 | 6.00 | 530 | 1.63 | 150 | 245 | 205 |
| CBPs | 15 | 17.6 | 17.22 | 6.50 | 542 | 1.02 | 150 | 240 | 205 |
| CBPs | 20 | 17.1 | 17.10 | 7.10 | 574 | 0.17 | 150 | 235 | 200 |
| CBPs | 100 | 9.1 | 13.80 | 31.50 | --- | 0 | 150 | 150 | 150 |
| DAPs | 5 | 13.5 | 17.58 | 4.90 | 495 | 3.01 | 150 | 250 | 210 |
| DAPs | 10 | 12.6 | 17.92 | 5.10 | 560 | 2.41 | 150 | 250 | 210 |
| DAPs | 15 | 12.0 | 18.00 | 5.20 | 595 | 1.75 | 150 | 250 | 210 |
| DAPs | 20 | 11.6 | 18.26 | 5.10 | 615 | 1.32 | 150 | 250 | 250 |
| DAPs | 100 | 6.5 | 17.85 | 9.80 | --- | 0 | 150 | 180 | 180 |
| CCPs | 5 | 16.6 | 17.30 | 5.50 | 615 | 1.75 | 150 | 250 | 210 |
| CCPs | 10 | 16.3 | 17.70 | 6.20 | 620 | 1.15 | 150 | 245 | 205 |
| CCPs | 15 | 15.8 | 17.80 | 6.30 | 630 | 0.65 | 150 | 245 | 205 |
| CCPs | 20 | 15.2 | 17.93 | 6.50 | 640 | 0.58 | 150 | 240 | 205 |
| CCPs | 100 | 7.0 | 17.63 | 33.93 | --- | 0 | 150 | 150 | 150 |

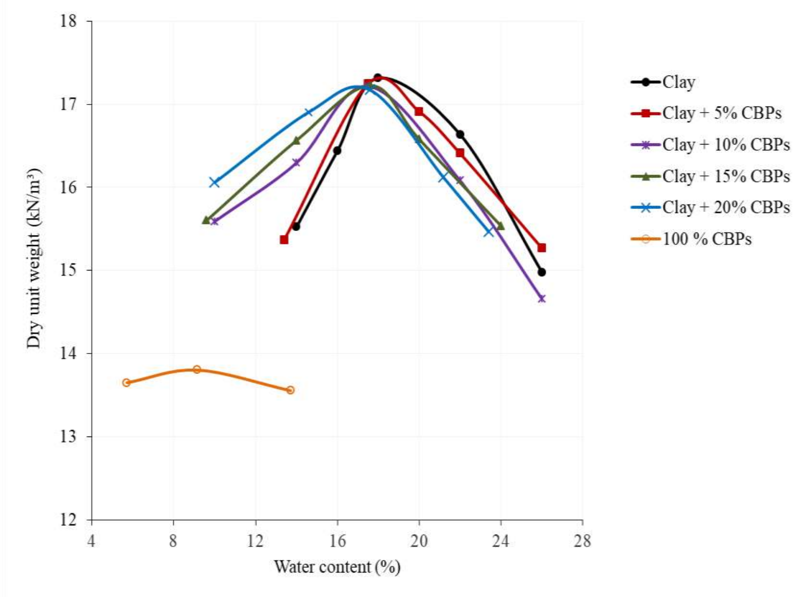


(a)

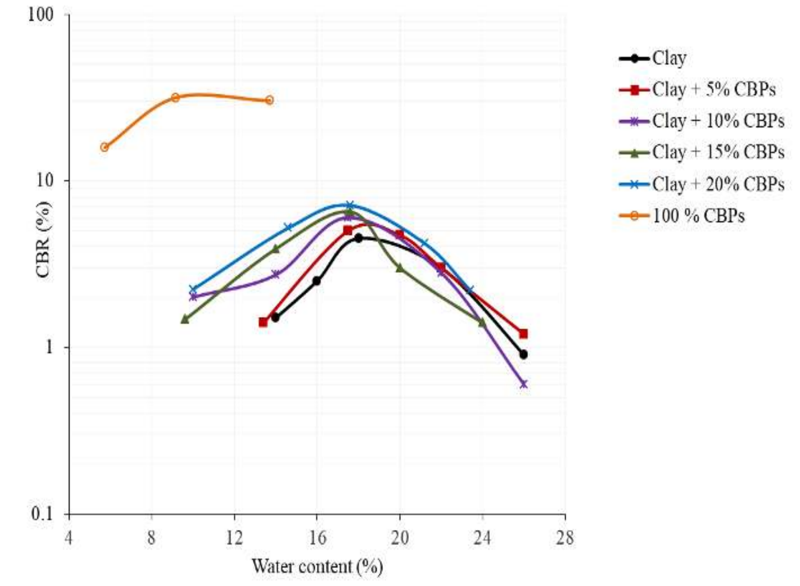


(b)

**Figure 5.7** Variation of dry unit weight (a) and CBR value (b) as a function of water content for the clay mixed with crushed bricks pieces (CBPs)

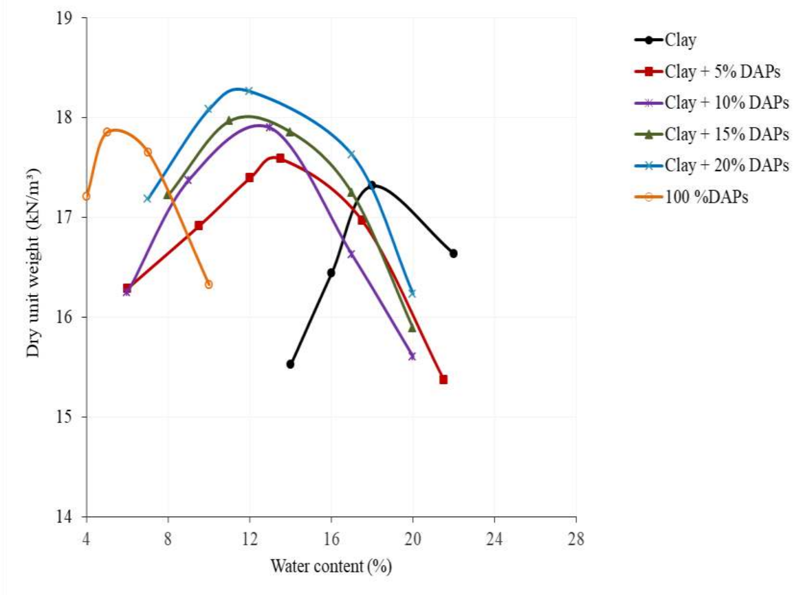


(a)

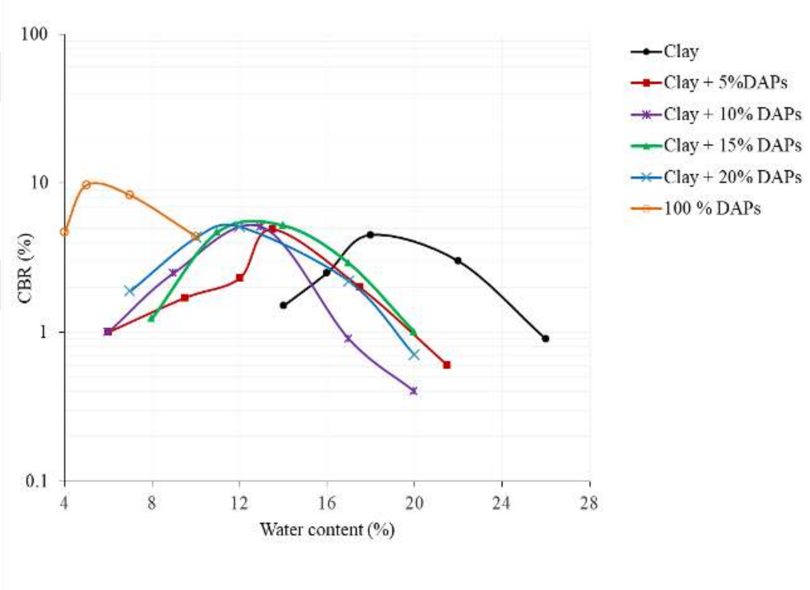


(b)

**Figure 5.8** Variation of dry unit weight (a) and CBR value (b) as a function of water content for the clay mixed with dumped asphalt pieces (DAPs)

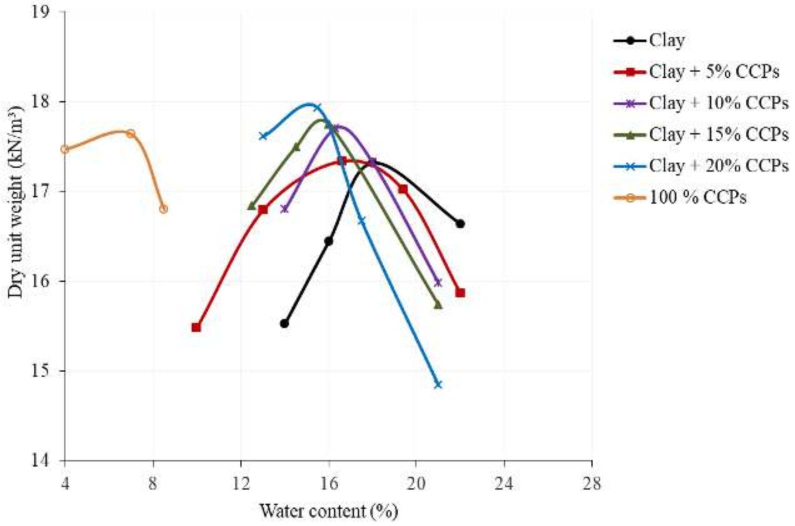


(a)

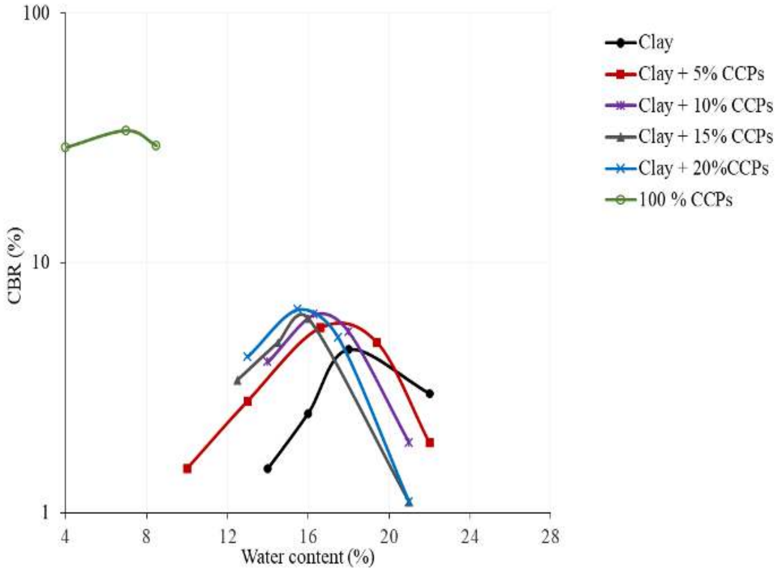


(b)

**Figure 5.9** Variation of dry unit weight (a) and CBR value (b) as a function of water content for the clay mixed with crushed concrete pieces (CCPs)

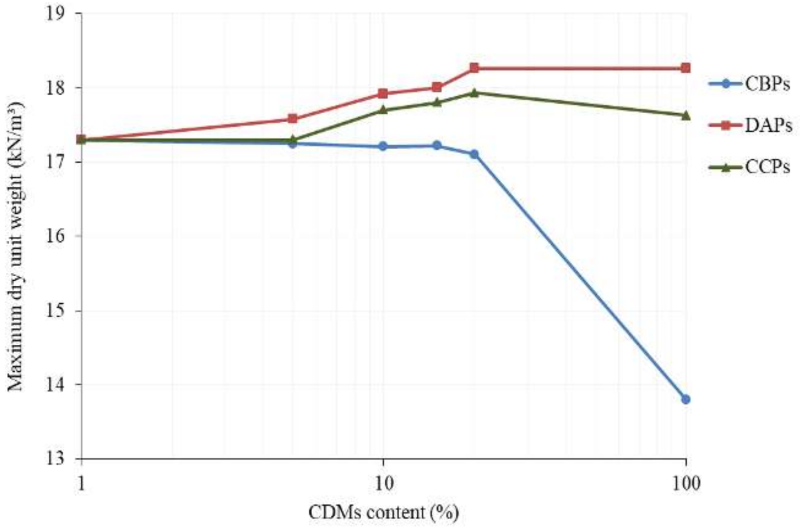


**Figure 5.10** Variation of the $\gamma_{drymax}$ with the CDMs content

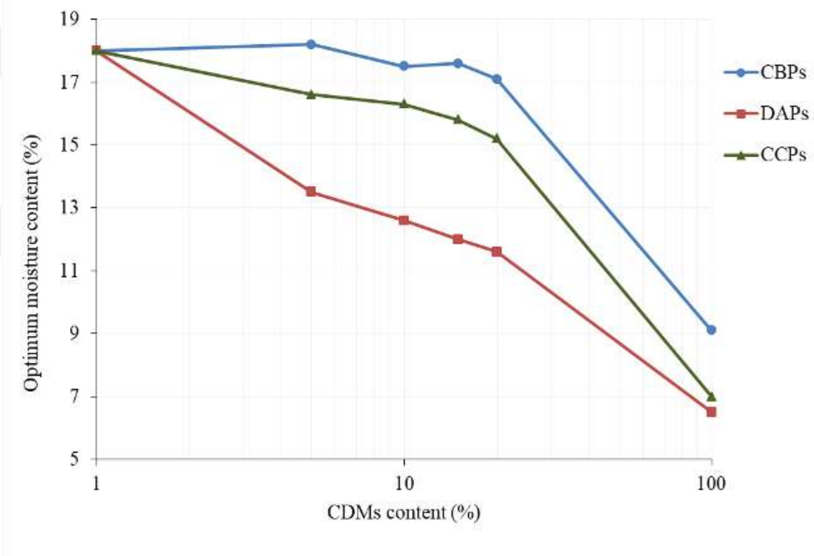


**Figure 5.11** Variation of the $w_{opt}$ with the CDMs content

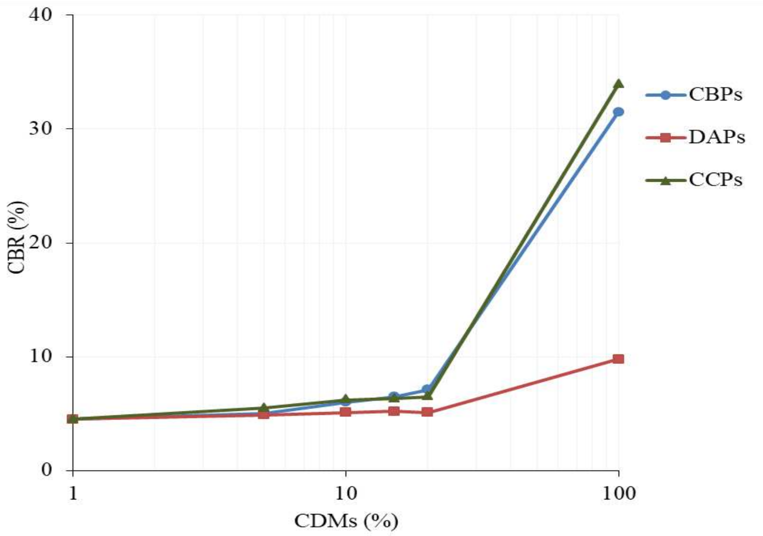


**Figure 5.12** Variations of the CBR values with the CDMs content

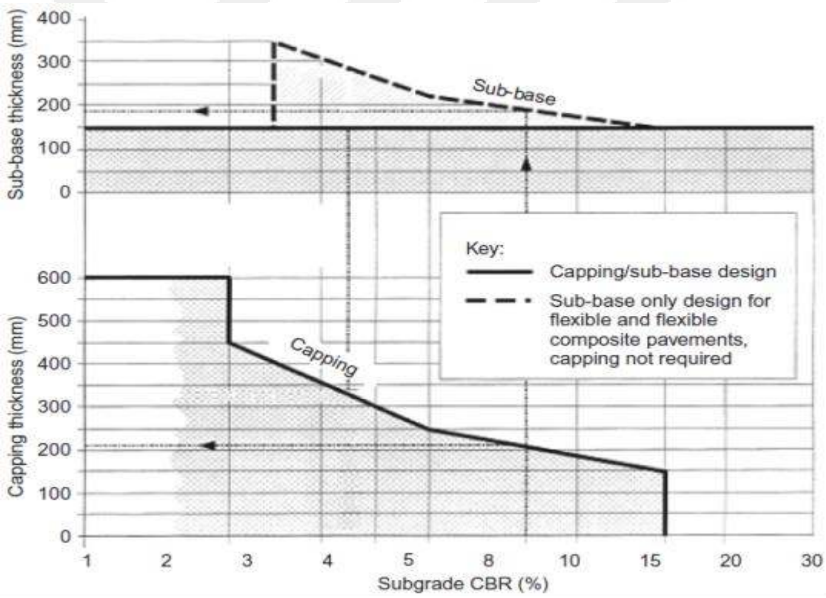


**Figure 5.13** Capping and sub-base thickness design (Highways Agency, 1994)

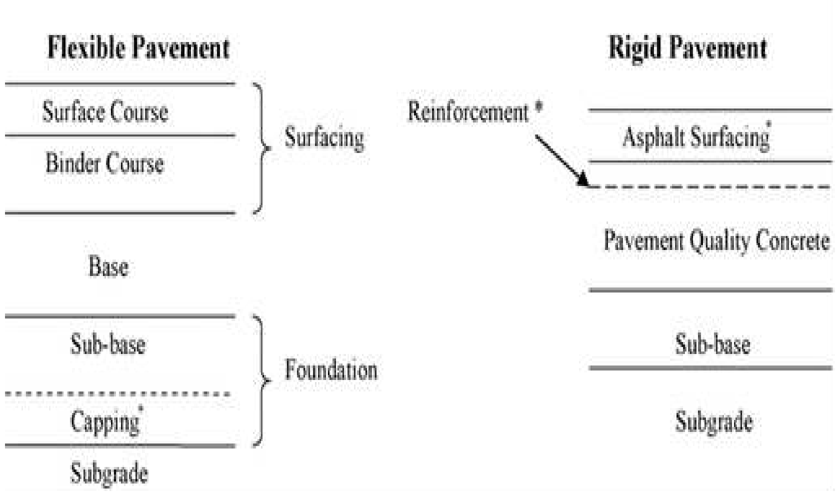


*indicates optional

**Figure 5.14** Structural layers of flexible and rigid pavements(Huang et al., 2007)

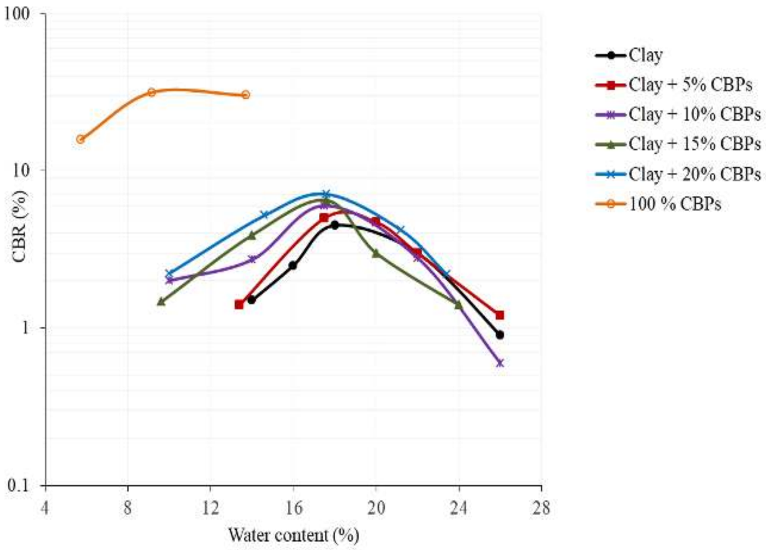


**Figure 5.15** Swelling percentage changes with water content for the clay with Crushed Bricks Pieces (CBPs)

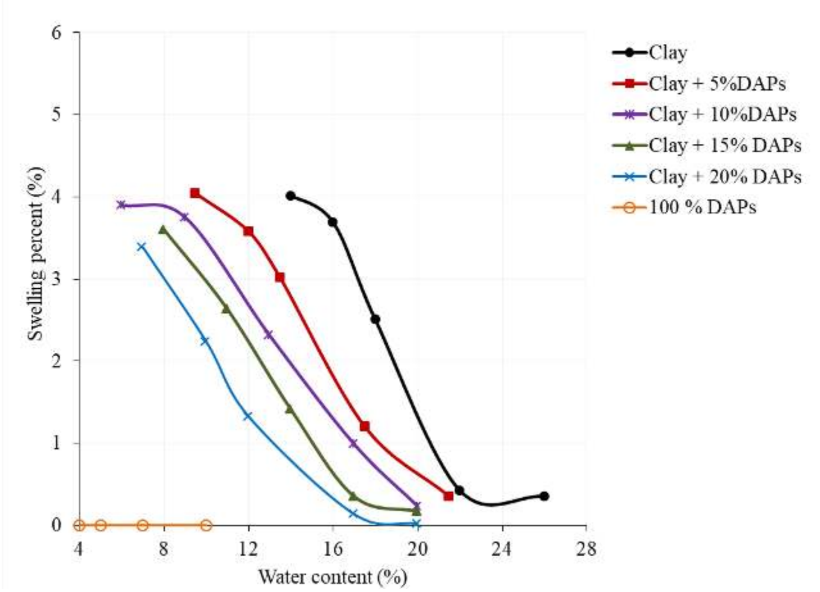


**Figure 5.16** Swelling percentages change with water content for the clay with dumped asphalt pieces (DAPs)

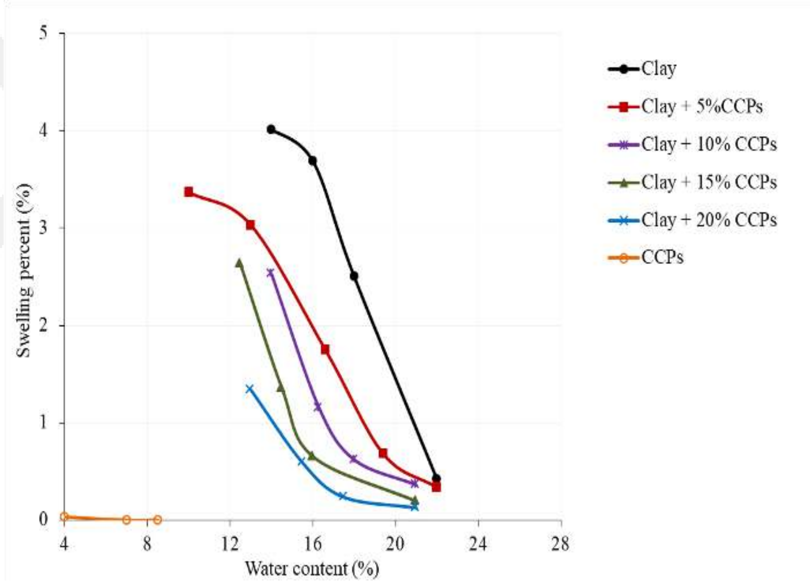


**Figure 5.17** Swelling percentage changes with water content for the clay with crushed concrete pieces (CCPs)

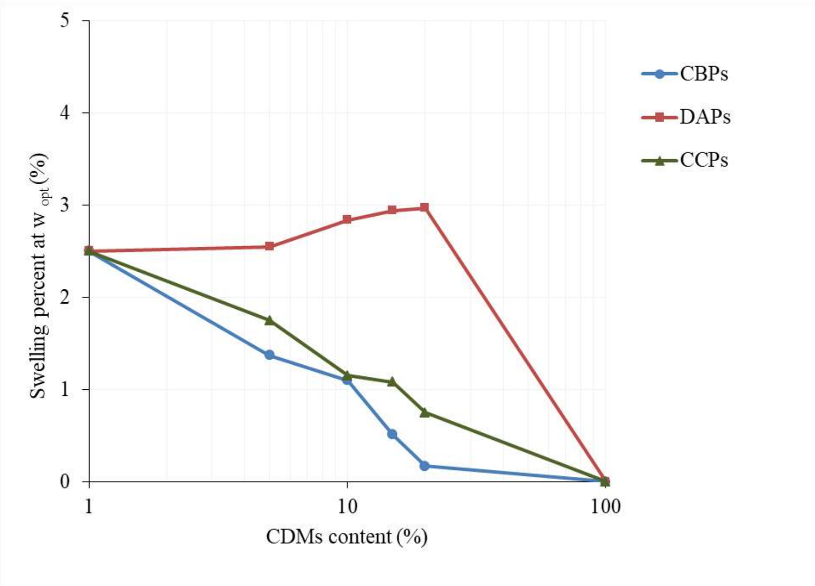


**Figure 5.18** Swelling percentage at $w_{opt}$ with the varying CDMs content

### 5.1.3.2 Unconfined compressive strength test results

The UCS testing results indicate that the strength behavior of the specimens was markedly affected by the addition of CDMs (Figure 5.19). The UCS tests were carried out on the specimens compacted to $w_{opt}$. The peak compressive strength values of the specimens continuously increased as the amount of waste materials increased. As has been noted, the UCS values of clay-CDMs mixtures were enhanced with similar increasing trends, comparing with UCS values of clay. Furthermore, the increments in strength observed in the clay with crushed concrete paving slab aggregates were found to be higher than those in the clay with other two waste materials. The increases in strength in the clay with CBPs were found to be the lowest.

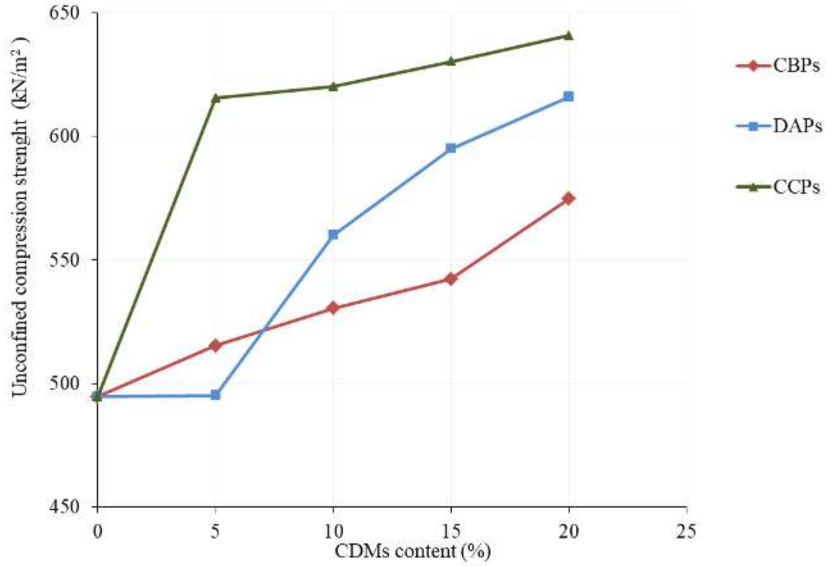


**Figure 5.19** Variations of unconfined compressive strength with the CDMs contents

#### 5.1.3.3 Direct shear test results

Table 5.4 summarizes the results of the strength parameters given by the direct shear test. The effective angle of internal friction (ϕ′) and the effective cohesion (c′) for clay and clay-CDMs mixtures were given at the maximum dry density and optimum moisture content. Figures 5.20 and 5.21 showed the variations of the angle of internal friction (ϕ′) and, the cohesion (c′) with the increasing proportions of CDMs, respectively. From the Table and the Figures, it is apparent that the addition of 10% CDMs leads to a maximum angle of internal friction (ϕ′). Nevertheless, the same percentage of CDMs leads to minimum cohesion (c′). The general impression given by results is that the CBPs and CCPs additions increased the angle of internal friction (ϕ′) while the DAPs addition decreased the angle of internal friction (ϕ′). The viscosity of bituminous materials coating the aggregate in the DAPs materials reduced the strength parameters of the soil by acting as lubricating materials between soil-aggregate particles. Originally, the DAP materials had very low strength, as shown by Arulrajah et al., (2013c).

The results show some fluctuations, especially in soil cohesion (c′), with increasing CDMs proportions. One possible explanation for these findings is that the fluctuations are effects of the type of test, especially the predetermined plane of failure in the direct shear test (Grim, 1953; Coduto, 1999; Das and Sobhan, 2014).

As shown in Figure 5.22, the concentration of CDMs in the middle of soil samples, which represents the predetermined plane of failure in the direct shear test, will affect the strength parameters of soil, $\phi'$ and $c'$.

Table 5.5 gives the vertical and horizontal displacements associated with direct shear test clay and clay-CDMs mixtures. The vertical displacements, which represent the vertical consolidation of the sample under normal load, were measured at two stages of the test. The first stage was at the end of consolidation and before the shearing of the samples, which gave less than values compared to the second stage, after the shearing of the samples, as shown in Figure 5.23. The same Figure shows that the values of vertical movement for clay for all normal loads are higher than those of most of the clay-CDMs mixtures. This finding is consistent with findings of the consolidation test, with some differences from the differences of direct shear and consolidation tests procedures.

The horizontal displacements-shear stress relations for clay and clay-CDMs mixtures are given in Figures 5.24 through 5.26. From the data in these Figures, it is apparent that for a specific displacement, the CCP materials provide almost the highest shear stress, whereas the DAP materials have the lowest stress. The CBP material provides shear stress equal to that of clay. This CDMs behavior was for the entire normal load (100, 200, and, 300kN/m$^2$). This stress-strain manner of clay-CDMs was due to the nature and concentration of specific CDMs in the direct shear samples. The rigidity of CCP, the elasticity of DAP, and the cohesive soil likeness of CBP play prominent roles in determining the stress-strain relationship of clay-CDMs mixtures in the direct shear test.

**Table 5.4** Direct shear test parameters for clay and clay-CDMs mixtures

| Mixtures type | CDMs content (%) | Optimum moisture content (%) | Maximum dry unit weight (kN/m³) | Effective cohesion (c′) | Effective angle of internal friction (ϕ′) |
|---|---|---|---|---|---|
| Clay | 0 | 18.00 | 17.30 | 20.0 | 29.0 |
| CBPs [a] | 5 | 18.20 | 17.25 | 17.0 | 30.5 |
| CBPs | 10 | 17.50 | 17.21 | 10.0 | 34.0 |
| CBPs | 15 | 17.60 | 17.22 | 42.0 | 31.0 |
| CBPs | 20 | 17.10 | 17.10 | 30.0 | 30.0 |
| CBPs | 100 | 9.10 | 13.80 | --- | --- |
| DAPs [b] | 5 | 13.50 | 17.58 | 12.0 | 28.0 |
| DAPs | 10 | 12.60 | 17.92 | 10.0 | 30.5 |
| DAPs | 15 | 12.00 | 18.00 | 11.0 | 29.0 |
| DAPs | 20 | 11.6 | 18.26 | 15.0 | 25.8 |
| DAPs | 100 | 6.50 | 17.85 | --- | --- |
| CCPs [c] | 5 | 16.60 | 17.30 | 20.5 | 31.0 |
| CCPs | 10 | 16.30 | 17.70 | 12.0 | 34.0 |
| CCPs | 15 | 15.80 | 17.80 | 28.0 | 31.5 |
| CCPs | 20 | 15.20 | 17.93 | 19.0 | 33.0 |
| CCPs | 100 | 7.00 | 17.63 | --- | --- |

a: Crushed bricks pieces (CBPs) b: Dumped asphalt pieces (DAPs) c: Crushed concrete pieces (CCPs)

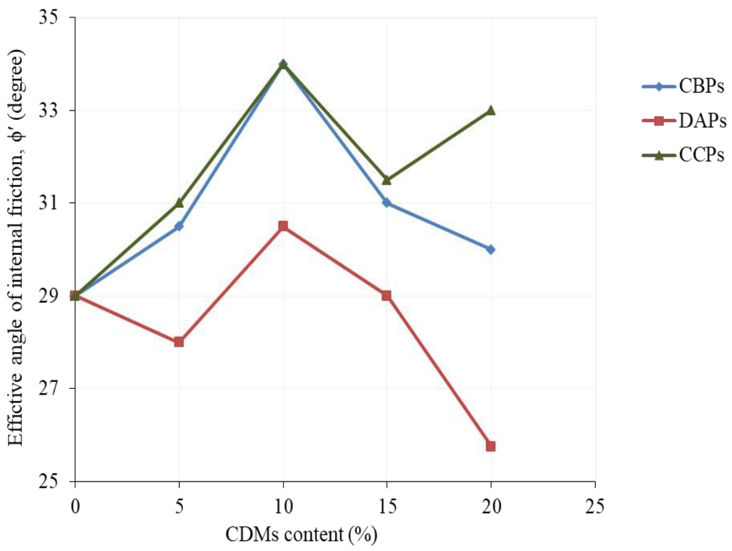


**Figure 5.20** Variations of the effective angle of internal friction (ϕ′) with the CDMs content

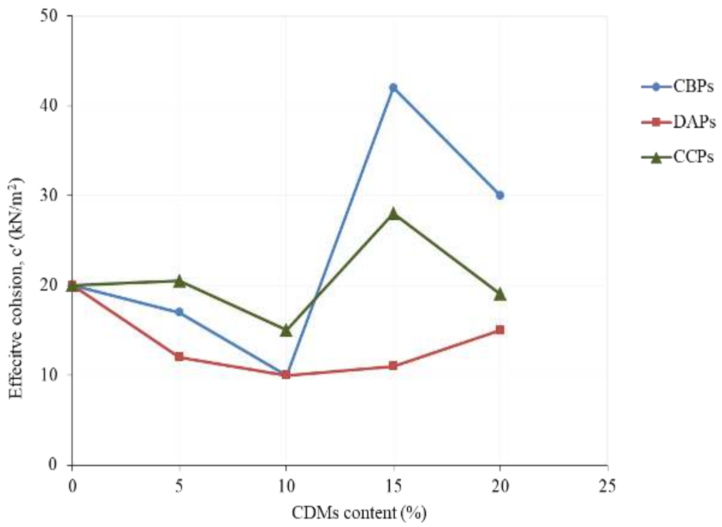


**Figure 5.21** Variations of the effective cohesion (c′) with the CDMs contents

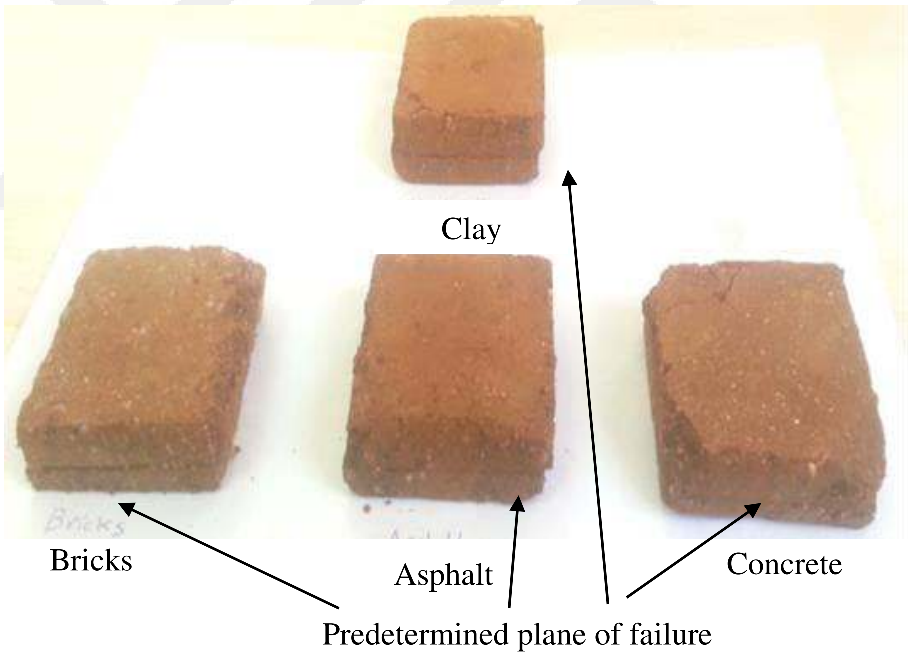


**Figure 5.22** Pictures of direct shear samples after test for clay and clay-CDMs mixtures

**Table 5.5** Vertical and horizontal displacements for samples in direct shear test

| CDMs type | CDMs content (%) | Horizontal displacement at failure (mm) | | | Vertical displacement before shearing (mm) | | | Vertical displacement after shearing (mm) | | |
|---|---|---|---|---|---|---|---|---|---|---|
| | | N.P. [d]100 $kN/m^2$ | N.P.200 $kN/m^2$ | N.P.300 $kN/m^2$ | N.P.100 $kN/m^2$ | N.P.200 $kN/m^2$ | N.P.300 $kN/m^2$ | N.P.100 $kN/m^2$ | N.P.200 $kN/m^2$ | N.P.300 $kN/m^2$ |
| Clay | 0 | 3.58 | 2.82 | 3.70 | 0.22 | 0.78 | 1.05 | 0.24 | 0.80 | 1.33 |
| CBPs [a] | 5 | 2.30 | 2.15 | 3.47 | 0.70 | 0.52 | 0.92 | 0.77 | 0.58 | 0.99 |
| CBPs | 10 | 3.05 | 4.05 | 4.2 | 0.32 | 1.30 | 0.85 | 0.52 | 1.53 | 1.12 |
| CBPs | 15 | 3.59 | 3.65 | 3.99 | 0.44 | 0.66 | 1.02 | 0.67 | 0.91 | 1.15 |
| CBPs | 20 | 2.82 | 3.22 | 3.75 | 0.73 | 0.64 | 0.93 | 0.92 | 0.82 | 1.05 |
| DAPs [b] | 5 | 4.00 | 4.69 | 5.41 | 0.82 | 0.24 | 0.40 | 0.92 | 0.45 | 1.18 |
| DAPs | 10 | 3.41 | 3.82 | 4.50 | 0.73 | 0.80 | 1.51 | 1.00 | 1.50 | 1.85 |
| DAPs | 15 | 2.30 | 3.38 | 3.45 | 0.71 | 1.05 | 1.28 | 0.80 | 1.22 | 1.37 |
| DAPs | 20 | 2.86 | 4.17 | 5.45 | 0.14 | 0.28 | 1.16 | 0.30 | 1.45 | 2.50 |
| CCPs [c] | 5 | 3.24 | 2.47 | 5.19 | 0.38 | 0.44 | 0.72 | 0.54 | 0.60 | 1.00 |
| CCPs | 10 | 1.52 | 3.11 | 3.90 | 0.68 | 0.55 | 0.83 | 0.77 | 0.71 | 1.05 |
| CCPs | 15 | 2.58 | 2.57 | 3.32 | 0.29 | 0.32 | 0.85 | 0.46 | 0.40 | 1.07 |
| CCPs | 20 | 2.78 | 4.78 | 3.80 | 0.42 | 0.71 | 1.25 | 0.62 | 0.98 | 1.53 |

a: Crushed bricks pieces (CBPs) b: Dumped asphalt pieces (DAPs) c: Crushed concrete pieces (CCPs) d: Normal pressure

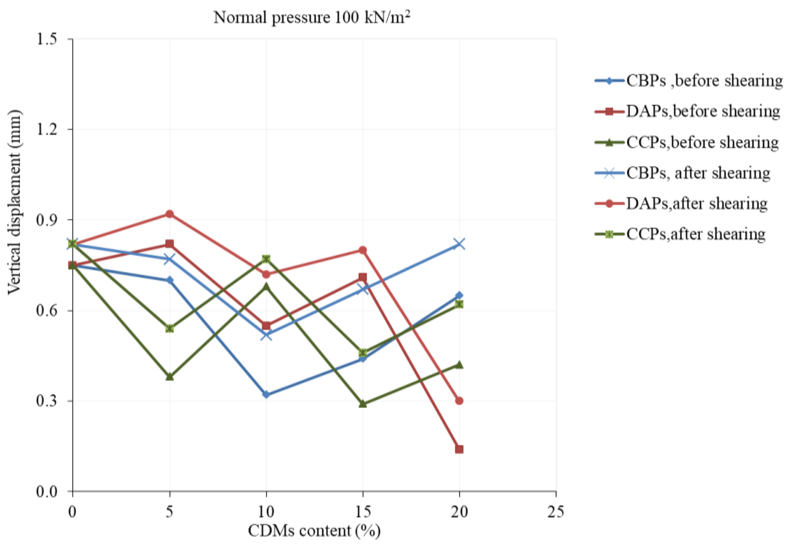
Normal pressure 100 kN/m²
1.5
1.2
0.9
0.6
0.3
0.0
Vertical displacment (mm)
0
5
10
15
20
25
CDMs content (%)
CBPs ,before shearing
DAPs,before shearing
CCPs,before shearing
CBPs, after shearing
DAPs,after shearing
CCPs,after shearing

(a)

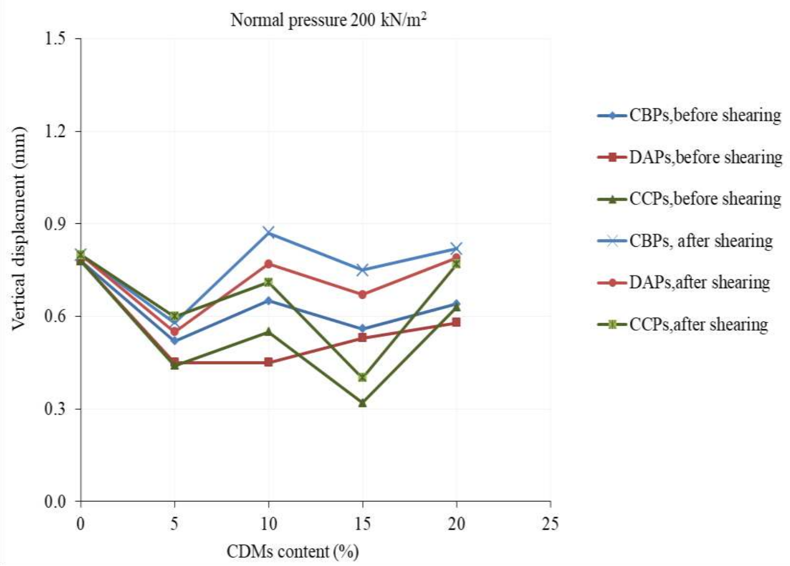
Normal pressure 200 kN/m²
1.5
1.2
0.9
0.6
0.3
0.0
Vertical displacment (mm)
0
5
10
15
20
25
CDMs content (%)
CBPs,before shearing
DAPs,before shearing
CCPs,before shearing
CBPs, after shearing
DAPs,after shearing
CCPs,after shearing

(b)

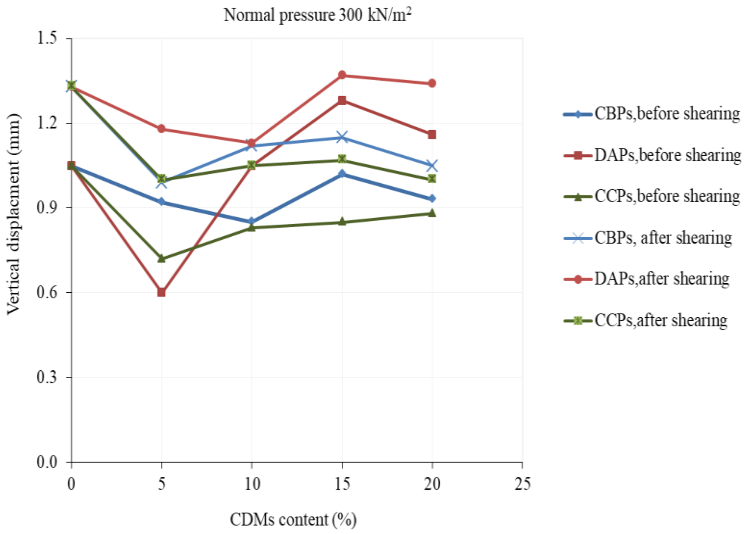


(c)

**Figure 5.23** Vertical displacements of direct shear samples for clay and clay-CDMs mixtures for normal pressure (a) 100 kN/$m^2$ (b) 200 kN/$m^2$ (c) 300 kN/$m^2$

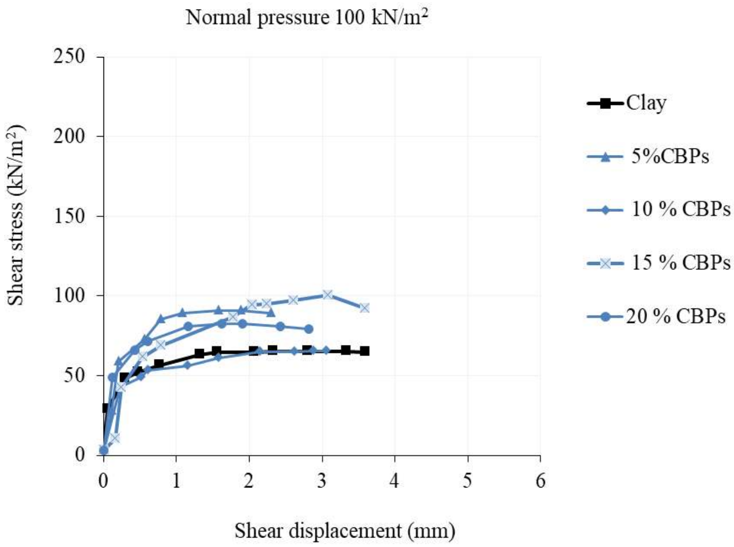


(a)

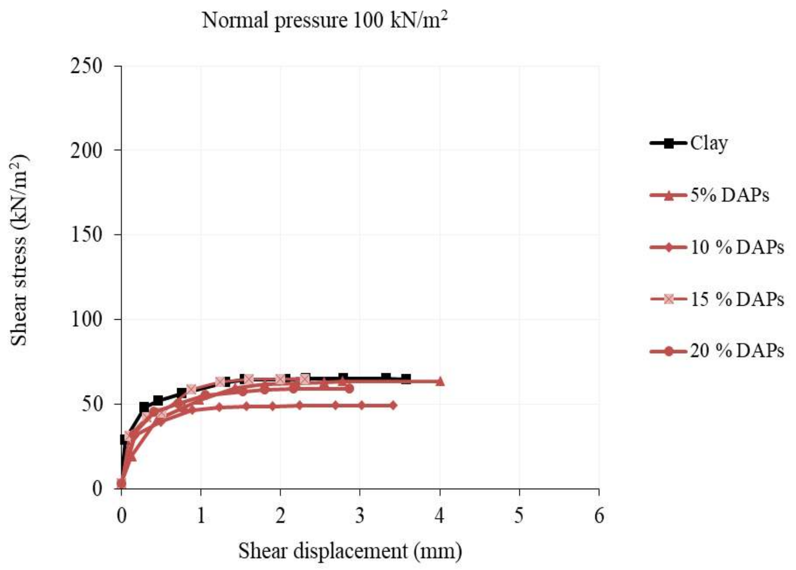


(b)

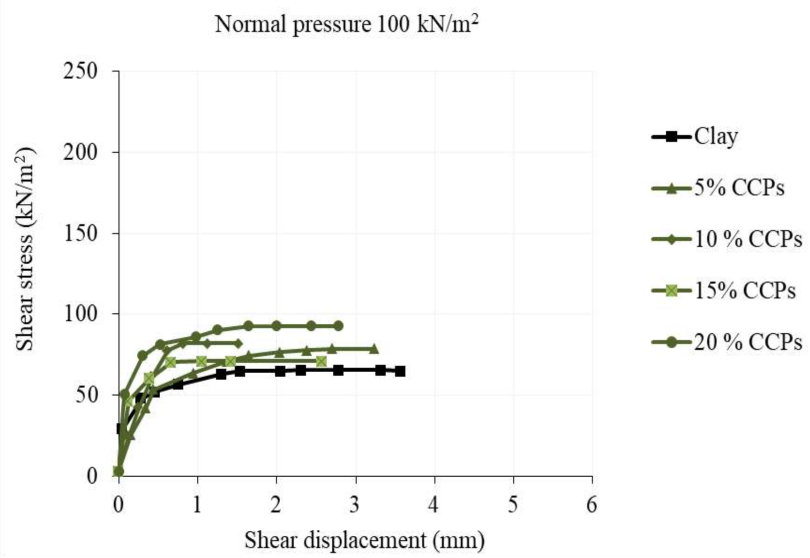


(c)

**Figure 5.24** Horizontal displacements at failure for clay and clay-CDMs mixtures in direct shear test for normal pressure 100 kN/m$^2$ (a)CBPs (b)DAPs (c)CCPs

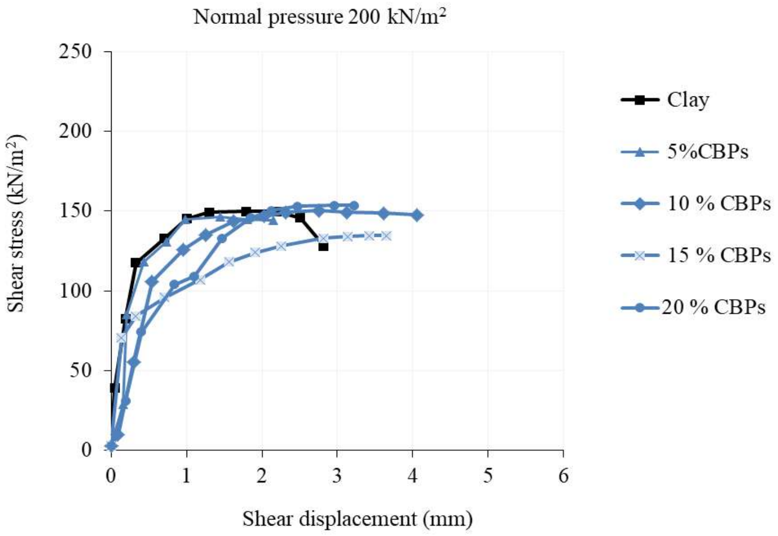
Normal pressure 200 kN/m²
Shear stress (kN/m²)
Shear displacement (mm)
Clay
5%CBPs
10 % CBPs
15 % CBPs
20 % CBPs
0
50
100
150
200
250
0
1
2
3
4
5
6

(a)

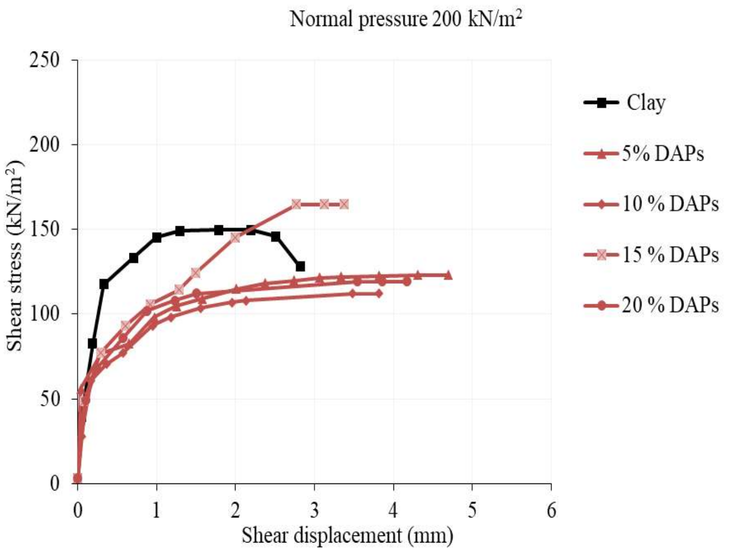
Normal pressure 200 kN/m²
Shear stress (kN/m²)
Shear displacement (mm)
Clay
5% DAPs
10 % DAPs
15 % DAPs
20 % DAPs
0
50
100
150
200
250
0
1
2
3
4
5
6

(b)

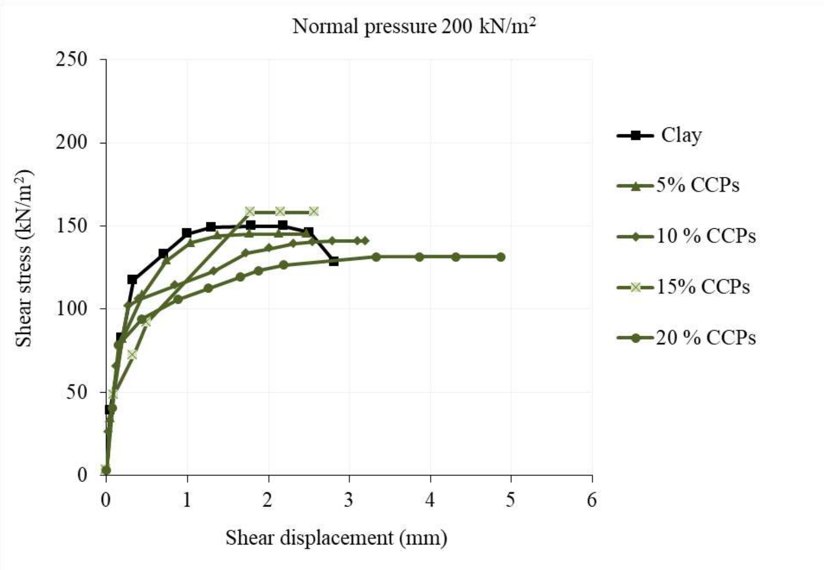


(c)

**Figure 5.25** Horizontal displacements at failure for clay and clay-CDMs mixtures in direct shear test for normal pressure 200 kN/m$^2$ (a)CBPs (b)DAPs (c)CCPs

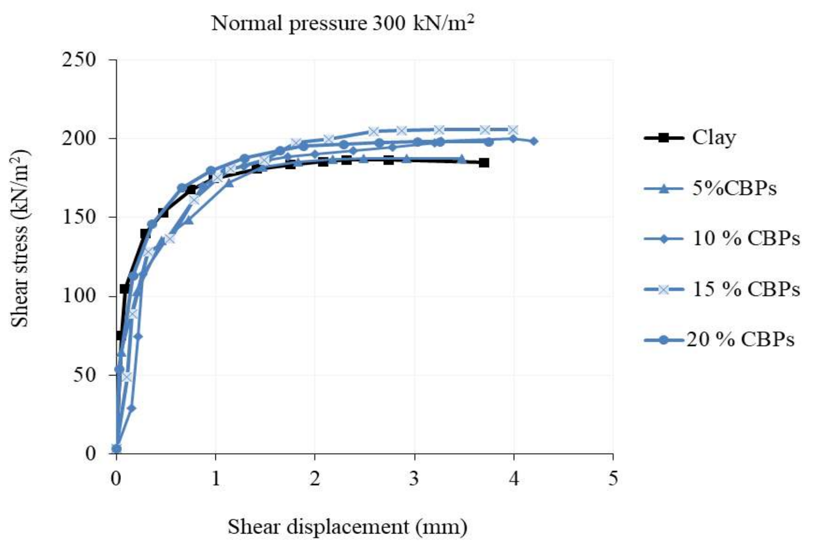


(a)

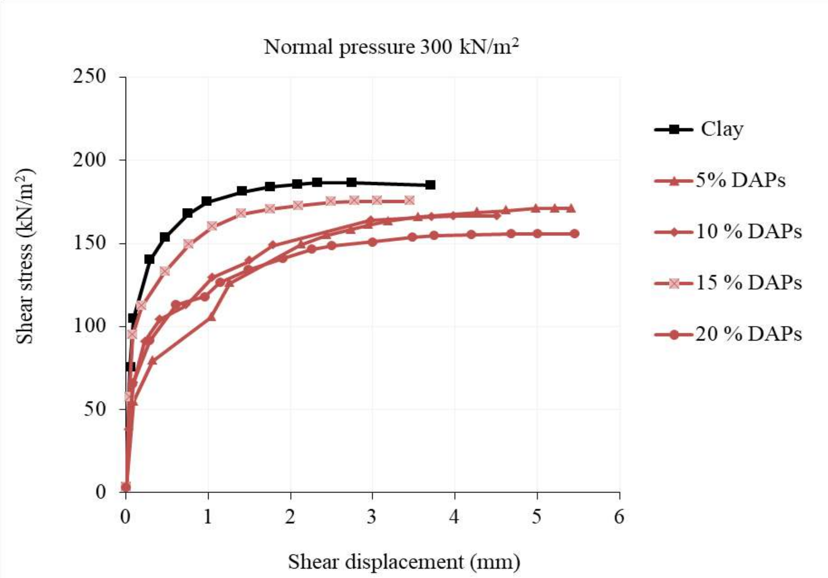


(b)

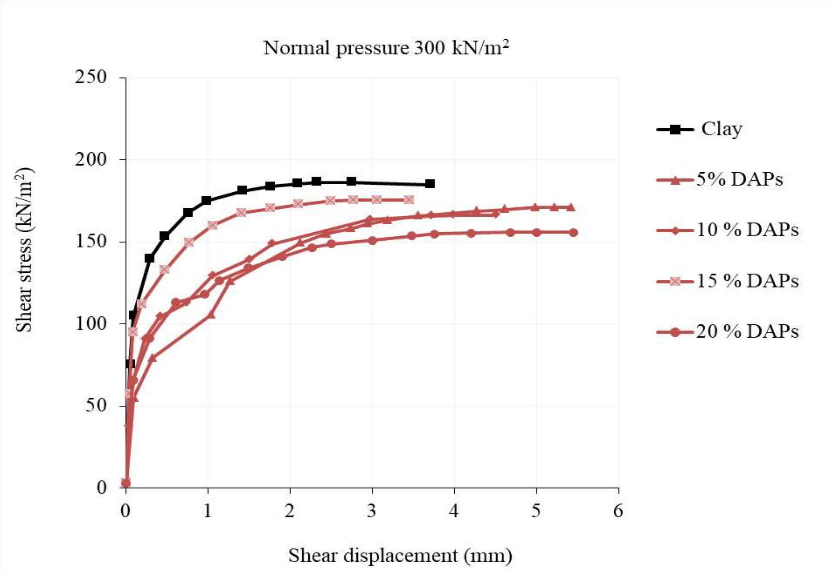


(c)

**Figure 5.26** Horizontal displacements at failure for clay and clay-CDMs mixtures in direct shear test for normal pressure 300 kN/m$^2$ (a)CBPs (b)DAPs (c)CCPs

### 5.1.3.4 Plate load test results

Plate load tests were done in a box model for clay and clay mixed with 10% CDMs. According to the direct shear test results, the 10% CDMs gives the highest angle of internal friction ($\phi'$), as shown in Figure 5.20. Therefore, 10% CDMs was considered to be a suitable percentage for use in the plate load test. Table 5.6 gives the settlements of clay and clay and 10% CDMs mixtures at different pressures applied in the plate load test in the box model. Figures 5.27 through 5.30 illustrate the load-settlements curves record by three strain gauges and their averages in the plate load test for clay and clay-10% CDMs mixtures. In Figure 5.31, the load-settlements curve obtained from the average of the three strain gauges is shown to make a comparison between the results of the plate load tests of clay and clay-10% CDMs mixtures.

It appears from Table 5.6 and Figures 5.27 through 5.31 that CDMs improve the strength of clay due to the increased bearing loads of the clay-10%CDMs mixtures. Also, the specific settlement for CDMs at any specific high load (larger than the 150kN/m$^2$) was less than the settlement of clay for the same load. The addition of 10% CDMs changed the construction and behavior of clay under the applied loads. The physical replacement of a specific part of fine soil by graduated coarse materials (CDMs) changed the classification of clay from A-7-6 to A-2-6 according to the AASTHO classification system, which made it considered as a better filling material. Besides, the CDMs used in this study came from high strength materials used in construction activities. Consistent with these findings, Figure 5.32 shows the time-settlement curve for 200 kN/m$^2$ of pressure for clay and the clay-CDMs mixtures. In this figure, the clay curve indicates the highest settlement at any specific time than the clay-CDMs mixtures. Figure 5.33 shows show the time-settlement curve for 300kN/m$^2$ of pressure. The data in this figure clearly shows that CCP had lower settlement at any specific time than the other CDMs. The clay does not appear in this figure because the failure happened in clay at 200kN/m$^2$.

The rebound load-settlement curves for clay and clay-10%CDMs mixtures showed a slight decrease in settlements for all tests, as shown in Figure 5.34. The same behavior of bearing failure (punching failure) was noted for clay and clay-10%CDM mixtures. However, the most obvious failure was seen in clay, as shown in Figures 5.35 through 5.38.

**Table 5.6** Vertical settlements for clay and clay-10% CDMs mixtures in plate load test

| | Average settlement of three strain gauges (mm) | | | |
|---|---|---|---|---|
| **Applied pressure ($kN/m^2$)** | **Clay** | **10% CBPs [a]** | **10% DAPs [b]** | **10% CCPs [c]** |
| **Loading** | | | | |
| 0 | 0.00 | 0.00 | 0.00 | 0.00 |
| 25 | 0.44 | 1.69 | 1.17 | 1.17 |
| 50 | 0.93 | 2.47 | 1.88 | 1.88 |
| 100 | 4.13 | 4.58 | 5.42 | 5.57 |
| 150 | 10.00 | --- | --- | --- |
| 200 | 22.89 | 12.14 | 13.02 | 13.38 |
| 300 | --- | 28.71 | 24.09 | 18.57 |
| 350 | --- | --- | 27.04 | 24.24 |
| **Unloading** | | | | |
| 200 | --- | 27.46 | --- | --- |
| 175 | --- | --- | 25.93 | 22.97 |
| 100 | --- | 27.02 | --- | --- |
| 87.5 | --- | --- | 25.67 | 22.74 |
| 50 | --- | 26.81 | --- | --- |
| 43.75 | --- | --- | 25.45 | 22.37 |
| 0 | 21.61 | --- | --- | --- |

a: Crushed bricks pieces (CBPs) b: Dumped asphalt pieces (DAPs) c: Crushed concrete pieces (CCPs)

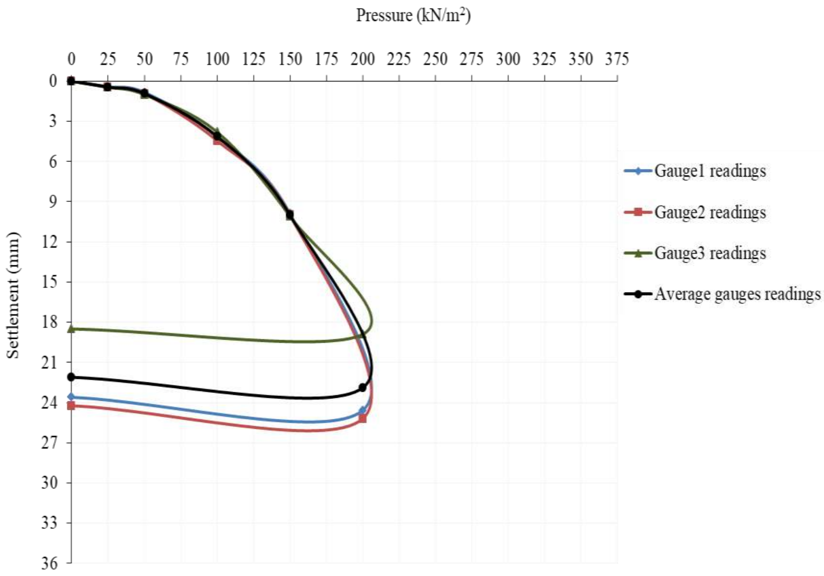


**Figure 5.27** Pressure-settlement curves for clay in plate load test (results obtained using three strain gauges)

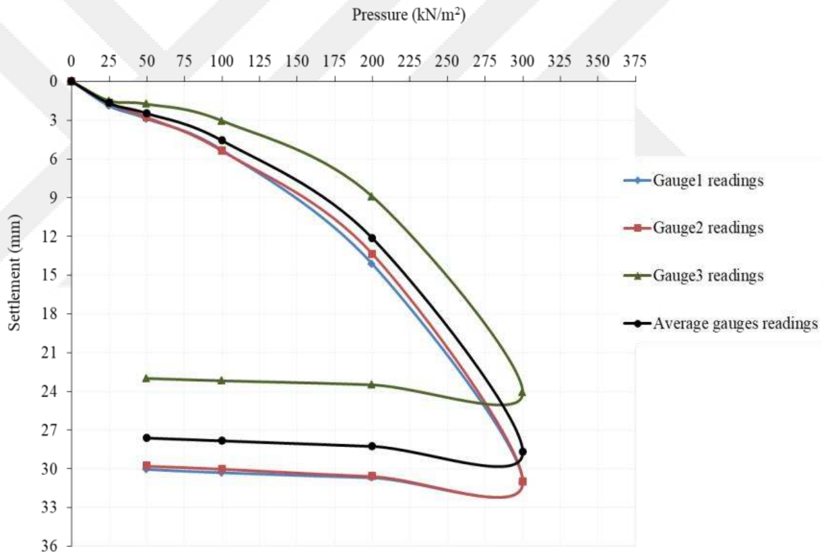


**Figure 5.28** Pressure-settlement curves for 10% CBPs in plate load test (results obtained using three strain gauges)

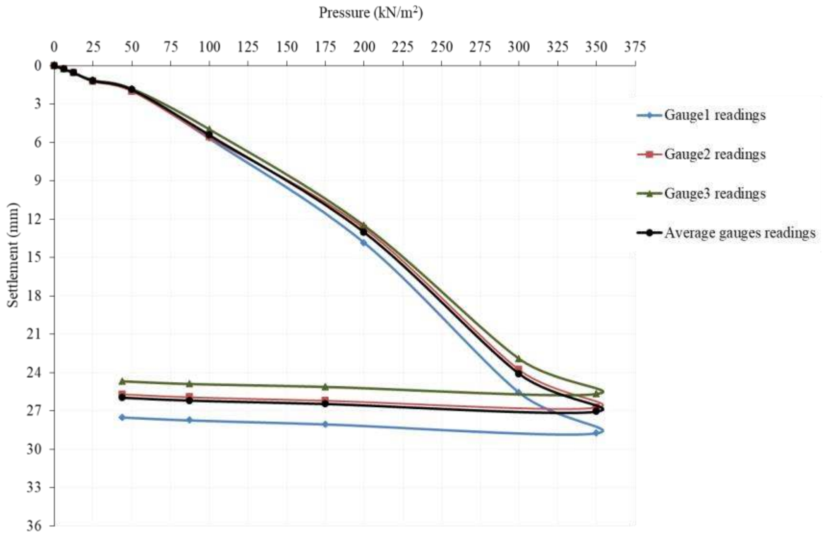


**Figure 5.29** Pressure-settlement curves for 10% DAPs in plate load test (results obtained using three strain gauges)

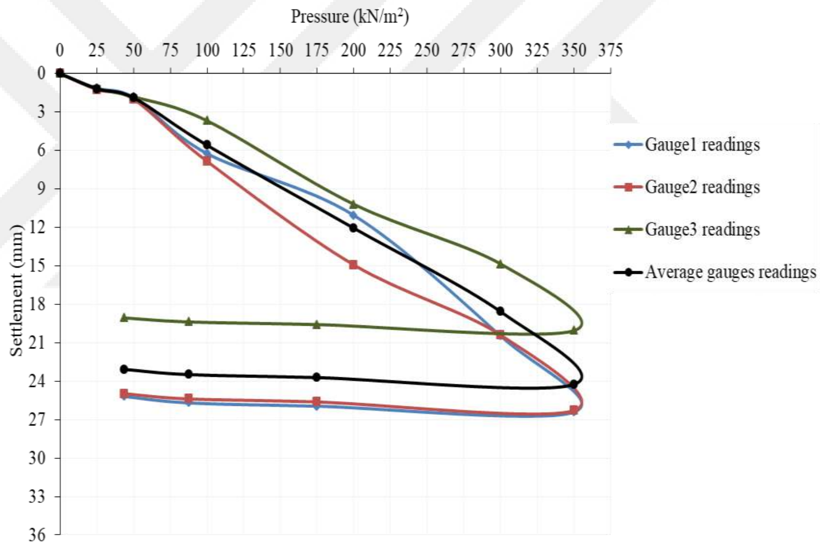


**Figure 5.30** Pressure-settlement curves for 10% CCPs in plate load test (results obtained using three strain gauges)

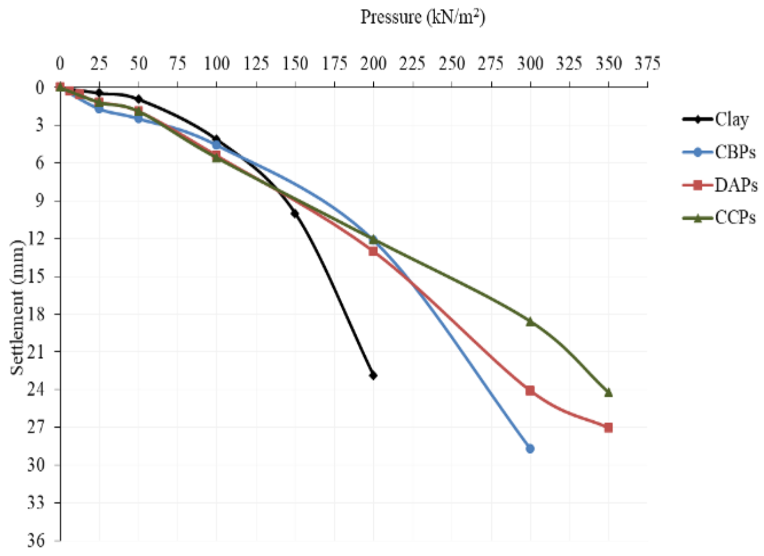


**Figure 5.31** Pressure-settlement curves for clay and clay-10% CDMs in plate load test (the results obtained by the average of three strain gauges)

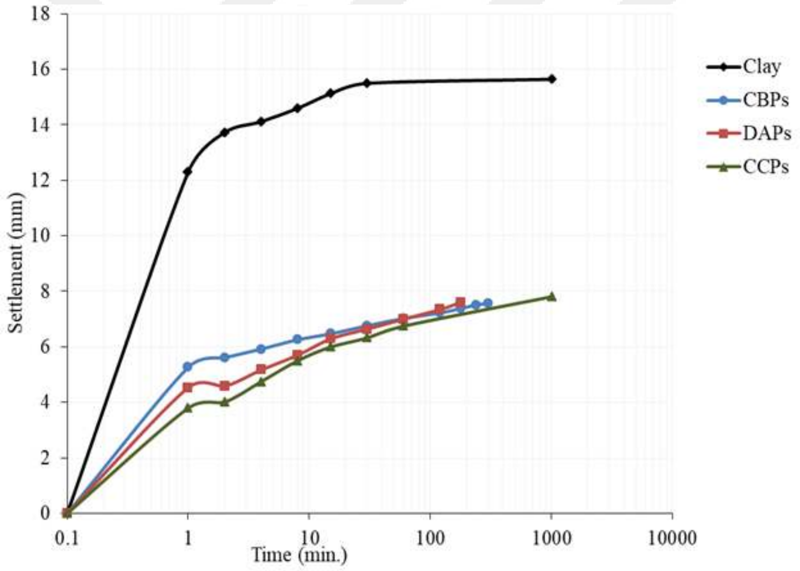


**Figure 5.32** Time-settlement curves of 200 kN/m$^2$ pressure for clay and clay-10% CDMs in plate load test (results based on the average from three strain gauges)

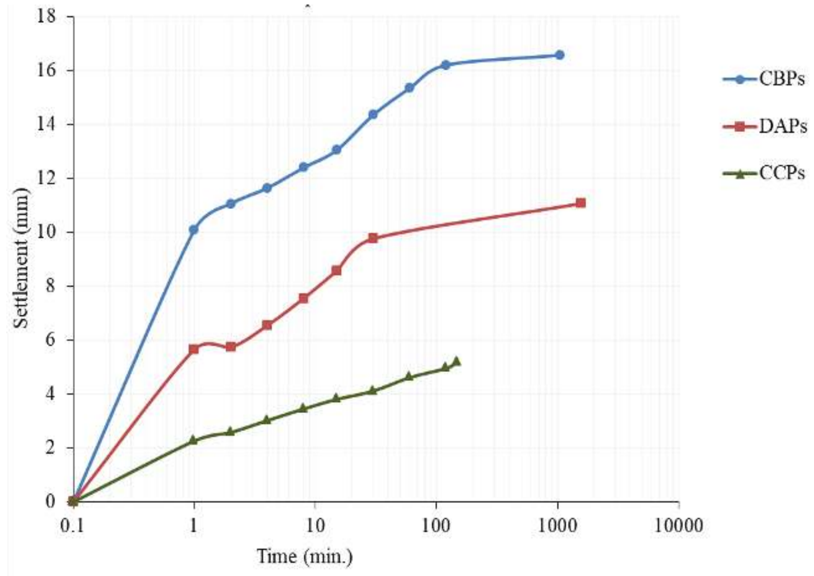


**Figure 5.33** Time-settlement curves of 300 kN/m$^2$ pressure for clay-10% CDMs in plate load test (results based on the average from three strain gauges)

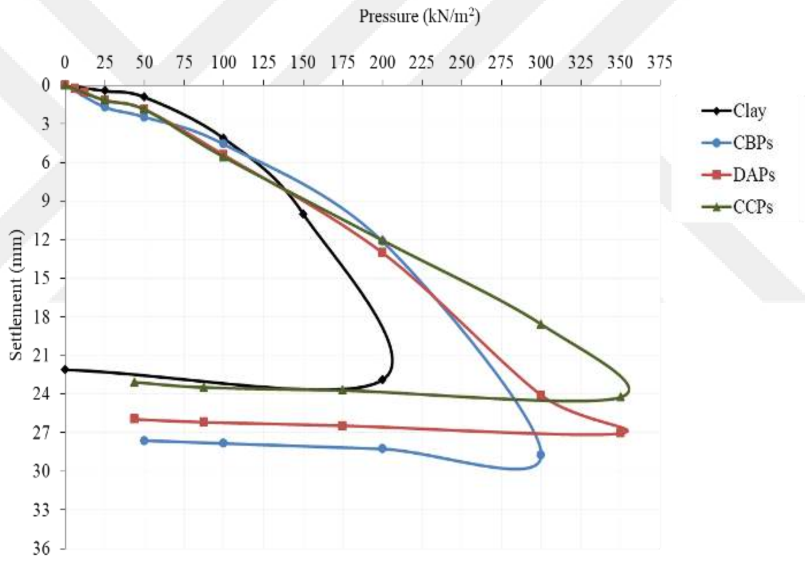


**Figure 5.34** Rebound pressure-settlement curves for clay and clay-10% CDMs in plate load test (results based on the average from three strain gauges)

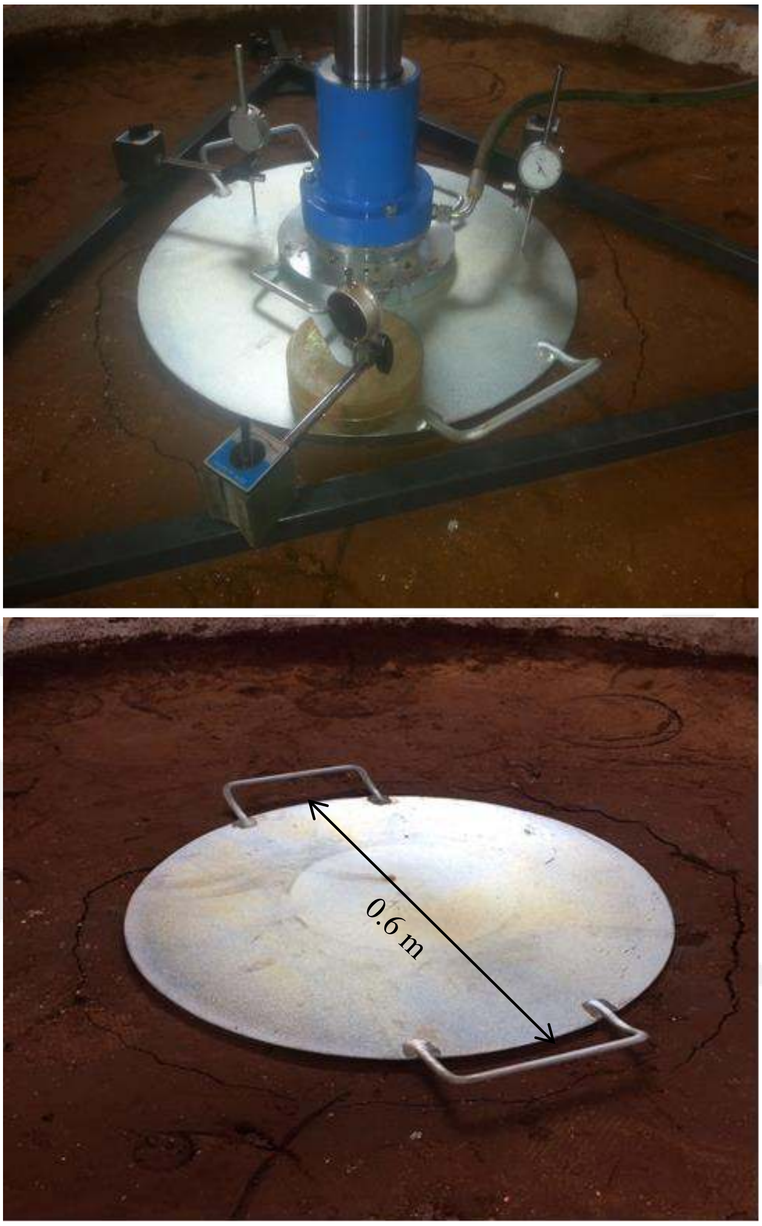


**Figure 5.35** Failure shape for clay at the end of plate load test


**Figure 5.36** Failure shape for CBPs at the end of plate load test


**Figure 5.37** Failure shape for DAPs at the end of plate load test


**Figure 5.38** Failure shape for CCPs at the end of plate load test

#### 5.1.3.5 Total geostatic and induced stress results

The total geostatic stress (overburden pressure) and induced stress developed in soil was studied on clay and clay-10% CDMs mixtures during the plate load test using two pressure cell transducers set on the bottom of the box model. The first pressure cell transducer was installed at the center of the box, and the second one was installed at the center of one-quarter of the box. Due to symmetry, the reading of second pressure cell transducer represents the pressure at a ring of 0.5m from the center of the box bottom, as shown in Figure 5.39. Figures 5.40 and 5.41 illustrates the reading of pressure cell transducers after filling the box, which represents the overburden pressure (before plate load test applied), and the pressure cell transducer readings of induced stress (during the plate load test applied).

As Figures 4.40 and 4.41 shows, there is a significant difference between the geostatic and induced stress (before and after the plate load test applied). Also, pressure cell transducer 1, which represents the pressure reading at the center of the bottom of the box, gave a higher reading than pressure cell transducer 2 for both the geostatic and induced pressure. These results are compatible with soil mechanics assumptions for geostatic and induced stress. The data in the previous two Figures shows significant increases in the geostatic and external stress for the clay-10%CDMs mixtures, especially DAP and CCP. These increases are mainly due to two reasons. First, the increases of the maximum dry density of clay-10% CDMs mixtures lead to increases in total geostatic stress in the soil. Another reason is the improvement of clay bearing capacity because of the addition of materials with high strength, like CDMs. because the data logger was installed to record pressure cell transducer readings each 15 minutes, Figures 5.42 through 5.45 show the relationship between the pressure cell transducer readings in $kN/m^2$ and the time of pressure generation for clay and clay-10% CDMs mixtures. The readings at one minute represent the beginning of the plate load test.

The readings increase very slowly with increasing bearing loads at the start because of the very small effect of small bearing loads on the soil pressure at pressure cell transducer depth (1.4m from surface). The pressure cell transducer readings start to increase after that, as well as during the increasing of the bearing load at the surface due to the large pressure reaching the soil at pressure cell transducers depth. Some reductions in the pressure cell transducers values were seen in the final reading due to the relaxation of the bearing pressure as a result of soil settlement under the bearing plate.

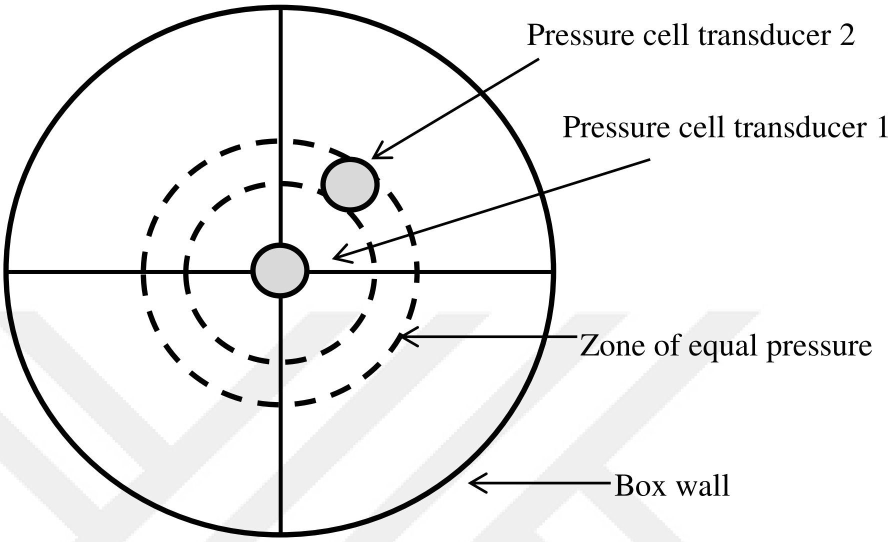


**Figure 5.39** Top view of box model with the location of pressure cell transducers and equal pressure zone

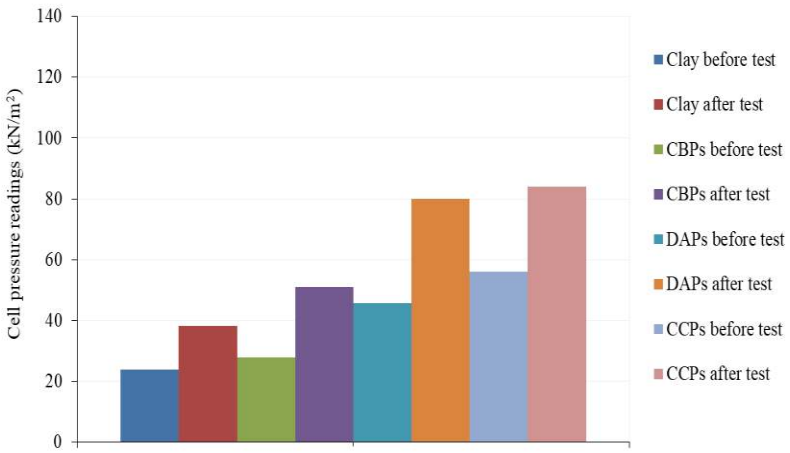


**Figure 5.40** Pressure cell transducer 1 reading before and after plate load test

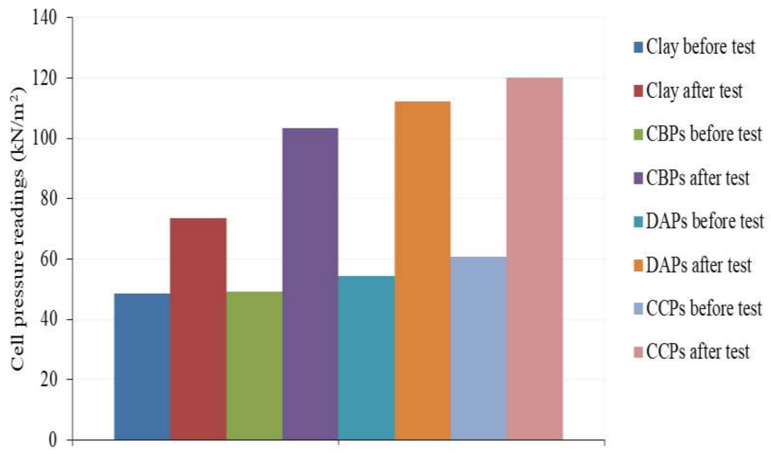


**Figure 5.41** Pressure cell transducer 2 reading before and after plate load test

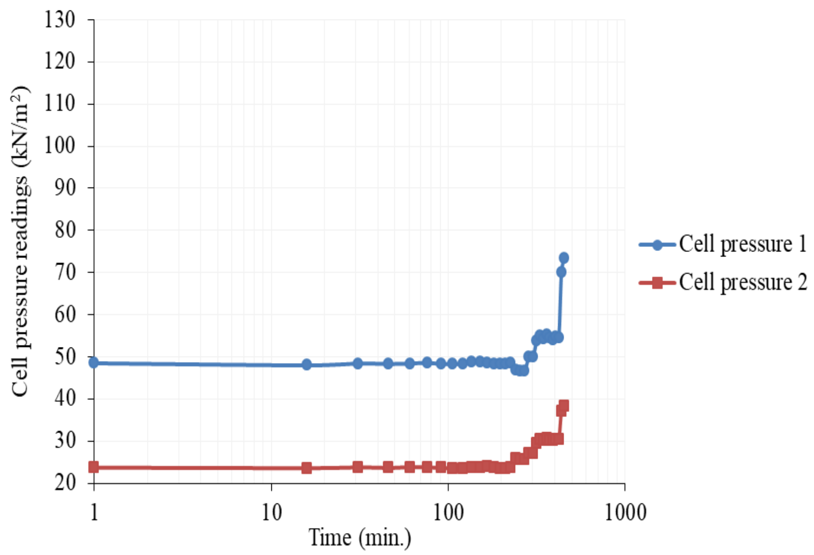


**Figure 5.42** Relationship between pressure cell transducer readings and time of pressure generation during plate load test for clay

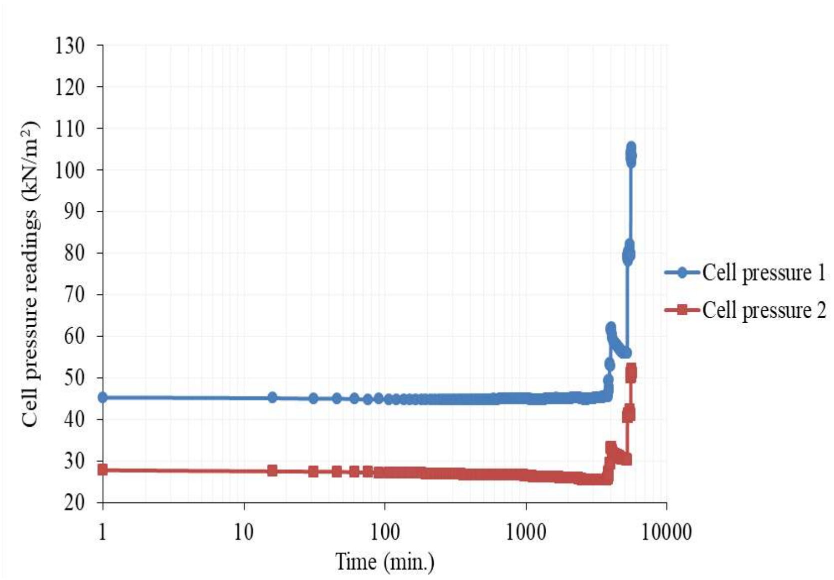


**Figure 5.43** Relationship between pressure cell transducer readings and time of pressure generation during plate load test for CBPs

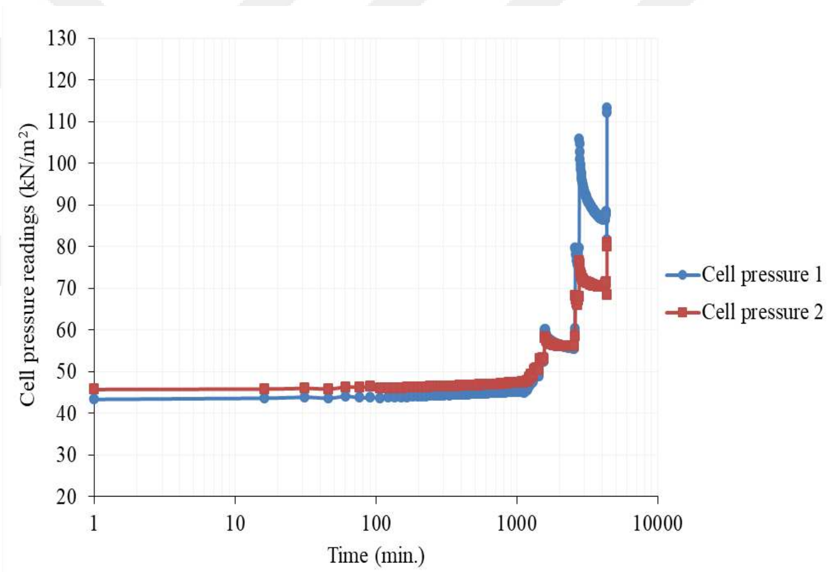


**Figure 5.44** Relationship between pressure cell transducer readings and time of pressure generation during plate load test for DAPs

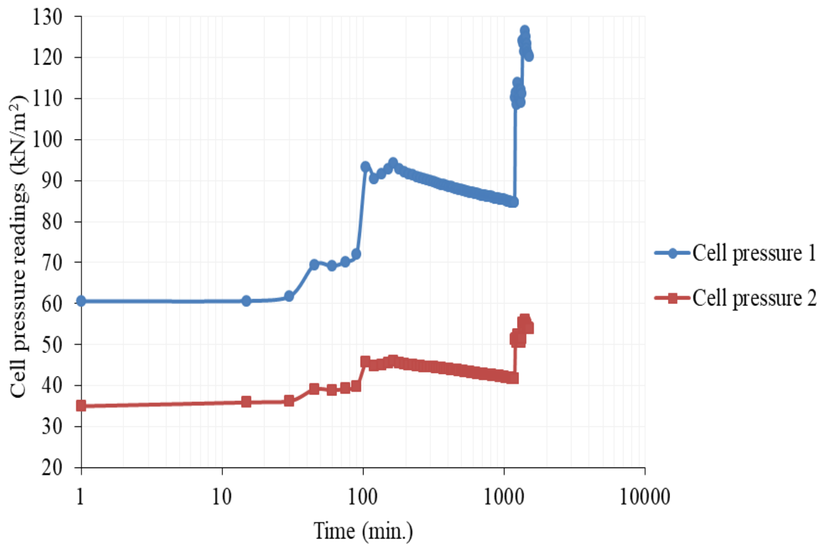


**Figure 5.45** Relationship between pressure cell transducer readings and time of pressure generation during plate load test for CCPs

### 5.1.4 Swelling characteristics and water absorption

Table 5.7 shows the swelling percentages calculated at the maximum dry density and optimum moisture content. These values were obtained using two different tests, CBR and oedometer tests. Table 5.7 and Figure 5.46 show that the swelling values from the oedometer test were higher than the values of the CBR test. There are two possible reasons for this difference. The first is the test condition, including specimen size and seating load. The second reason is the difference in size of the CDMs used in the two tests.

The large CDMs particles (19mm) used in the CBR test reduced the swelling percentages because it is considered as a heavy, non-plastic material, which obstructs the swelling process. As a result, the swelling percentages decreased as the CDMs content increased in the CBR tests, except in the situation of the DAPs material. Table 5.6 and Figure 5.46 show that the swelling percentages increased when the DAPs and CCPs content increased in the oedometer test. This increase was due to the increase to the maximum dry density. Figure 5.49 confirms that expansive clay generally decreases swelling percentages when the PI decreases (Holtz and Gibbs, 1956; Seed et al., 1960; Van Der Merwe, 1964). The PI decreased when the CDMs content increased, except in the situation of the DAPs material, in which the PI increased. The behavior of the DAPs materials has two explanations. Firstly, there are many organic (increase swelling) materials in DAPs materials, as shown by Arulrajah et al., (2013). Another reason is the high-water absorption of this material, as exposed by Arulrajah et al., (2013c).

Figure 5.50 clearly shows this behavior of the DAPs material. In this figure, the relation between the CDMs content and the absorption of water, represented by the difference between water content before and after the test, was shown. Figure 5.51 gives the relation between the swelling pressures in kN/m$^2$ and CDMs content. The increases in the swelling pressure when the DAPs and CCPs content increased were due to the increases of maximum dry density. Increasing the CBPs content was led to a decrease in swelling percentages and pressures. This behavior of CBPs material is due its non-plastic, light nature (Gs, 2.403), as well as its low water absorption compared to the other CDMs.

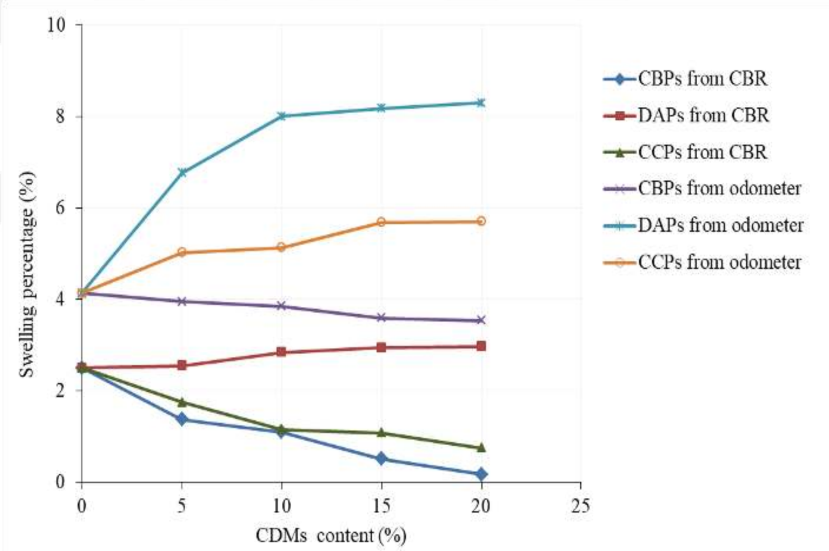


**Figure 5.46** Effect of CDMs content on the swelling percentages of clay using oedometer and CBR test

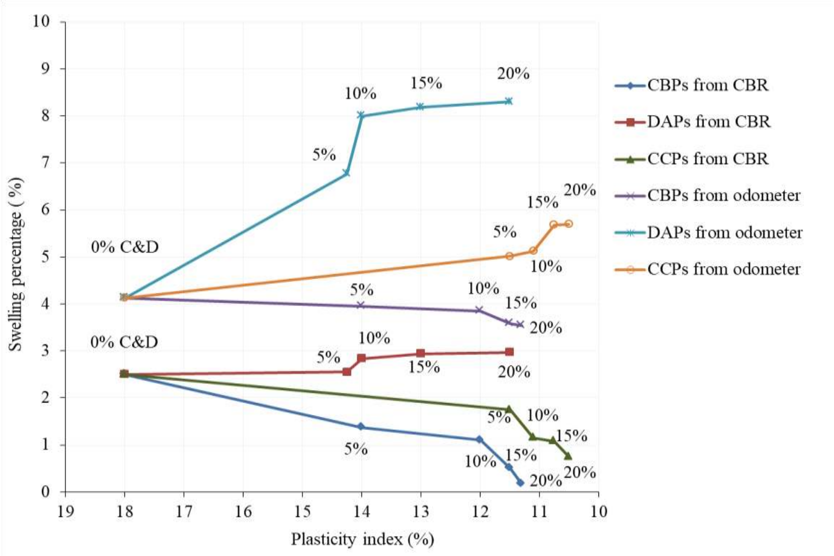


**Figure 5.47** Correlation between swelling percentages and PI for clay and clay-CDMs mixtures by oedometer test and CBR test

**Table 5.7** Swelling characteristics and absorption for clay and clay-CDMs mixtures

| **Mixtures type** | **CDMs content (%)** | **Optimum Moisture Content** | **Maximum dry unit weight** | **Swelling pressure at the OMC [a]** | **Swelling percent at the OMC (%) [b]** | **Swelling percent at the OMC [c]** | **Absorption from CBR (%)** | **Absorption from oedometer (%)** |
|---|---|---|---|---|---|---|---|---|
| Clay | 0 | 18 | 17.3 | 62.5 | 4.13 | 2.5 | 0.47 | 0.354 |
| CBPs | 5 | 18.2 | 17.25 | 60 | 3.95 | 1.37 | 0.41 | 0.370 |
| CBPs | 10 | 17.5 | 17.21 | 58.5 | 3.85 | 1.1 | 0.37 | 0.420 |
| CBPs | 15 | 17.6 | 17.22 | 58 | 3.59 | 0.51 | 0.36 | 0.428 |
| CBPs | 20 | 17.1 | 17.1 | 57 | 3.54 | 0.17 | 0.29 | 0.485 |
| CBPs | 100 | 9.1 | 13.8 | - | - | - | - | - |
| DAPs | 5 | 13.5 | 17.58 | 175 | 6.77 | 2.55 | 0.88 | 0.816 |
| DAPs | 10 | 12.6 | 17.92 | 250 | 8 | 2.84 | 0.90 | 0.830 |
| DAPs | 15 | 12 | 18 | 275 | 8.18 | 2.94 | 0.93 | 0.857 |
| DAPs | 20 | 11.6 | 18.26 | 280 | 8.3 | 2.97 | 0.96 | 0.865 |
| DAPs | 100 | 6.5 | 17.85 | - | - | - | - | - |
| CCPs | 5 | 16.6 | 17.3 | 78.125 | 5.02 | 1.75 | 0.464 | 0.438 |
| CCPs | 10 | 16.3 | 17.7 | 112 | 5.13 | 1.15 | 0.411 | 0.447 |
| CCPs | 15 | 15.8 | 17.8 | 118 | 5.68 | 1.08 | 0.361 | 0.451 |
| CCPs | 20 | 15.2 | 17.93 | 125 | 5.7 | 0.75 | 0.322 | 0.452 |
| CCPs | 100 | 7 | 17.63 | - | - | - | - | - |

a: from oedometer test b: from oedometer test c: from CBR test

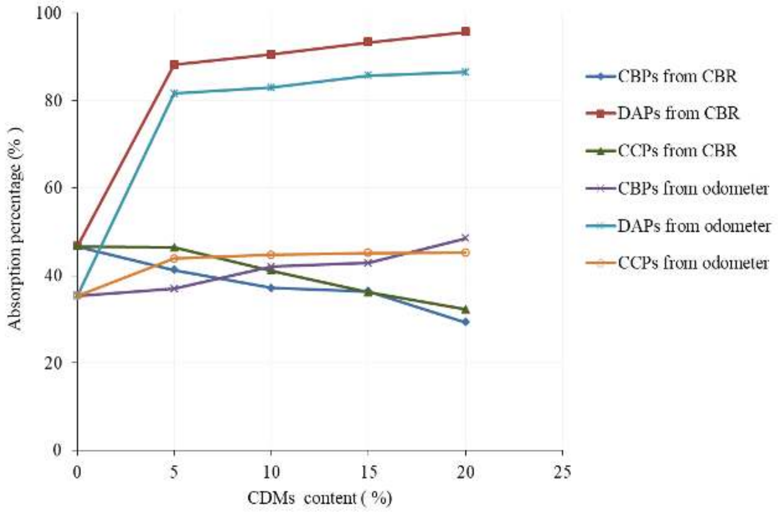


**Figure 5.48** Effect of CDMs content on the water absorption of clay and clay-CDMs mixtures by oedometer test and CBR test

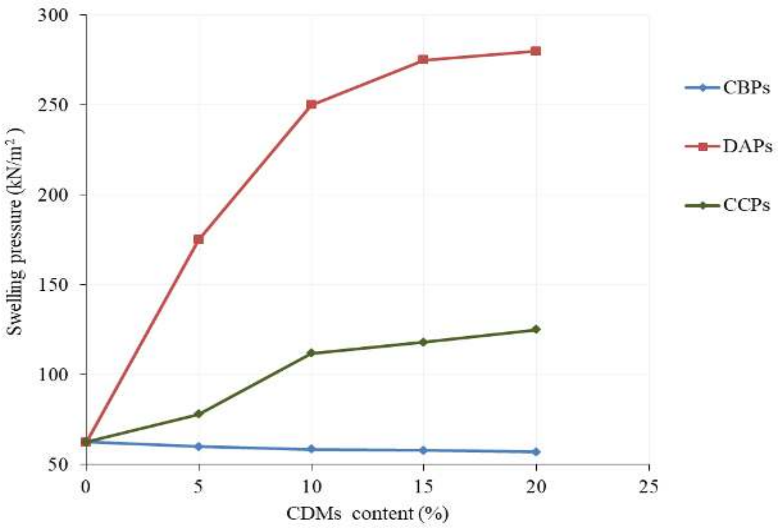


**Figure 5.49** Effect of CDMs content on the swelling pressure of clay using oedometer test

### 5.1.5 Effects of construction and demolition materials on compressibility

Consolidation is considered to be one of the foremost problems with clay. Massive consolidation happens in clay when it becomes saturated. The effects of mixing some CDMs with clay were investigated.

Figures 5.50 through 5.52 demonstrate the compression curves (e-log p) for the remolded soil of clay and clay-CDMs mixtures. Table 5.8 summarizes the results of all consolidation parameters, which were determined using a consolidation test, as represented by the void ratio-log pressure curves. The general shape of the (e-log p) curves of remolded clay and clay-CDMs mixtures has some differences from the undisturbed soil curve (Terzaghi and Peck, 1967). The addition of CBPs increases the ($e_0$) with the decreasing of ($e_0$-$e_f$) which gives less compressible curves, as shown in Figure 5.50. Clays normally have a compression curve (in the shape of void ratio e versus effective vertical stress in the semi-logarithmic plane) lying above that of reconstituted or remolded clays owing to the effect of soil structure (Schmertmann, 1991; Cotecchia and Chandler, 1997; Hong and Tsuchida 1999; Hong et al., 2012). Same behavior was noted by the addition of CCPs, with exception of increasing of ($e_0$).

Figure 5.53 demonstrates the relationship between initial void ratio ($e_0$), which was calculated at the beginning of the test, and the different proportions of CDMs content. A slight increase in $e_0$ coincided with an increase of CBP content due to the decreasing $\gamma_{drymax}$ values. Contrarily, $e_0$ decreased with increasing of DAP and CCP content as a result the increasing $\gamma_{drymax}$ values due to the addition of these materials. The CDMs were added in small amounts so that the CDMs particles were suspended among the clay particles, as shown in Figure 5.54. Figure 5.54 reveals that the enter-granular void ratio ($e_s$), which has been adopted by many researchers to evaluate the voids in coarse-fine soil mixtures, is not suitable for this study. The enter-granular void ratio is used when a small percentage (i.e., less than 25%) of fine materials is mixed with coarse soil (Monkul and Ozden, 2007; Çabalar, 2010; Çabalar and Hasan, 2013).

The changes in soil structure and the rearrangement of soil particles due to the addition of CDMs clearly affected the compressibility of the clay. Figures 5.55 and

5.56 respectively show the reduction of compression index (Cc) and swelling index (Cs) by due to increases in CDMs for load increments from 200kN/$m^2$ to 400kN/$m^2$. The same behavior was seen for compressibility parameters ($C_c$ and $C_s$) for load increments between 400kN/$m^2$ and 800kN/$m^2$, as shown in Figures 5.57 and 5.58. This change in consolidation parameters can be considered as an improvement of the consolidation characteristics of clay that leads to reduced settlement for structures built on this type of soil.

The improvement is in the amount of consolidation represented by the reduction of $C_c$ and the rate of consolidation represented by $C_v$. From the data in Figures 5.59 and 5.61, it is apparent that the increase in the coefficient of consolidation ($C_v$) was highlighted. In these two Figures, the relationships between the coefficients of consolidation ($C_v$) and the variations of CDMs for loads of 400kN/$m^2$ and 800 kN/$m^2$ are shown, respectively. This increase in the coefficient of consolidation ($C_v$) is due to the change in soil structure and fabric, which has significant effects on the coefficient of conductivity of soil (k). Figures 5.60 and 5.62 illustrate the relationship between the coefficient of conductivity (k) and the variations of CDMs for loads of 400kN/$m^2$ and 800kN/$m^2$ in the oedometer test. In these Figures, there is a clear trend of k increasing with the increases in CDMs content.

**Table 5.8** Consolidation characteristics of clay and clay-CDMs mixtures

| | | (400)kN/m² | | | | | (800)kN/m² | | | | |
|---|---|---|---|---|---|---|---|---|---|---|---|
| **Mixtures type** | **$e_o$[1]** | **$C_c$[2]** | **$C_s$[3]** | **$m_v$[4]** | **$c_v$[5]** | **k[6]** | **$C_c$[7]** | **$C_s$[8]** | **$m_v$** | **$c_v$** | **k** |
| Clay | 0.511 | 0.061 | 0.0248 | 0.0061 | 0.005 | 3.29677E-05 | 0.092 | 0.0184 | 0.0046 | 0.005 | 2.47927E-05 |
| 5%CBPs | 0.514 | 0.056 | 0.0217 | 0.0046 | 0.011 | 4.88263E-05 | 0.072 | 0.0163 | 0.0028 | 0.010 | 2.81349E-05 |
| 10%CBPs | 0.517 | 0.052 | 0.0207 | 0.0045 | 0.012 | 5.2555E-05 | 0.069 | 0.0160 | 0.0027 | 0.012 | 3.19733E-05 |
| 15%CBPs | 0.519 | 0.048 | 0.0188 | 0.0044 | 0.013 | 5.56037E-05 | 0.061 | 0.0157 | 0.0026 | 0.013 | 3.32878E-05 |
| 20%CBPs | 0.532 | 0.043 | 0.0162 | 0.0043 | 0.014 | 5.90183E-05 | 0.060 | 0.0153 | 0.0029 | 0.014 | 4.07701E-05 |
| 5%DAPs | 0.487 | 0.055 | 0.0184 | 0.0029 | 0.012 | 3.49146E-05 | 0.085 | 0.0172 | 0.0046 | 0.009 | 4.12784E-05 |
| 10%DAPs | 0.479 | 0.051 | 0.0148 | 0.0028 | 0.014 | 4.08418E-05 | 0.084 | 0.0140 | 0.0046 | 0.011 | 5.11601E-05 |
| 15%DAPs | 0.454 | 0.047 | 0.0137 | 0.0026 | 0.020 | 5.03741E-05 | 0.079 | 0.0120 | 0.0044 | 0.015 | 6.48000E-05 |
| 20%DAPs | 0.433 | 0.043 | 0.0120 | 0.0045 | 0.021 | 5.77839E-05 | 0.075 | 0.0112 | 0.0040 | 0.018 | 7.29343E-05 |
| 5%CCPs | 0.504 | 0.048 | 0.0227 | 0.0045 | 0.011 | 5.06637E-05 | 0.073 | 0.0172 | 0.0039 | 0.009 | 3.51175E-05 |
| 10%CCPs | 0.480 | 0.034 | 0.0194 | 0.0051 | 0.013 | 6.40831E-05 | 0.057 | 0.0162 | 0.0027 | 0.015 | 4.00178E-05 |
| 15%CCPs | 0.465 | 0.032 | 0.0182 | 0.0036 | 0.022 | 7.97916E-05 | 0.053 | 0.0170 | 0.0028 | 0.017 | 4.70455E-05 |
| 20%CCPs | 0.465 | 0.028 | 0.0127 | 0.0036 | 0.022 | 8.16246E-05 | 0.052 | 0.0134 | 0.0026 | 0.021 | 5.69354E-05 |

1: Initial void ratio 2: Compression index for pressure (200-400) kN/m$^2$ 3: Swelling index for pressure (200-400) kN/m$^2$ 4: Coefficient of volume change cm$^2$/gm
5: coefficient of consolidation cm$^2$/sec 6: Coefficient of conductivity cm/sec 7: Compression index for pressure (400-800) kN/m$^2$
8: Swelling index for pressure (400-800) kN/m$^2$

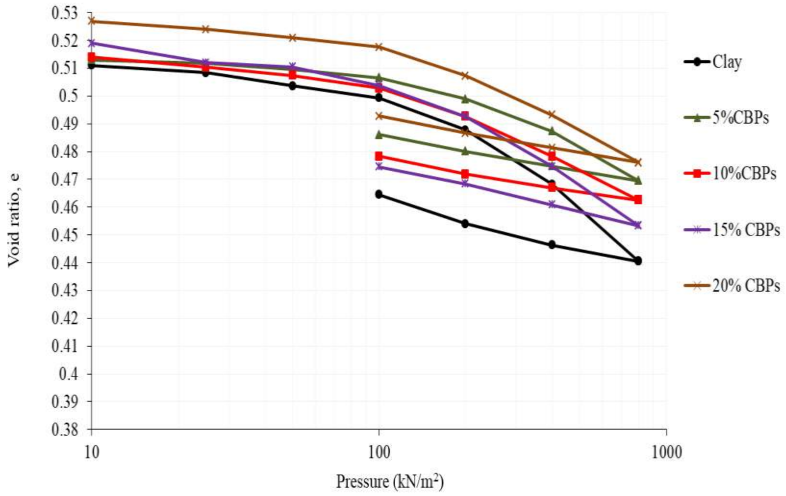


**Figure 5.50** Compression curve (e-log p) for clay and clay-CBPs mixtures

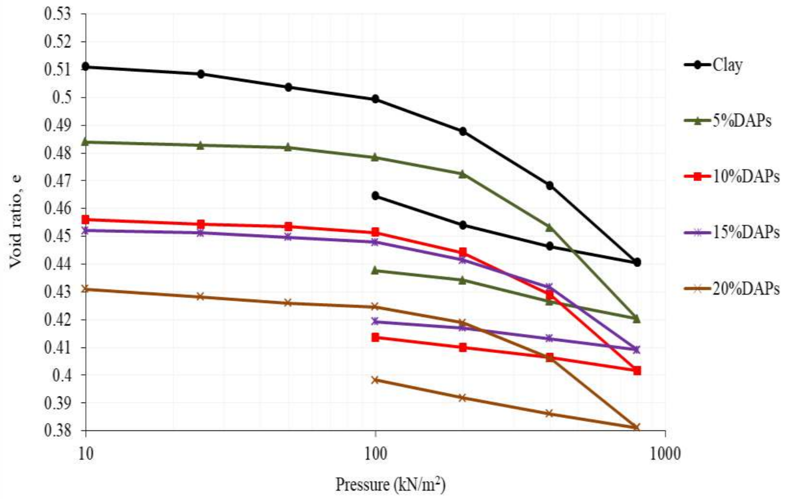


**Figure 5.51** Compression curve (e-log p) for clay and clay-DAPs mixtures

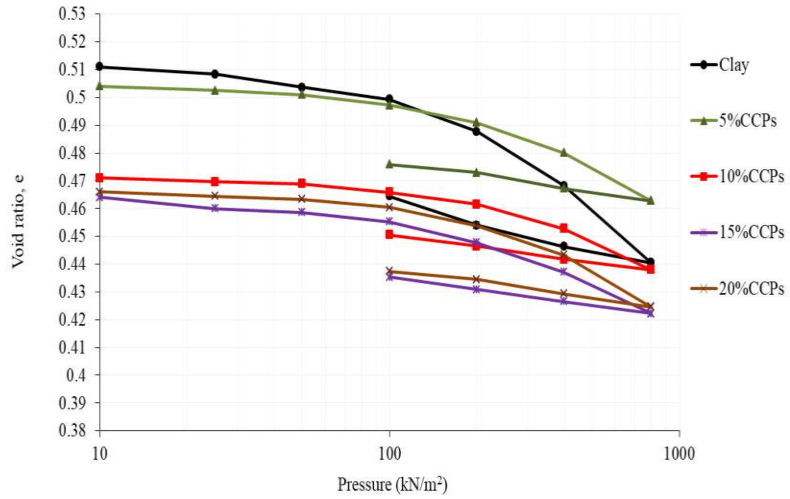


**Figure 5.52** Compression curve (e-log p) for clay and clay-CCPs mixtures

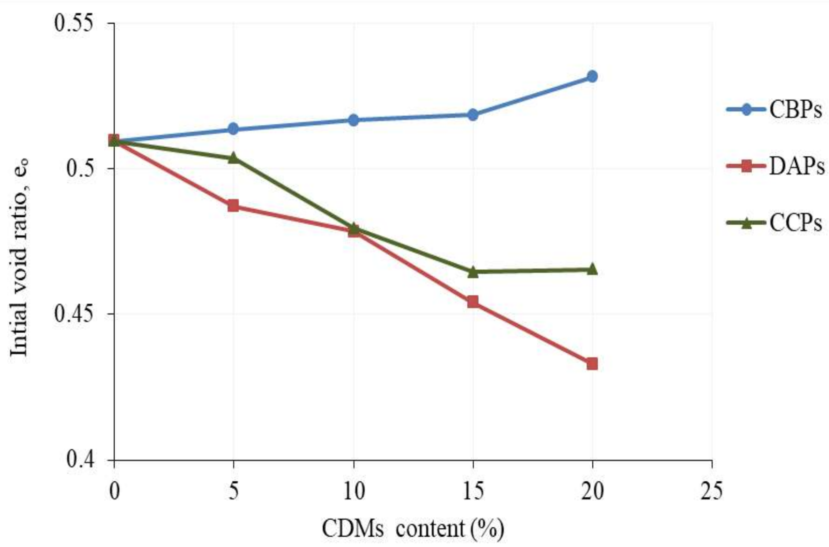


**Figure 5.53** Relation between the initial void ratio ($e_o$) and the variation of CDMs content

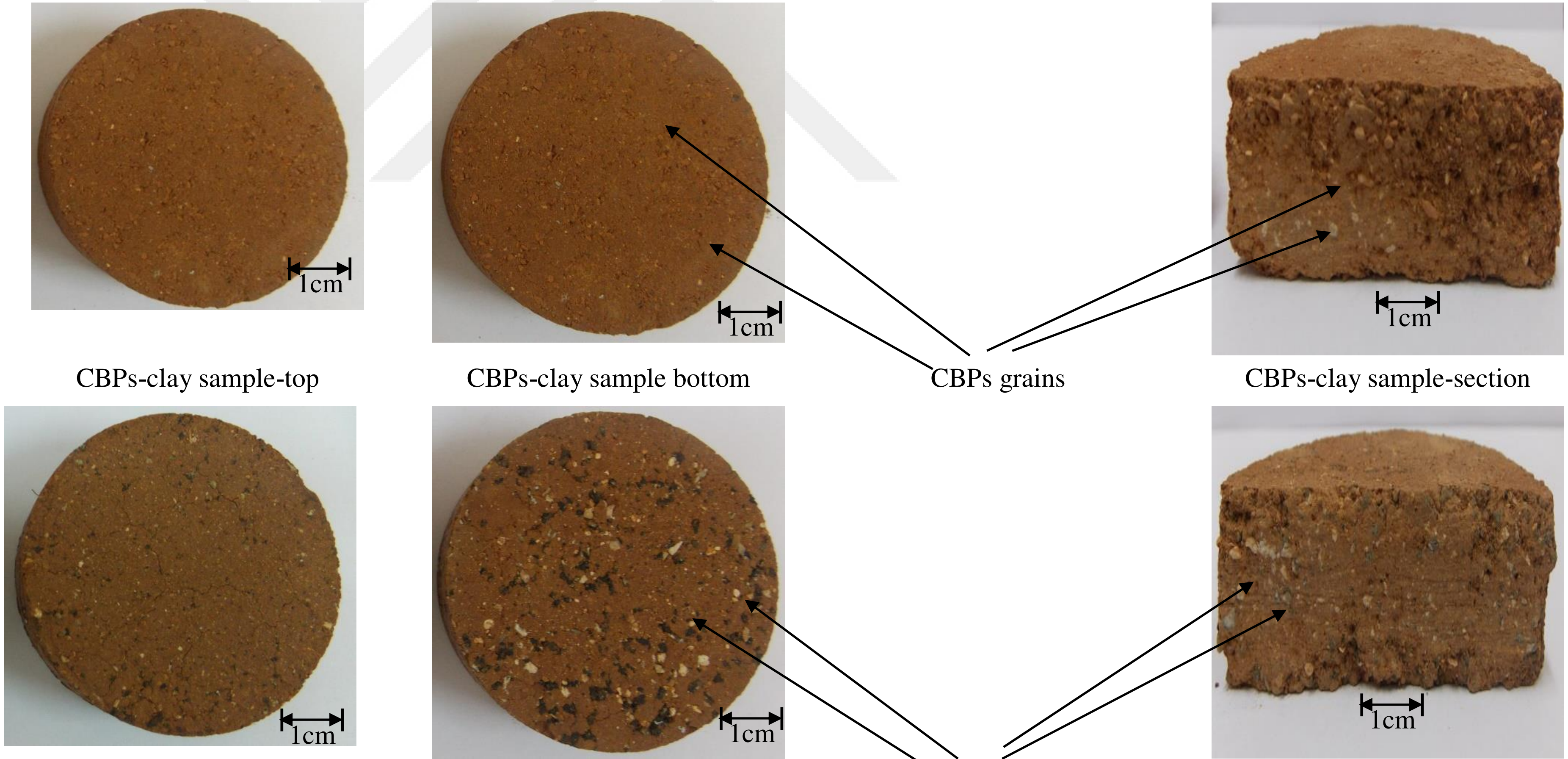


CBPs-clay sample-top | CBPs-clay sample bottom | CBPs grains | CBPs-clay sample-section

DAPs-clay sample-top | DAPs-clay sample bottom | DAP grains | DAPs-clay sample-section

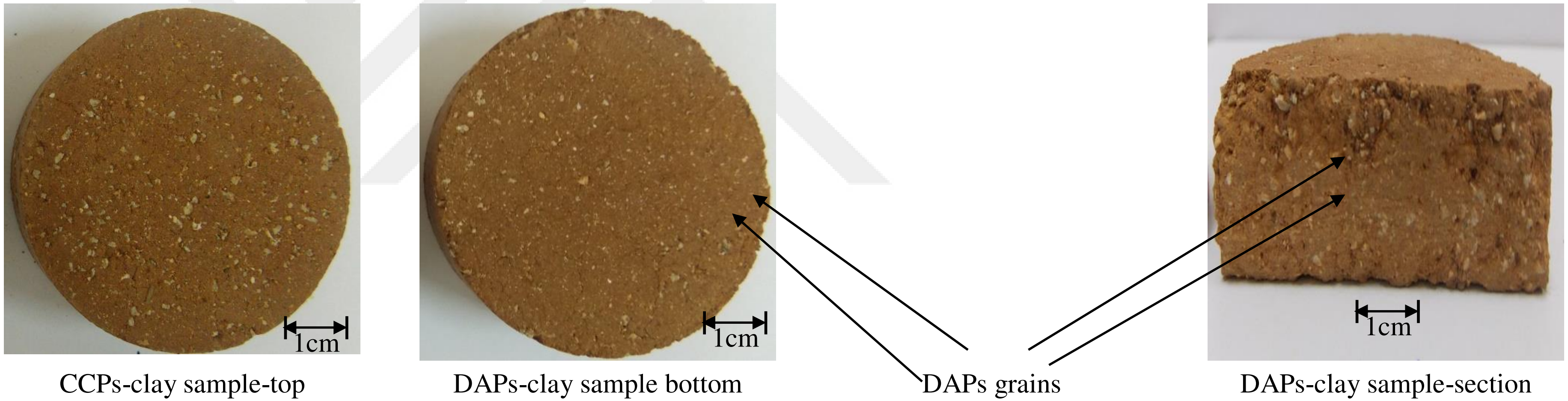


**Figure 5.54** Pictures of clay-CDMs oedometer samples (left) samples top, (medium) samples bottom (right) samples section

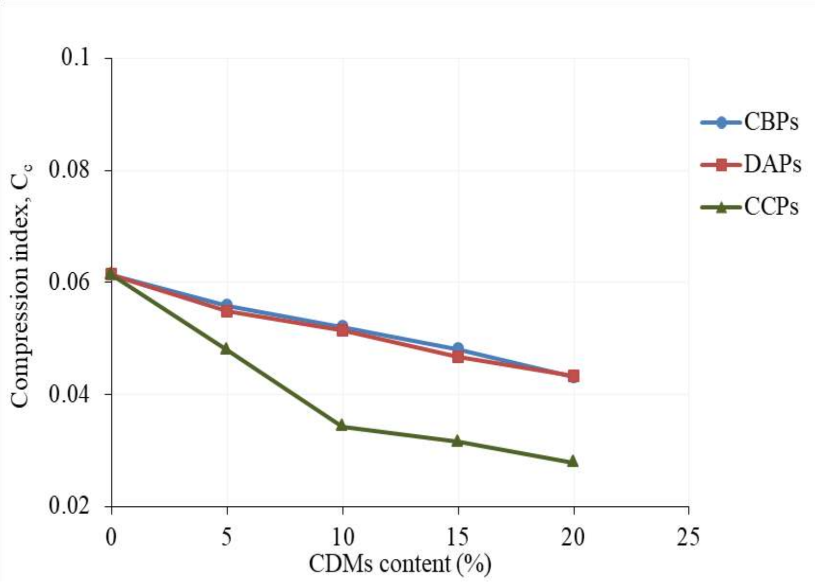


**Figure 5.55** Relation between the compression index ($C_c$) and variation of CDMs for pressure increment from 200 to 400 kN/m$^2$

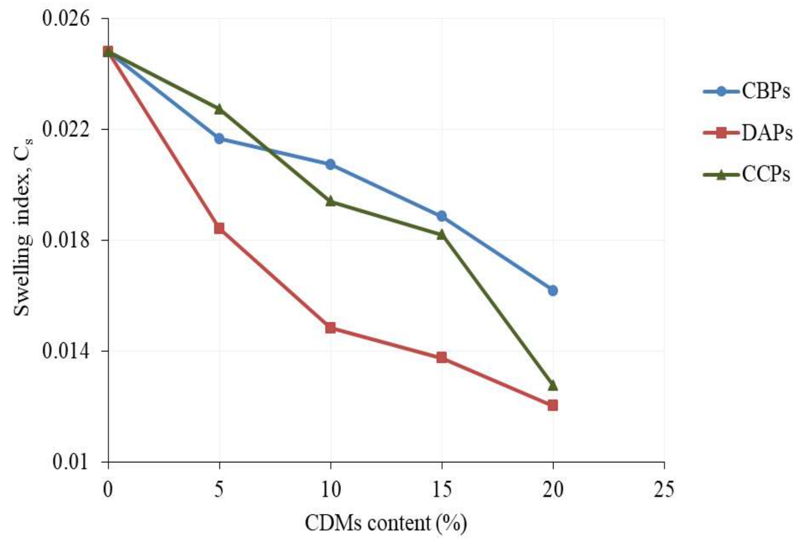


**Figure 5.56** Relation between the swelling index ($C_s$) and variation of CDMs for pressure increment from 200 to 400 kN/m$^2$

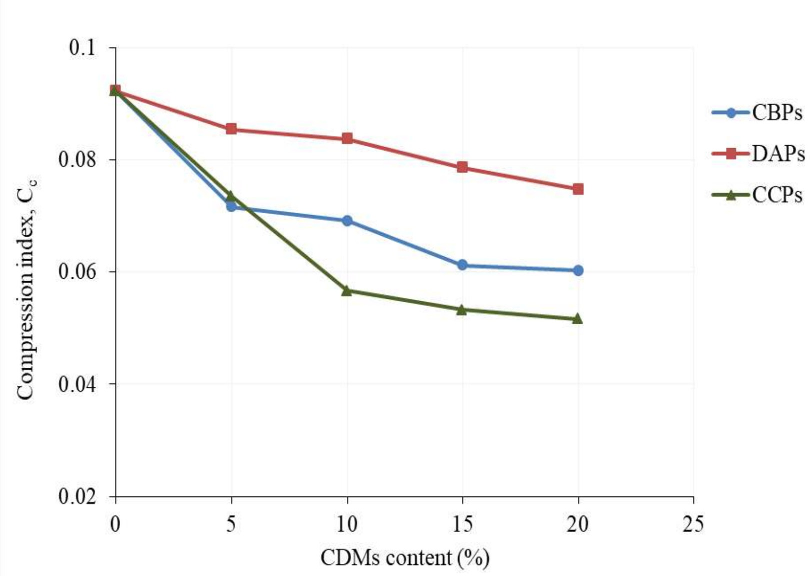


**Figure 5.57** Relation between the compression index ($C_c$) and variation of CDMs for pressure increment from 400 to 800 kN/m$^2$

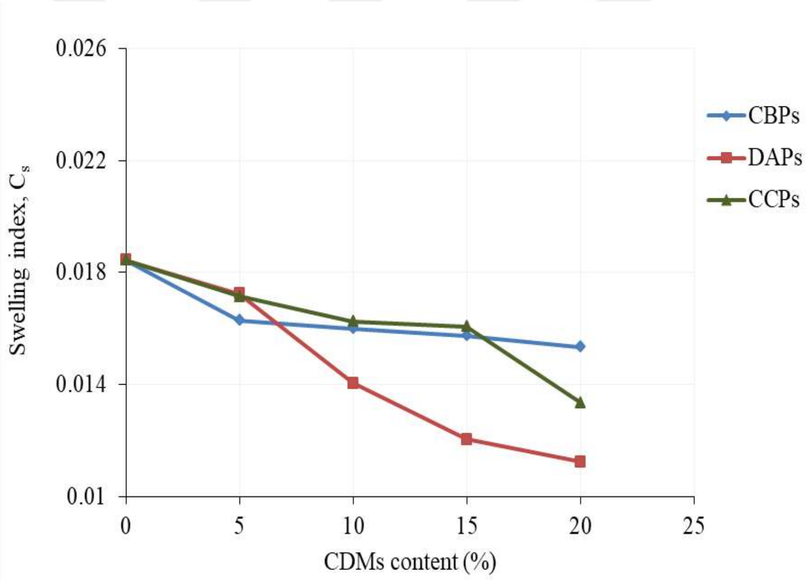


**Figure 5.58** Relation between the swelling index ($C_s$) and variation of CDMs for pressure increment from 400 to 800 kN/m$^2$

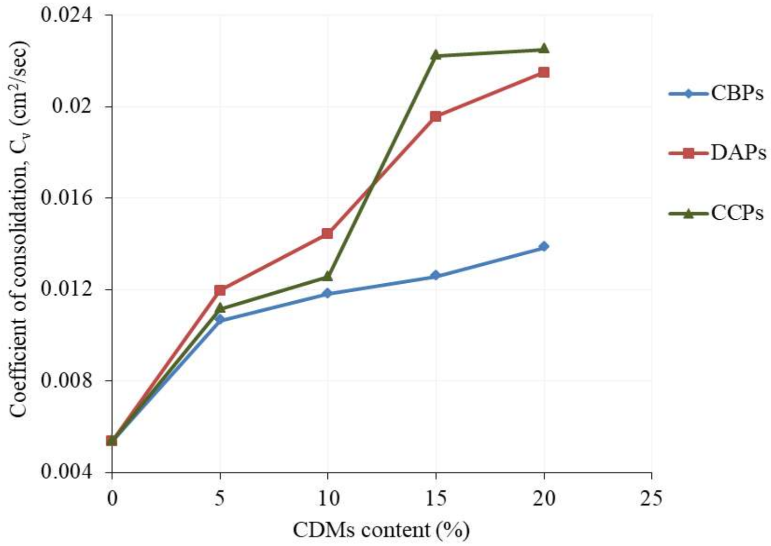


**Figure 5.59** Relation between the coefficient of consolidation ($C_v$) and variation of CDMs for pressure 400 kN/$m^2$

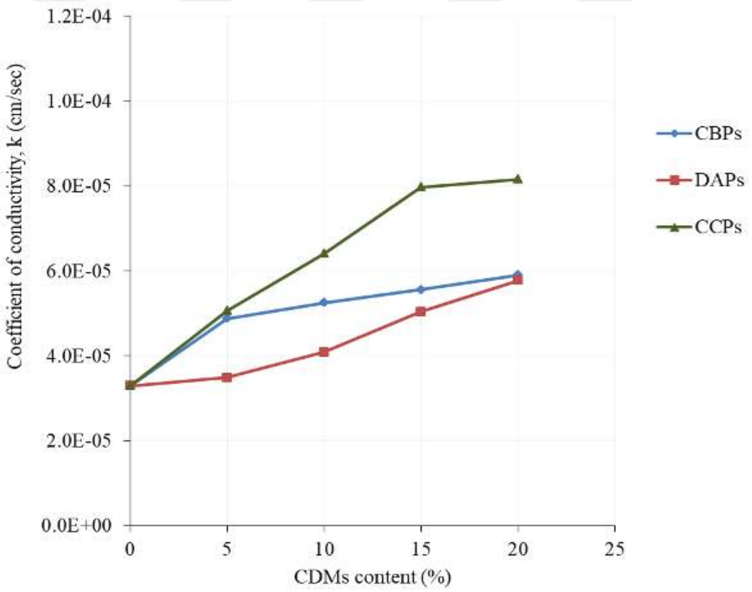


**Figure 5.60** Relation between the coefficient of conductivity (k) and the variation of CDMs for pressure 400 kN/$m^2$ in oedometer test

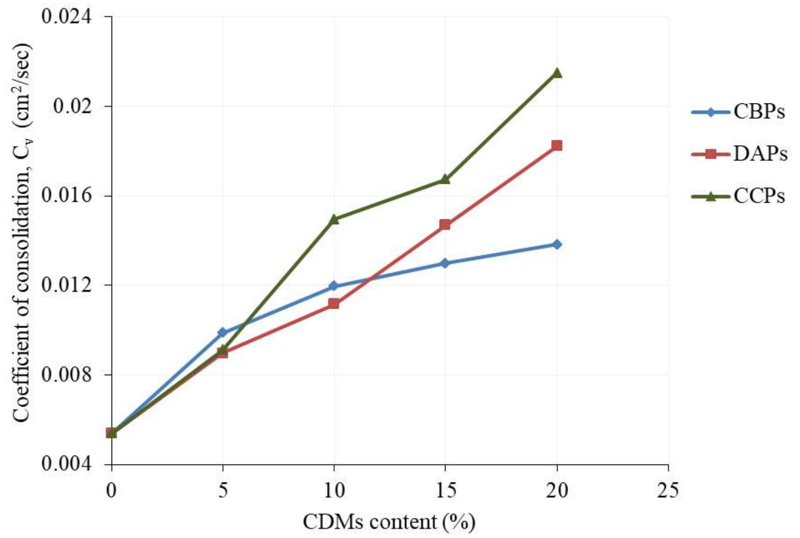


**Figure 5.61** Relation between the coefficient of consolidation ($C_v$) and variation of CDMs for pressure 800 kN/$m^2$

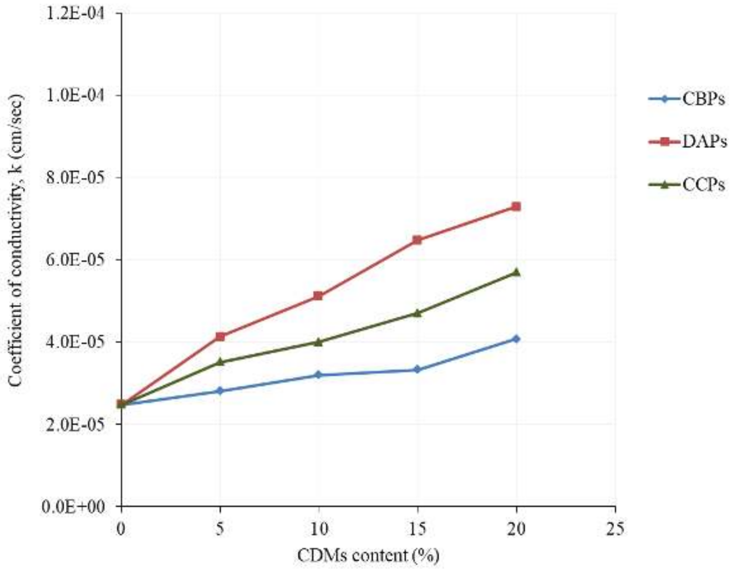


**Figure 5.62** Relation between the coefficient of conductivity (k) and the variation of CDMs for pressure 800 kN/$m^2$ in oedometer test

## 5.2 Theoretical Results

The first part of the theoretical study included the calculating of ultimate bearing capacity for clay and clay-CDMs mixtures using direct shear and plate load tests and comparing the results.

The second part included making a comparison between the pressure-settlements curve of footing obtained using plate load tests and those calculated using geotechnical software (Plaxis) for clay and clay-CDMs mixtures.

### 5.2.1 Bearing capacity results

The results of bearing capacity were obtained using the results of two tests, direct shear test for clay and clay-CDMs, and plate load test for clay and clay-10% CDMs.

Table 5.9 shows that the results of bearing capacity depend on the direct shear test and plate load test. In this table, the bearing capacity factors that rely on the angle of internal friction ($\phi'$) and the bearing capacity values were calculated using Terzaghi's ultimate bearing capacity equation. The calculations were based on the situation of circular footing with three different diameters and a 1.0m footing depth. Figure 5.63 shows the relation between the variations of CDMs and the ultimate bearing capacity in kN/m$^2$ for the three footing diameters, depending on the direct shear test parameters. The findings shown in Table 5.9 and Figures 5.63 reveal that there were general increases in ultimate bearing capacity with increasing amounts of CBP and CCP materials, whereas there was a clear decreasing trend in ultimate bearing capacity with increasing proportions of DAPs materials. This finding highlights the effect of the types and sizes of CDMs used to find strength parameters of soil ($\phi'$ and $c'$) in the direct shear test, which was used to calculate the ultimate bearing capacity. While the CBP and CCP are almost consider hard, homogenous materials, even when crushed to a fine material (2mm), the DAPs materials consist of two materials, hard aggregate coated with a weak asphalt film. When the DAPs materials are crushed into fine aggregate, the coating asphalt controls the behavior of the DAPs and the soil mixed with it. The concentration of CDMa in the middle of the predetermined failure plane in the direct shear test and had an effect on the strength parameters of soil ($\phi'$ and $c'$), which were used to calculate the bearing capacity. This finding provides evidence about the variation in both the increasing and decreasing of ultimate bearing capacity values with the increasing of CDMs content in soil mixtures. The effect of footing diameter on the bearing capacity was slight according to Terzaghi's ultimate bearing capacity equation.

The ultimate bearing capacity obtained from plate load testing is given in Table 5.9 for clay and clay-10%CDMs. As Table 5.9 shows, there is a significant difference between the two groups of ultimate bearing capacities obtained from the direct shear test and plate load test. The significant differences between the results are attributed to the type and boundary conditions for each test. The bearing capacity calculated according to the strength parameters of soil ($\phi'$) and ($c'$) in the direct shear test was calculated using small consolidated soil samples with predetermined failure planes. Conversely, the bearing capacities calculated from the plate load test results was obtained directly from the pressure reading of the equipment during application of the load. The test was done in a large box model filled with compacted soil samples.

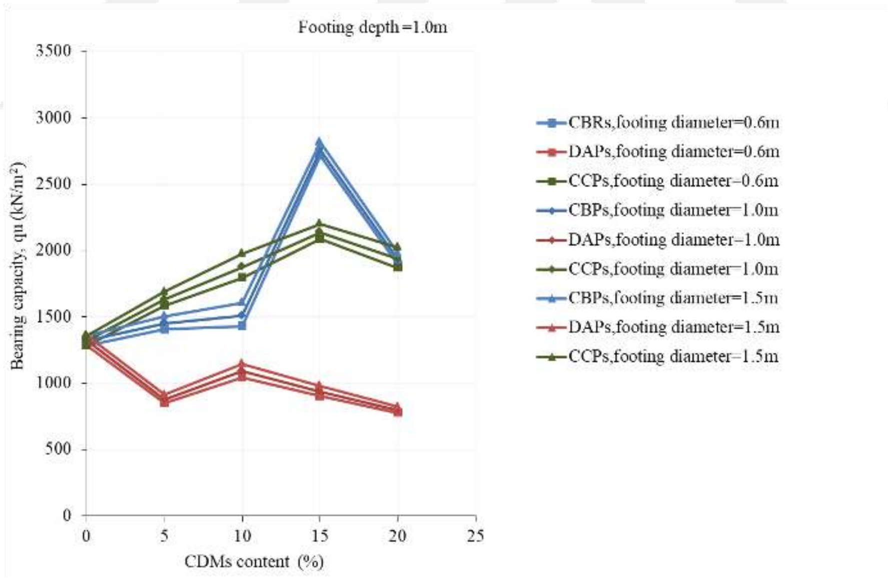


**Figure 5.63** Bearing capacity values for clay and clay-CDMs for different footing diameters (depending on direct shear test parameters)

**Table 5.9** Bearing capacity results for clay and clay-CDMs mixtures.

| Mixtures type | CDMs content (%) | Effective cohesion (c′) | Effective angle of internal friction (ϕ′) | Terzaghi's bearing capacity factors | | | Ultimate bearing capacity values kN/m$^2$ | | | |
|---|---|---|---|---|---|---|---|---|---|---|
| | | | | | | | From direct shear test | | | From plate load test |
| | | | | $N_c$ | $N_q$ | $N_\gamma$ | B=1.5m | B=1.0m | B=0.6m | B=0.6m |
| Clay | 0 | 20.0 | 29.0 | 16.18 | 19.98 | 34.24 | 1362 | 1320 | 1286 | 200 |
| CBPs [a] | 5 | 17.0 | 30.5 | 21.00 | 24.00 | 42.00 | 1505 | 1451 | 1407 | |
| CBPs | 10 | 5.0 | 34.0 | 38.04 | 36.5 | 52.64 | 1607 | 1509 | 1430 | 300 |
| CBPs | 15 | 42.0 | 31.0 | 22.65 | 25.28 | 40.41 | 2817 | 2759 | 2712 | |
| CBPs | 20 | 30.0 | 30.0 | 19.13 | 22.46 | 37.16 | 1981 | 1931 | 1892 | |
| DAPs [b] | 5 | 12.0 | 28.0 | 13.70 | 17.81 | 31.61 | 915 | 878 | 850 | |
| DAPs | 10 | 5.0 | 30.5 | 21.00 | 24.00 | 42.00 | 1145 | 1089 | 1044 | 350 |
| DAPs | 15 | 11.0 | 29.0 | 16.18 | 19.98 | 34.24 | 980 | 937 | 902 | |
| DAPs | 20 | 15.0 | 25.8 | 9.00 | 13.20 | 26.00 | 822 | 797 | 778 | |
| CCPs [c] | 5 | 20.5 | 31.0 | 22.65 | 25.28 | 40.41 | 1691 | 1632 | 1585 | |
| CCPs | 10 | 12.0 | 34.0 | 38.04 | 36.50 | 52.64 | 1976 | 1875 | 1794 | 350 |
| CCPs | 15 | 28.0 | 31.5 | 24.00 | 27.00 | 42.00 | 2202 | 2138 | 2086 | |
| CCPs | 20 | 19.0 | 33.0 | 31.94 | 32.23 | 48.09 | 2023 | 1938 | 1869 | |

a: Crushed bricks pieces (CBPs) b: Dumped asphalt pieces (DAPs) c: Crushed concrete pieces (CCPs)

### 5.2.2 Pressure- settlement curves results of Plaxis 2D simulation

#### 5.2.2.1 Estimation of modulus of elasticity

The input parameters used in the Plaxis 2D simulation for clay and clay-CDMs mixtures are shown in Table 5.11. The values of $E_{ref}$ used in the table are presented, and these values can be used to make the best pressure-displacement curves matching of the actual plate load test and the Plaxis simulation. The $E_{ref}$ values give the best matching pressure-displacement curve of the actual plate load test, and the Plaxis simulation depends on the nature of the CDMs and the geotechnical properties of clay-CDMs mixtures. The comparison between the $E_{ref}$ values for different soils in Table 5.11 and Table 5.10, which was given by Das and Sobhan (2014), shows two notable things. First, the $E_{ref}$ used in the simulation represent reasonable values according to Table 5.10 because these values can classify medium to hard clay, which represents the soil type used in the test. Second, the additions of CDMs increase the Es values of soil because these materials have high Es values compared to soil (10-50×$10^6$ kN/$m^2$ for bricks and 25-38×$10^6$ kN/$m^2$, according to materials data book, 2003).

**Table 5.10** Representative values of the modulus of elasticity (Das and Sobhan, 2014)

| Soil type | Es (modulus of elasticity) kN/$m^2$ |
|---|---|
| Soft clay | 1800- 3500 |
| Hard clay | 6000- 14000 |
| Loose sand | 10000- 28000 |
| Dense sand | 35000- 70000 |

#### 5.2.2.2 Pressure- Settlement curves of actual plate load and Plaxis 2D simulation

Table 5.11 shows the parameters used to estimate the pressure-settlement curves as output for the plate load test using the Plaxis2D simulation of the box model. Figures 5.64 through 5.67 illustrate the comparison between the real pressure-settlement curves and the Plaxis 2D simulation of the plate load test for clay and clay-CDMs mixtures. From the data in the previous figures, it is apparent that the simulation of plate load test using Plaxis 2D software gives accurate and reasonable results. The Plaxis simulation of pressure-settlement curves shows significant agreement for clay and clay-CDMs mixtures. The results show some divergence, especially at the failure stages (plastic stage). This variation of the results is due to the significant differences in the methods of calculation for the pressure-settlement curves. The actual plate load test is represented by pressures applied by a jack to a bearing plate sitting in the soil with settlements reading taken with pressure. The simulated plate load test involved putting the materials' input parameters into the program. On the one hand, the actual plate load test was carried out on clay and clay mixed with different sizes (less than 19mm) of CDMs aggregate, which had a large influence on the results. On the other hand, the Plaxis 2D results depend on the parameters results from the experimental tests, and the conditions may have varied from those of the physical box model.

In spite of some diverging results, the general results display close correlation between the experimental and theoretical results, as shown in Figures 5.68 through 5.71. In these figures, the pressure-settlement curves from the actual test and Plaxis 2D simulation were connected by a linear equation to determine the correlation factor ($R^2$), which used as an index for the results. It is apparent that the Plaxis 2D simulation gives a considerable representation of the curves' trends and the maximum pressure values of the actual pressure-settlement curves. Reasonably, increasing $E_{ref}$ increases the maximum pressure value at any specific settlement of the pressure-settlement curves, as shown in the Figures 5.64 through 5.67. This finding provides evidence about the effect of modulus of elasticity on soil settlement, especially elastic settlement based on elastic theory, as represented by Equation 5.1 (Das and Sobhan, 2014).

$$S_c = \Delta\sigma(\alpha\acute{B})\frac{1-\mu_s}{E_s}I_sI_f \tag{5.1}$$

Where Es in the previous equation represent the average modulus of elasticity of the soil, measured from under the foundation to (5B), whereas B is the foundation diameter.

**Table 5.11** Input parameters used in the Plaxis 2D simulation of the plate load test

| **Plaxis model properties** | **clay** | **10% CBPs** | **10% DAPs** | **10% CCPs** |
|---|---|---|---|---|
| Materials model | Mohr-Coulomb | Mohr-Coulomb | Mohr-Coulomb | Mohr-Coulomb |
| Materials type | Undrain | Undrain | Undrain | Undrain |
| General properties | | | | |
| $\gamma_{unsat.}$ (unsaturated field density) | 18.37 | 18.20 | 18.16 | 18.52 |
| $\gamma_{sat.}$ (saturated field density) | 19.13 | 18.67 | 18.98 | 18.97 |
| Horizontal permeability m/day | 3.814E-08 | 6.082E-8 | 4.726E-8 | 7.417E-8 |
| Vertical permeability m/day | 3.814E-08 | 6.082E-8 | 4.726E-8 | 7.417E-8 |
| Final $E_{ref}$* (modulus of elasticity) Kn/m$^2$ | 2500-5000 | 10000-15000 | 2500-8500 | 2500-11000 |
| ν (Poisson's ratio) | 0.34 | 0.305 | 0.33 | 0.305 |
| $C_{ref}$ (cohesion) Kn/m$^2$ | 20.0 | 5.0 | 5.0 | 12.0 |
| ϕ Effective angle of internal friction (ϕ′) | 29.0 | 34.0 | 30.5 | 34.0 |
| Ψ (psi) | 0.0 | 4.0 | 0.5 | 4.0 |

*: The final range of values of $E_{ref}$ used in this table present the values gave the best matching pressure-displacement curve of actual and the Plaxis simulation.

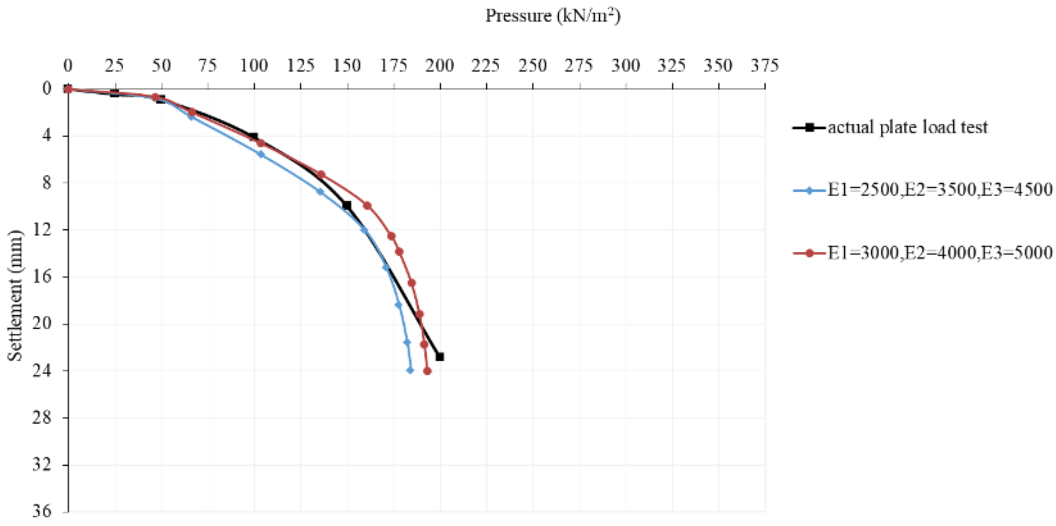


**Figure 5.64** Pressure-settlement curves for actual plate load test and Plaxis 2D simulation of clay

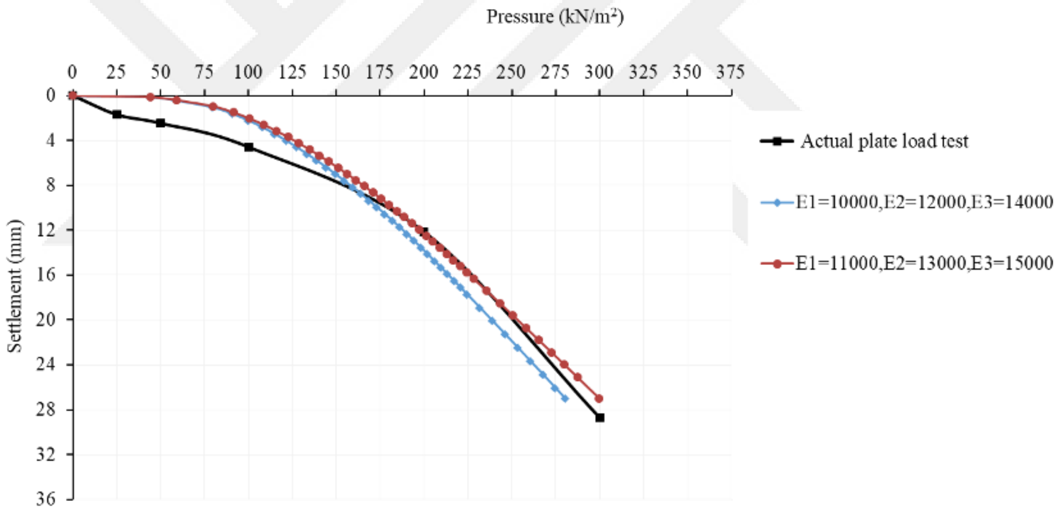


**Figure 5.65** Pressure-settlement curves for actual plate load test and Plaxis 2D simulation of 10% CBPs

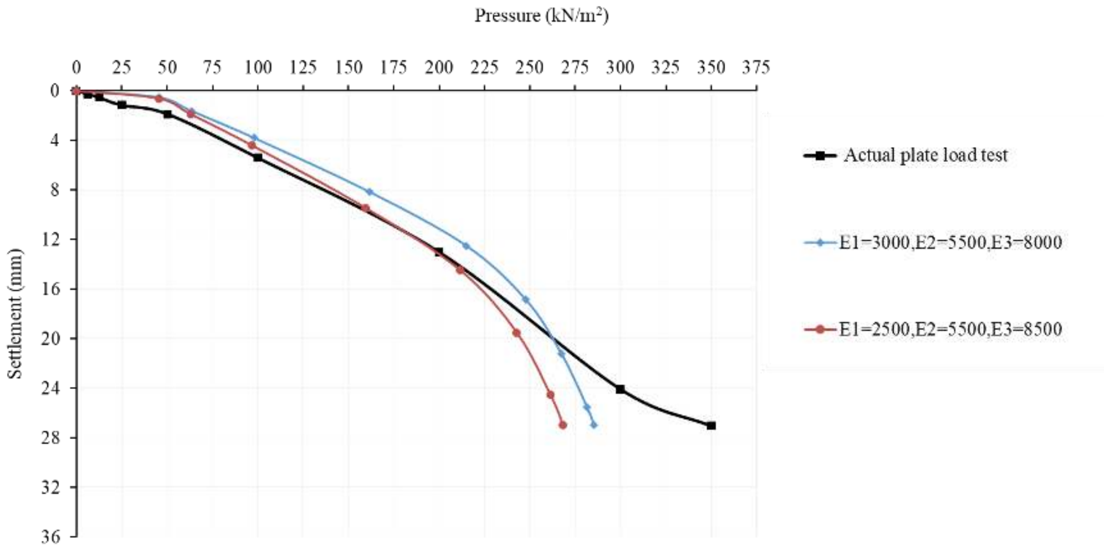


**Figure 5.66** Pressure-settlement curves for actual plate load test and Plaxis 2D simulation of 10% DAPs

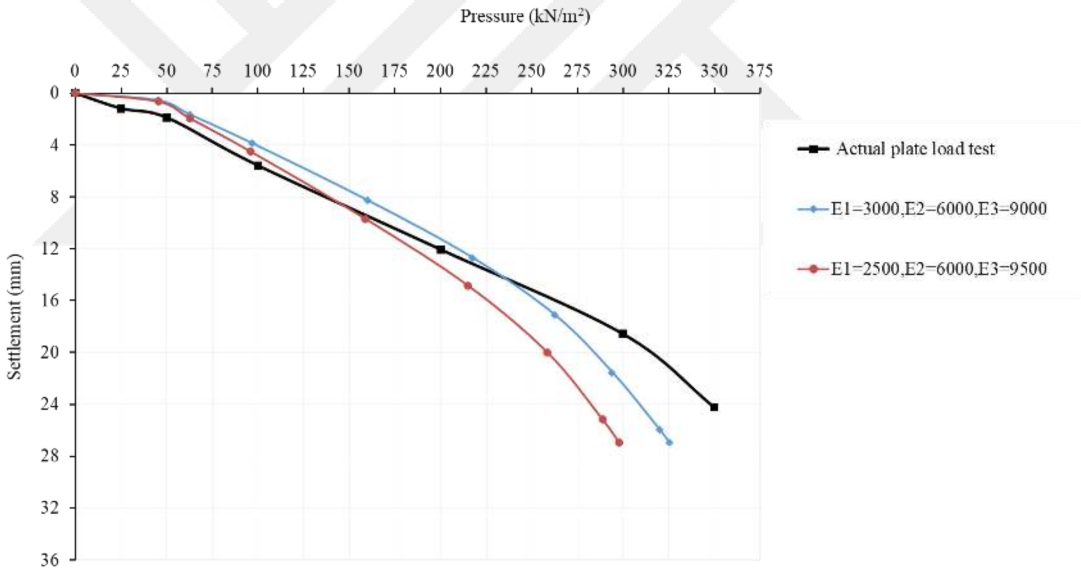


**Figure 5.67** Pressure-settlement curves for actual plate load test and Plaxis 2D simulation of 10% CCPs

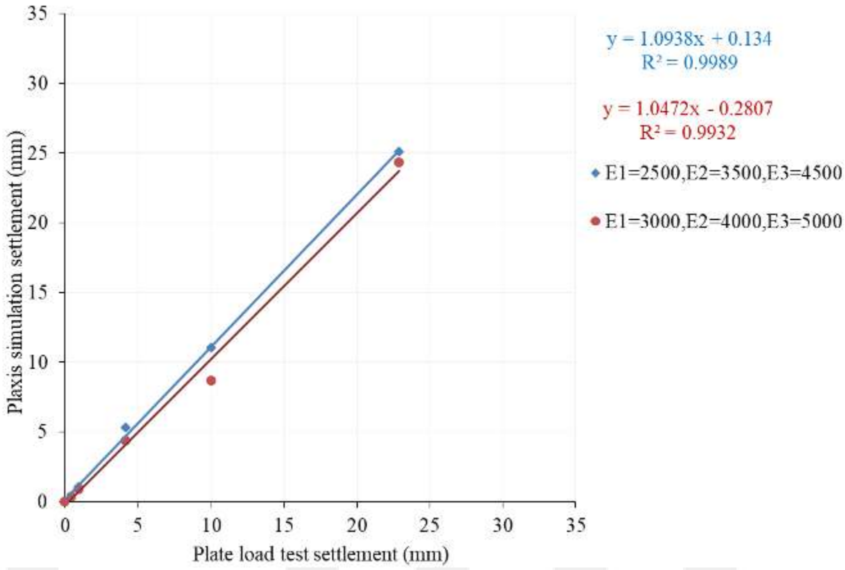


**Figure 5.68** Relation between settlement values at the same pressure for actual plate load test and Plaxis 2D simulation of clay

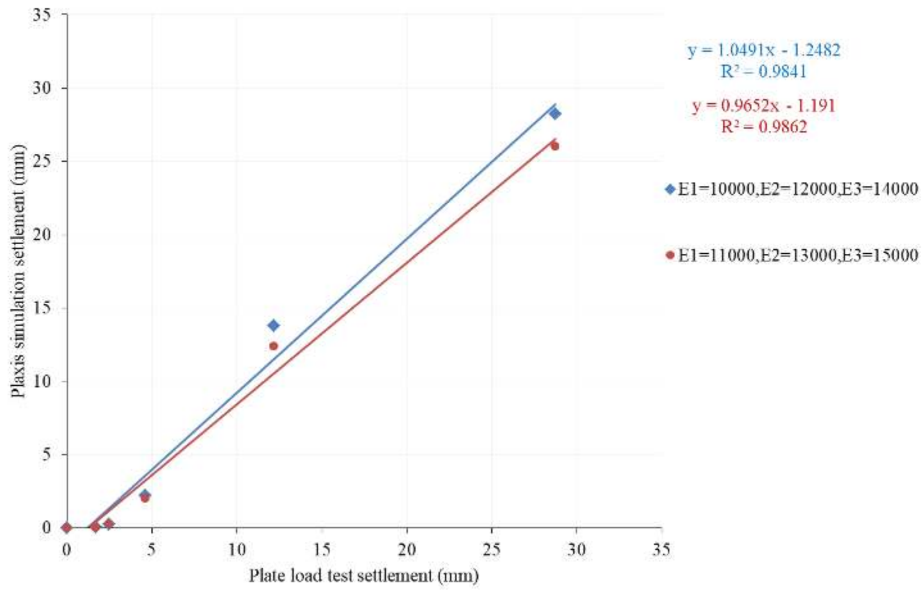


**Figure 5.69** Relation between settlement values at the same pressure for actual plate load test and Plaxis 2D simulation of 10% CBPs

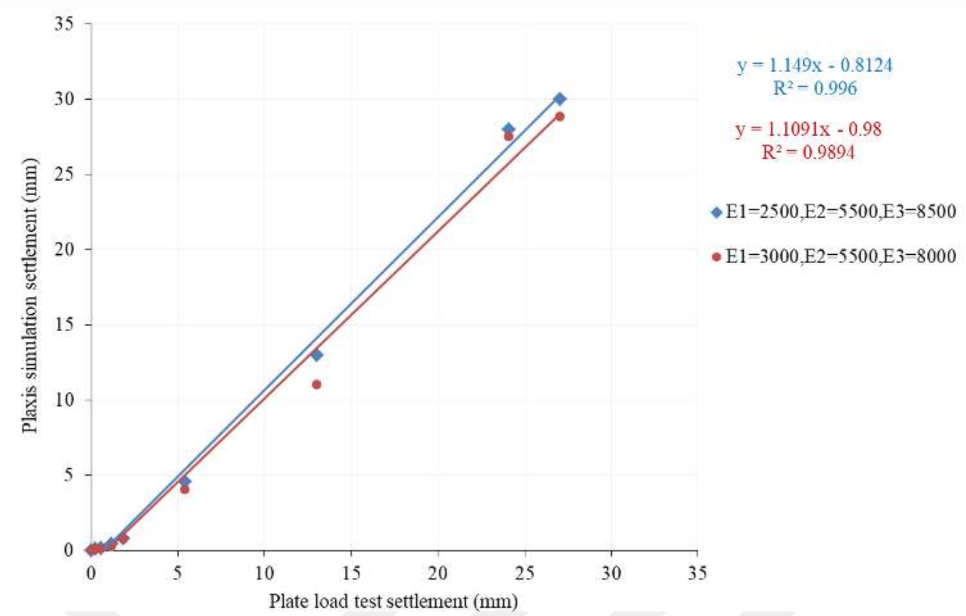


**Figure 5.70** Relation between settlement values at the same pressure for actual plate load test and Plaxis 2D simulation of 10% DAPs

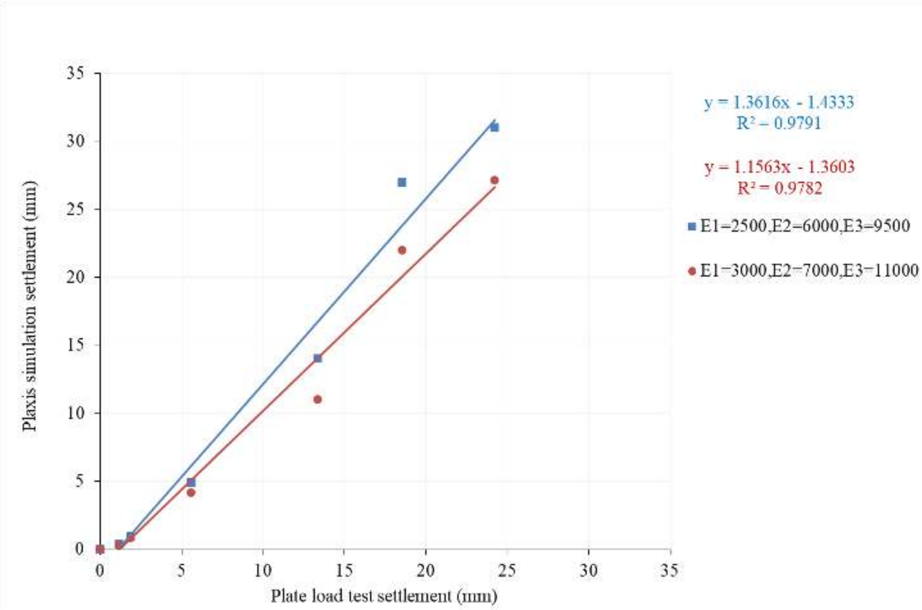


**Figure 5.71** Relation between settlement values at the same pressure for actual plate load test and Plaxis 2D simulation of 10% CCPs

# CHAPTER 6

# CONCLUSIONS AND RECOMMENDATIONS

## 6.1 Conclusions

This study was divided into two parts. The experimental part involved investigating the effects of three types of CDMs (CBPs, DAPs, and CCPs) on some geotechnical properties of clay. At the beginning, the experiment included taking SEM pictures and EDXs for clay and CDMs. After that, the index properties, including the consistency limits and sieve analysis, were done to determine the classification of clay and clay-CDMs mixtures.

The oedometer set of tests were done to estimate the swelling and consolidation characteristics of clay and clay-CDMs mixtures.

The strength of clay and clay-CDMs mixtures was investigated using four tests: CBR test, UCS test, direct shear test, and plate load test using a box model.

Therefore, the conclusions taken from the experimental study are presented in three groups: (1) the general and index properties of clay and clay-CDMs mixtures, (2) the oedometer test characteristics, and (3) the strength characteristics of clay and clay-CDMs mixtures.

(1) The conclusions are the general and index properties of clay and clay-CDMs mixtures:

The effects of the three CDMs on the plasticity of clay are represented by the consistency limits (liquid limit, plastic limit, and PI) and the classification of clay, which depend on the consistency limits and grain size distribution. In addition to the SEM pictures and EDXs for clay and CDMs, the consistency limits and grain size distribution give extensive indications of changes in the geotechnical properties of clay as a result of the addition of CDMs.

The index properties offer assistance in the explanation of clay-CDMs behavior and, the estimation of strength and oedometer parameters for clay-CDMs mixtures. There are little-known efforts to study the effect of CDMs on the plasticity and classification of clay.

- The EDX analysis of clay and CDMs gives evidence about the natural mineral compounds of these materials. This analysis led to the best understanding of the geotechnical properties of clay- CDMs mixtures.
- The liquid limits and PI of clay decrease as the CDMs percentages increase. These decreases are reflected in the geotechnical properties (swelling, consolidation, and soil strength).
- The classification of clay changes from CL to ML with CBP and CCP additives according to USCS while it changes from A-7-6 to A-6 for all CDMs additives according to AASHTO.

(2) The conclusions are taken from oedometer tests of clay and clay-CDMs mixtures:

This study deals with one of the biggest problems with the clay. Large volume changes happen in clay when the water content changes in this type of soil. The effects of mixing some types of CDMs with clay were investigated. To the author's best knowledge, previous studies on CDMs were only focused on the strength properties of these materials. Although these investigations reported many interesting results, little work has been done to examine the effects of CDMs on the oedometer characteristics of clay.

- The results showed that the oedometer test (swelling test) gives swelling percentages greater than CBR test for all clay-CDMs mixtures.
- The addition of CDMs with small particles (less than 2mm) in the oedometer test led to more swelling percentage than when large particles (i.e., less than 19mm) were used in the CBR test.

- Due to its high organic content and water absorption, increasing the DAPs content gives causes an increased swelling percentage and pressure for clay in both CBR and oedometer tests.

- Increasing the DAPs and CCPs content increased the maximum dry density of clay and causes increased swelling percentages and pressures.

- Increasing the CBPs content gives reduces the swelling percentage and pressure. Therefore, it is promising for use as a stabilizer for clay after further studies.

- Generally, increasing the CDMs content has a positive effect on the consolidation features of clay.

- All CDMs decreased the consolidation of clay by decreasing the compression index ($C_c$).

- The time of consolidation for clay was decreased due to the increasing of the coefficient of consolidation ($C_v$) and coefficient of conductivity (k) for clay-CDMs mixtures.

(3) The conclusions are taken from the strength tests of clay and clay-CDMs mixtures:

To gain a deep understanding of the effects of adding CDMs to clay on clay strength, the strength of clay was first tested using the CBR test. Then the UCS test was used as another indicator of clay-CDMs strength. The direct shear test was used to identify the strength parameters ($\phi'$ and $c'$) of soil of clay and clay-CDMs mixtures. The behavior of clay and clay-CDMs mixtures under plate load was checked using a large box model. These four tests have dissimilar test procedures and conditions. It appears from previous investigations that numerous studies have been conducted to determine the strength of clay and CDMs individually. However, to the best of the author's knowledge, no researchers have studied the effects of CDMs on the strength of clay.

- Generally, the strength of clay, as represented by CBR and UCS values, increased with increasing CDMs percentages. The CCPs was found to increase strength more than the other materials. The strength enhancement depends on the type of test and the type of CDMs mixed with clay.

- A small increase in maximum dry unit weight ($\gamma_{drymax}$) for clay was found after increasing CDMs percentages.

- A slight reduction in optimum water content ($w_{opt}$) was found for clay after increasing the CBPs and CCPs percentages, more than the reduction caused by increasing DAPs percentages.

- Generally, adding CBPs and CCPs increases the angle of internal friction ($\phi'$) while adding DAPs decreases it.

- The addition of 10% CDMs gives the maximum angle of internal friction ($\phi'$). However, the same percentage leads to minimum cohesion ($c'$).

- In the direct shear test, the predetermined plane of failure, the size of CDMs, and the concentration of these materials in the middle of the soil samples had significant effects on the fluctuations of the results.

- The results also show that, for any specific displacement obtained by the direct shear test, the CCPs materials give almost the highest shear stress, whereas the DAPs materials give the lowest shear stress.

- The results of the plate load test show that the addition of CDMs increased the ultimate bearing capacity of clay.

- The results of the plate load test also showed that for any specific time, the CCPs had the less settlement than the other CDMs.

- Generally, the clay and the CBP material exhibit the same bearing failure (punching failure) behavior. Nevertheless, the most obvious failure region was seen in clay.

- The internal stress (pressure cell transducer reading) at the bottom of the clay was increased due to the increasing induced stress (plate load pressure), by about 100% (double) for the clay and clay-10% CDMs mixtures.

- Generally, the results from the strength tests of clay and clay-CDMs mixtures indicated the possibility of using CCP and CBP to stabilize this type of clay with a degree of confidence larger than obtained when using DAPs materials.

The two theoretical objectives of the study were, first, to estimate the ultimate bearing capacity for clay and clay-CDMs mixtures using direct shear and plate load tests and comparing the test results and, second, to compare the settlements of footing obtained by plate load testing and geotechnical software (Plaxis 2D) for clay and clay-CDMs mixtures. Some notable conclusions may be considered.

- Generally, the ultimate bearing capacity of clay was increased by the addition of CDMs with different percentages depending on the CDMs type and the method of bearing capacity estimation.

- Remarkable alignment between the results of the numerical simulation and the plate load testing was observed ($R^2$=0.97).

- The modulus of elasticity ($E_{ref}$) had a considerable effect on the soil settlement, especially elastic settlement.

### 6.2 Recommendations for Future Studies

The investigation of the effects of different types of SWMs on soil, especially CDMs, may be a wide area in current and future geo-environmental research. Some recommendations can be drawn from the conclusions of the current research to detect the geotechnical properties of soil-CDMs mixtures in more depth than this study. Therefore, further investigations may be considered concerning the following items:

1. These studies were conducted using clay taken from one location (the Campus of University of Gaziantep, Turkey). The use of the studied CDMs with other problematic soils like organic or collapsible soils is strongly recommended.

2. The current study may be extended using other types of CDMs or SWMs with different percentages or mixtures of these materials.

3. The triaxial test can be used to study the static and dynamic strength properties of clay and clay-CDMs mixtures to improve the understanding of the performance of these materials when used as stabilizers for clay or any soil.

4. Modifications to the box model to investigate the shape of the bearing plate or depth of the pressure cell transducer may add valuable information about clay-CDMs bearing capacity.

5. Experimental studies on soil-SWMs could be associated with theoretical studies using different geotechnical software, and a comparison should be made between experimental and theoretical results.

# REFERENCES

Aatheesan, T., Arulrajah, A., Bo, M.W., Vuong, B., and Wilson, J. (2010). Crushed brick blends with crushed rock for pavement systems, Proc. Institution of Civil Engineers, *Waste& Resource Management*, **163**, 1, 29-35.

Abd Elsamee, W. N. (2013). An experimental study on the effect of foundation depth, size and shape on subgrade reaction of cohesionless soil, *Engineering*, **5**, 10, 785-795

Al-Rawas, A. A., Taha R., Nelson, J.D., Al-Shab, B. T. and Al-Siyabi, H. (2002). A comparative evaluation of various additives used in the stabilization of expansive soils, *Geotechnical Testing Journal*, GTJODJ, **25**, 2, 199-209.

Al-Rawas, A. A., Hagoa, A.W., and Al-Sarmib, H. (2005). Effect of lime, cement and Sarooj (artificial pozzolan) on the swelling potential of an expansive soil from Oman, *Building and Environment*, **40**, 5, 681-687.

Anik, D., Boonstra, C., and Mak, J. (1996). Handbook of sustainable building. James & James, London.

Apotheker, S. (1990). Construction and demolition debris-the invisible waste stream, *Resource Recycling*, **9**, 12, 66-74.

Arm, M. (2003). Mechanical properties of residues as unbound road materials. Land and Water, Royal Institute of Technology, Ph.D. thesis, 1007. Resources Engineering. Stockholm.

Arslan, H., Salgın, B., and Coşgun, N. (2012). Construction and demolition waste management in Turkey. INTECH Open Access Publisher.

Arulrajah, A., Piratheepan, J., Disfani, M., and Bo, M. W. (2013). Geotechnical and geoenvironmental properties of recycled construction and demolition materials in pavement subbase applications, *Journal of Materials in Civil Engineering*, **25**, 8, 1077-1088.

Arulrajah, A., Rahman, M. A., Piratheepan, J., Bo, M. W., and Imteaz, M. A. (2013b). Evaluation of interface shear strength properties of geogrid-reinforced construction and demolition materials using a modified large-scale direct shear testing apparatus, *Journal of Materials in Civil Engineering*, **26**, 5, 974-982.

Arulrajah, A., Piratheepan, J. and Disfani, M. M. (2013c). Reclaimed asphalt pavement/recycled concrete aggregate blends in pavement sub-bases: laboratory and field evaluation, *Journal of Materials in Civil Engineering*, **26**, 2, 349-357.

Arulrajah, A., Piratheepan, J., Aatheesan, T., and Bo, M. W. (2011). Geotechnical properties of recycled crushed brick in pavement applications, *Journal of Materials in Civil Engineering*, **23**, 10, 1444-1452.

Arulrajah, A., Piratheepan, J., Bo, M. W., and Sivakugan, N. (2012). Geotechnical characteristics of recycled crushed brick blends for pavement sub-base applications, *Canadian Geotechnical Journal*, **49**, 7, 796-811.

ASTM. American Society for Testing and Materials. (2010). Standard test methods for liquid limit, plastic limit, and plasticity index of soils. D4318-2010West Conshohocken, PA.

ASTM. American Society for Testing and Materials. (2012). Standard test methods for laboratory compaction characteristics of soil using modified effort. D1557-2012West Conshohocken, PA.

ASTM. American Society for Testing and Materials. (2009). Standard test method for California Bearing Ratio of laboratory compacted soils. D1883-2009West Conshohocken, PA.

ASTM. American Society for Testing and Materials. (2010). Standard test methods for laboratory determination of water (moisture) content of soil and rock by mass. D2216-2010West Conshohocken, PA.

ASTM. American Society for Testing and Materials. (2013). Standard test methods for one-dimensional swell or collapse of soils. D2166-2013West Conshohocken, PA.

ASTM. American Society for Testing and Materials. (2014). Standard test method for the unconfined compressive strength of cohesive soils. D4546-2014West Conshohocken, PA.

ASTM. American Society for Testing and Materials. (2011). Standard test method for one-dimensional consolidation properties of soils using incremental loading. D2435M-2011West Conshohocken, PA.

ASTM. American Society for Testing and Materials. (2011). Standard test method for direct shear test of soils under consolidated drained conditions. D3080- 2011West Conshohocken, PA.

ASTM. American Society for Testing and Materials. (1994). Standard test method for bearing capacity of soil for static load and spread footings. D1194-1994West Conshohocken, PA.

Azam, S. (2007). Study on the swelling behaviour of blended clay-sand soils, *Geotechnical and Geological Engineering*, **25**, 3,369-381.

Azam, A.M. and Cameron, D.A. (2013). Geotechnical properties of blends of recycled clay masonry and recycled concrete aggregates in unbound pavement construction, *Journal of Materials in Civil Engineering*, **25**, 6, 788-798.

Bakoss, S. L., and Ravindrarajah, R. S. (1999). Recycled construction and demolition materials for use in road works and other local government activities: scoping report. University of technology, Sydney, center for built infrastructure research.

Bareither, C. A., Benson, C. H., and Edil, T. B. (2011). Compression behavior of municipal solid waste: immediate compression, *Journal of Geotechnical and Geoenvironmental Engineering*, **138**, 9, 1047-1062.

Başer, O. (2009). Stabilization of expansive soils using waste marble dust. MSc thesis, the graduate school of natural and applied sciences of Middle East Technical University.

Behiry, A. E. (2013). Utilization of cement treated recycled concrete aggregates as base or subbase layer in Egypt, *Ain Shams Engineering Journal*, **4**, 4, 661-673.

Bennert, T., Papp Jr, W., Maher, A., and Gucunski, N. (2000). Utilization of construction and demolition debris under traffic-type loading in base and sub-base applications. Transportation research record, *Journal of the Transportation Research Board*, **1714**, 33-39.

Brinkgreve, R. B. J. (2002). PLAXIS (version 8) user's manual. Delft university of technology and PLAXIS BV, Netherlands.

Budhu, M. (2011). Soil mechanics and foundations, 3rd edition. (With CD). John Wiley & Sons.

Burland, J.B. (1990). On the compressibility and 250, shear strength of clays, *Géotechnique*, **40**, 3, 329-378.

Chai, J. C., Miura, N., Zhu, H. H., and Yudhbir. (2004). Compression and consolidation characteristics of structured clay, *Canadian Geotechnical Journal*, **41**, 6, 1250-1258.

Chen, F. H. (2012). Foundations on expansive soils (Vol. 12). Elsevier.

Chini, A. R., Kuo, S. S., Armaghani, J. M., and Duxbury, J. P. (2001). Test of recycled concrete aggregate in accelerated test track, *Journal of Transportation Engineering*, **127**, 6, 486-492.

Chidiroglou, I., Goodwin, A. K., Laycock, E., and O'Flaherty, F. (2008). Physical properties of demolition waste material, *Proceedings of the Institution of Civil Engineering Journal Construction Materials*, 97-103.

Chu, S. C. and Kao, H. S. (1993). A Study of Engineering Properties of Clay Modified by Fly Ash and Slag, Proceedings, Fly Ash for Soil Improvement, *American Society of Civil Engineers*, Geotechnical Special Publication, 36, 89-99.

Coduto, D.P., (1999). Geotechnical engineering principles and practices. 2nd edition. Upper Saddle River, NJ07458. Prentice Hall.

Consoli, N. C., Rosa, F. D., and Fonini, A. (2009). Plate load tests on cemented soil layers overlaying weaker soil, *Journal of Geotechnical and Geoenvironmental Engineering*, **135**, 12, 1846-1856.

Consoli, N. C., Schnaid, F., and Milititsky, J. (1998). Interpretation of plate load tests on residual soil site, *Journal of Geotechnical and Geoenvironmental Engineering*, 124, **9**, 857-867.

Consoli, N. C., Vendruscolo, M. A., and Prietto, P. D. M. (2003). Behavior of plate load tests on soil layers improved with cement and fiber, *Journal of Geotechnical and Geoenvironmental Engineering*, **129**, 1, 96-101.

Cooley, D. A. (2005). Effects of reclaimed asphalt pavement on mechanical properties of base materials. MSc. thesis, Department of Civil and Environmental Engineering, Brigham Young University.

Cotecchia, F. and Chandler, R. J. (1997). The influence of structure on the pre-failure behaviour of a clay, *Géotechnique*, **47**, 3, 523-544.

Cabalar A. F., Karabash Z., and Mustafa, W. S. (2014). Stabilizing a clay using tire buffing's and lime, *Road Materials and Pavement Design*, **15**, **4**, 872-891.

Cabalar, A. F., and Karabash, Z. (2014). California bearing ratio of a sub-base material modified with tire buffings and cement addition, *Journal of Testing and Evaluation*, **43**, 6, 1279-1287.

Cabalar, A. F., and Hasan, R. A. (2013). Compressional behaviour of various size/shape sand–clay mixtures with different pore fluids, *Engineering Geology*, **164**, 36-49.

Cabalar, A. F. (2010). Applications of the oedometer, triaxial and resonant column tests to the study of micaceous sands, *Engineering Geology*, **112**, 1-4, 21-28.

Dalla Rosa, F., Consoli, N. C., and Baudet, B. A. (2008). An experimental investigation of the behaviour of artificially cemented soil cured under stress. *Géotechnique*, **58**, 8, 675-679.

Das, B.M., and Sobhan, K. (2014). Principles of geotechnical engineering. 8$^{th}$ edition. Global Engineering: Christopher M. Shortt. USA.

Day, R. W. (1999). Geotechnical and foundation engineering design and construction. McGraw- Hill Companies, New York.

Del Río Merino, M., Izquierdo Gracia, P., and Weis Azevedo, I. S. (2010). Sustainable construction: construction and demolition waste reconsidered, *Waste Management & Research*, **28**, 2, 118-129.

Disfani, M. M., Arulrajah, A., Haghighi, H., Mohammadinia, A., and Horpibulsuk, S. (2014). Flexural beam fatigue strength evaluation of crushed brick as a supplementary material in cement stabilized recycled concrete aggregates, *Construction and Building Materials*, **68**, 667-676.

Donovan, C.T. (1990). C.T. Donovan Associates Inc., P.O. Box 5665, Burlington, VT05402, 802, 658-9385.

Durmusoglu, E., Sanchez, I. M., and Corapcioglu, M. Y. (2006). Permeability and compression characteristics of municipal solid waste samples, *Environmental Geology*, **50**, 6, 773-786.

Esin, T., and Cosgun, N. (2007). A study conducted to reduce construction waste generation in Turkey, *Building and Environment*, **42**, 4, 1667-1674.

Evans, J. C., Costa, M. J., and Cooley, B. (1995). The state-of-stress in soil-bentonite slurry trench cutoff walls. In *Geoenvironment 2000@ sCharacterization, Containment, Remediation, and Performance in Environmental Geotechnics*, 1173-1191.

Fan, R. D., Dua, Y. J., Reddy, K. R., Liua, S. Y., and Yang, Y. L. (2014). Compressibility and hydraulic conductivity of clay mixed with calcium bentonite for slurry wall backfill: Initial assessment, *Applied Clay Science*, **101**, 119-127.

Firat, S., Yllmaz G., Cömert, A. T. and Sümer M. (2012)**.** Utilization of marble dust, fly ash and waste sand (silt-quartz) in road sub-base filling materials, *KSCE Journal of Civil Engineering*, **16**, 7, 1143-1151.

Gavilan, R. M., and Bernold, L. E. (1994). Source evaluation of solid waste in building construction, *Journal of Construction Engineering and Management*, **120**, 3, 536-552.

Grim, R.E. (1953). Clay mineralogy. McGraw-Hill. New York.

Guo, Y., Wu, Y., and Zhang, X. (2009). Application of recycled brick-stone aggregate in road base. In Material Design, Construction, Maintenance, and Testing of Pavements: Selected Papers from the 2009 GeoHunan International Conference, 43-48.

Gupta, R. and Trivedi, A. (2009). Behavior of model circular footing on silty soil with cellular support, *International Journal of Engineering-Transactions B: Applications*, **23**, 1, 21-35.

Hardin, B. O., and Black, W. L. 1968. Vibration modulus of normally consolidated clay, *Journal of the Soil Mechanics and Foundations Division*, **92**, 2, 353-369.

Harnas, F. R., Rahardjo, H., and Wang, J. Y. (2013). Design of Landfill Cover using Construction and Demolition Waste: Material Characterization and Numerical Modelling. In Proceedings of 18th Southeast Asian Geotechnical & Inaugural AGSSEA Conference, 29–31 May 2013, Singapore.

Herrador, R., Pérez, P., Garach, L., and Ordóñez, J. (2011). Use of recycled construction and demolition waste aggregate for road course surfacing, *Journal of Transportation Engineering*, **138**, 2, 182-190.

Highways Agency. (1994). HD 25-94, 7. Pavement design and maintenance-foundations. Design manual for roads and bridges, The Stationery Office, London, UK.

Horpibulsuk, S., Shibuya, S., Fuenkajorn, and K., Katkan, W., (2007). Assessment of engineering properties of Bangkok clay, *Canadian Geotechnical Journal*, **44**, 2, 173-187.

Holtz, R.D., and W, D. Kovacs. (1981). An introduction to geotechnical engineering, Englewood Cliffs, New Jersey: Prentice-Hall.

Holtz, W. G., and Gibbs, H. J. (1956). Engineering properties of expansive clays, *Transactions of the American Society of Civil Engineers*, **121**, 1, 641-663.

Hossain, M.S. (2002) Mechanics of Compressibility and Strength of Solid Waste in Bioreactor Landfills. Ph.D. Dissertation, Department of Civil Engineering, North Carolina State University at Raleigh, NC.

Hoyos, L. R., Puppala, A. J., and Ordonez, C.A. (2011). Characterization of cement fiber treated reclaimed asphalt pavement aggregates: preliminary investigation, *Journal of Materials in Civil Engineering*, **23**, 7, 977-989.

Hong, Z. and Tsuchida, T. (1999). On compression characteristics of Ariake clays, *Canadian Geotechnical Journal*, **36**, 5, 807-814.

Hong, Z. S., Zeng, L. L., Cui, Y. J., Cai, Y. Q., and Lin, C. (2012). Compression behaviour of natural and reconstituted clays, *Géotechnique*, **62**, 4, 291-301.

Huang, W. L., Lin, D. H., Chang, N. B., and Lin, K. S. (2002). Recycling of construction and demolition waste via a mechanical sorting process, *Resources, Conservation and Recycling*, **37**, 1, 23-37.

Hoppe, E. J., Lane, D. S., Fitch, G. M., and Shetty, S. (2015). Feasibility of reclaimed asphalt pavement (RAP) use as road base and subbase material, Virginia center for transportation innovation and research report (No. VCTIR 15-R6).

Hoque, E., and Tatsuoka, F. (1998). Anisotropy in elastic deformation of granular materials, *Soils and Foundations*, **38**, 1, 163-179.

Hoy, M., Horpibulsuk, S., and Arulrajah, A. (2016). Strength development of recycled asphalt pavement–Fly ash geopolymer as a road construction material, *Construction and Building Materials*, **117**, 209-219.

Huang, Y., Bird, R.N., Heidrich, O. (2007). A review of the use of recycled solid waste materials in asphalt pavements, *Resources, Conservation and Recycling*, **52**,1, 58-73.

Jaky, J. (1944). The coefficient of earth pressure at rest, *Journal of the Society of Hungarian Architects and Engineers*, 355-358.

Jones, D. E., and Holtz, W. G. (1973). Expansive soils-the hidden disaster, *Civil Engineering*, **43**, 49-51.

Kalkan, E. (2011). Impact of wetting–drying cycles on swelling behavior of clays modified by silica fume,*Applied Clay Science*, **52**, 4, 345-352.

Kavazanjian Jr, E. D., Matasovic, N. E., and Bachus, R. C. (1999). Large-diameter static and cyclic laboratory testing of municipal solid waste, In *Proceedings Sardinia*, **99**, 437-444.

Khanal, S. (2013). Back calculation of plate loading tests using Plaxis 2D and the hardening soil model. MSc thesis, department of civil and transport engineering, Norwegian University of Science and Technology.

Kim, B., Prezzi, M., and Salgado, R. (2005). Geotechnical properties of fly and bottom ash mixtures for use in highway embankments, *Journal of Geotechnical and Geoenvironmental Engineering*, **131**, **7**, 914-924.

Kolay, P. K., Kumar, S., and Tiwari, D. (2013). Improvement of bearing capacity of shallow foundation on geogrid reinforced silty clay and sand, Hindawi Publishing Corporation, *Journal of Construction Engineering*, **2013**.

Kumar, M. A. and Prasada, G. V. (2009). Use of lime cement stabilized pavement construction, *Indian Journal of Engineering and Material Science*, **16**, 4, 269-276.

Lee, M. T. and Nicholson, P. G. (1997). An Engineering test program of MSW ash mixed with quarry tailings for use as a landfill construction material, Testing Soil Mixed with Waste or Recycled Materials, *Journal of ASTM International*. STP 1275, Mark A. Wasemiller, Keith B. Hoddinott, Eds, 205-218.

Leite, da Conceição. F., dos Santos Motta, R., Vasconcelos, K. L., and Bernucci, L. (2011). Laboratory evaluation of recycled construction and demolition waste for pavements, *Construction and Building Materials*, **25**, 6, 2972-2979.

Lima, J. A. R., (1999). Proposition of directives for the production and standardization of recycled construction waste and its applications in mortars and concretes in Portuguese. MSc Thesis. University of São Paulo, São Paulo, SP

Maher, M. H., Gucunski, N., and Papp Jr, W. J. (1997). Recycled asphalt pavement as a base and sub-base material, Testing Soil Mixed with Waste or Recycled Materials, *Journal of ASTM International*. STP 1275, Mark A. Wasemiller, Keith B. Hoddinott, Eds, 42-53.

Marcuson, W. F., and Wahls, H. E. (1972). Time effects on dynamic shear modulus of clays, *Journal of the Soil Mechanics and Foundations Division*, **98**, 12, 1359-1373.

Materials data book, (2003). Cambridge University Engineering Department, 2003 edition, U.K.

McMainis, K. L. and Nataraj, M. (1997). Characterization of filter cake ash and applications for soil stabilization, Testing Soil Mixed with Waste or Recycled Materials, *Journal of ASTM International*. STP 1275, Mark A. Wasemiller, Keith B. Hoddinott, Eds, 219-231.

McMahon, S. G. (1997). A valuable product from a construction and demolition facility, Testing Soil Mixed with Waste or Recycled Materials, *Journal of ASTM International*. STP 1275, Mark A. Wasemiller, Keith B. Hoddinott, Eds, 54-61.

Melbouci, B. (2009). Compaction and shearing behavior study of recycled aggregates, *Construction and Building Materials*, **23**, 8, 2723-2730.

Melton, J. S., Clark, C. J., and Regis, P. T. (2012). Feasibility study on building-derived concrete debris for use in highway construction, Testing and Specification of Recycled Materials for Sustainable Geotechnical Construction, *Journal of ASTM International*. STP154020120005, T. Edil, Ed., West Conshohocken, PA, 95-111.

Miller, G. A., Azad, S., and Dhar, B. (1997). The effect of kiln dust on the collapse potential of compacted shale, Testing Soil Mixed with Waste or Recycled Materials, *Journal of ASTM International*. STP 1275, Mark A. Wasemiller, Keith B. Hoddinott, Eds, 232-245.

Miller, G. A. and Azad, S. (2000). Influence of soil type on stabilization with cement kiln dust, *Construction and Building Materials*, **14**, 2, 89-97.

Mirzababaei, M., Miraftab, M., Mohamed, M., and McMahon, P. (2013). Impact of carpet waste fiber addition on swelling properties of compacted clays, *Geotechnical and Geological Engineering*, **31**, 1, 173-182.

Mishra, A. K., Ohtsubo, M., Li, L., and Higashi, T. (2011). Controlling factors of the swelling of various bentonites and their correlations with the hydraulic conductivity of soil-bentonite mixtures, *Applied Clay Science*, **52**, 1-2, 78-84.

Mitchell, James K. and Soga, Kenichi. (2005). Fundamentals of soil behavior3rd ed. Hoboken, New Jersey, John Wiley & Sons, Inc., Published simultaneously in Canada, 330-331.

Modarres, A., and Nosoudy, Y. M. (2015). Clay stabilization using coal waste and lime-technical and environmental impacts, *Applied Clay Science*, **116**, 281-288.

Mohammadinia, A., Arulrajah, A., Sanjayan, J., Disfani, M. M., Bo, M. W., and Darmawan, S. (2014). Laboratory evaluation of the use of cement-treated construction and demolition materials in pavement base and subbase applications, *Journal of Materials in Civil Engineering*, **27**, 6.

Mohammadinia, A., Arulrajah, A., Sanjayan, J., Disfani, M. M., Bo, M. W., and Darmawan, S. (2015). Geotechnical Properties of Lightly Stabilized Recycled Demolition Materials in Base/Sub-Base Applications. In IFCEE (2015, March), American Society of Civil Engineers, 2767-2776

Molenaar, A., and van Niekerk, A. (2002). Effects of gradation, composition, and degree of compaction on the mechanical characteristics of recycled unbound materials, *Transportation Research Record: Journal of the Transportation Research Board*, **1787**, 73-82.

Monkul, M. M., and Ozden, G. (2007). Compressional behavior of clayey sand and transition fines content, *Engineering Geology*, **89**, 3-4, 195-205.

Nawagamuwa, U. P., Madarasinghe, D. L., Goonatillake, M. D. M. J., Karunarathna, H. J. D., and Gunaratne, M. (2013). Sustainable reuse of Brownfield properties in Sri Lanka as a gabion fill material. In: ICSBE-2012: International Conference on Sustainable Built Environment, Kandy, Sri Lanka.

Neves, J., Freire, A. C., Roque, A. J., Martins, I., Antunes, M. L., and Faria, G. (2013). Utilization of recycled materials in unbound granular layers validated by experimental test sections. In Ninth International Conference on the Bearing Capacity of Roads, Railways and Airfields, 2013 Trondheim, Norway.

Nicholson, P. G., and Ding, M., (1997). Improvement of tropical soils with waste Ash and lime admixtures, Testing of Soil Mixed with Waste or Recycled Materials, *Journal of ASTM International* ASTM STP 1275, Mark A. Wasemiller, Keith B. Hoddinott, Eds, 195-204.

Nunes, M. C. M. (1997). Enabling the use of alternative materials in road construction Ph.D. thesis, University of Nottingham.UK

Oglesby CH, Parker HW, and Howell GA. (1989). Productivity improvement in construction. New York, NY: McGraw-Hill.

Okagbue, C., and Ene, E., (2009). Some basic geotechnical properties of expansive soil modified using pyroclastic dust, *Engineering Geology*, **107**, 1-2, 61-65.

O'Mahony, M. M., and Milligan, G. W. E. (1991). Use of recycled materials in subbase layers, *Transportation Research Record*, 1310, 73-80.

Ornek, M., Laman, M., Demir, A., and Yildiz, A. (2012). Prediction of bearing capacity of circular footings on soft clay stabilized with granular soil, *Soils and Foundations*, **52**, 1, 69-80.

Outwater, A., and Tansel, B. (1994). Reuse of sludge and minor wastewater residuals. CRC Press.

Öztürk M. (2005) Ministry of environment and forestry construction waste management. Ankara, Turkey: www.cevreorman. gov.tr [in Turkish].

Otani, J., Ochiai, H., and Yamamoto, K. (1998). Bearing capacity analysis of reinforced foundations on cohesive soil, *Geotextiles and Geomembranes*, **16**, 4, 195-206.

Pappu A, Saxena M, Asolekar SR. (2007). Solid wastes generation in India and their recycling potential in building materials, *Building and Environment*, **42**, 6, 2311-2320.

Park, Y. Kim, S., and Kim, M. (2000). Liquefaction of embankments on sandy soil and the optimum countermeasure against the liquefaction. Twelfth conference on earthquake engineering, New Zaland.2000.

Park, T. (2003). Application of construction and building debris as base and subbase materials in rigid pavement, *Journal of Transportation Engineering*, **129**, 5, 558-563.

Pasandín, A. R., and Pérez, I. (2013). Laboratory evaluation of hot-mix asphalt containing construction and demolition waste, *Construction and Building Materials*, **43**, 497–505.

Poon, C. S., and Chan, D. (2006). Feasible use of recycled concrete aggregates and crushed274 clay brick as unbound road sub-base, *Construction and Building Materials*, **8**, 578-585.

Rahman, M. A., Imteaz, M., Arulrajah, A., and Disfani, M. M. (2014). Suitability of recycled construction and demolition aggregates as alternative pipe backfilling materials. *Journal of Cleaner Production*, **66**, 75-84.

Rahman, M. A., Imteaz, M. A., Arulrajah, A., Piratheepan, J., and Disfani, M. M. (2015). Recycled construction and demolition materials in permeable pavement systems: geotechnical and hydraulic characteristics, *Journal of Cleaner Production*, **90**, 183-194.

Reddy, K. R., Gangathulasi, J., Parakalla, N. S., Hettiarachchi, H., Bogner, J. E., and Lagier, T. (2009). Compressibility and shear strength of municipal solid waste under short-term leachate recirculation operations, *Waste Management & Research*, **27**, 6, 578-587.

Rojas, J. C., Salinas, L. M., and Sejas, C. (2007). Plate-load tests on an unsaturated lean clay. In Experimental unsaturated soil mechanics, *Springer Berlin Heidelberg.*, 445-452.

Saeed, A., Ashtiani, R., and Boudreau, R. L. (2012). Performance related tests on recycled materials for sustainable design of pavement systems, Testing and Specification of Recycled Materials for Sustainable Geotechnical Construction, *Journal of ASTM International*, STP154020120001, T. Edil, Ed., West Conshohocken, PA, 3-26.

Safiuddin, M., Jumaat, M. Z., Salam, M. A., Islam, M. S., and Hashim, R. (2010). Utilization of solid wastes in construction materials, *International Journal of the Physical Sciences*, **5**, 13, 1952-1963.

Sanjeev, K. V. Jain, P. K. and Kumar, R. (2013). Prediction of bearing capacity of granular layered soils by plate load test, *International Journal of Advanced Engineering Research and Studies*, **2**, 3, 142-149.

Santos, E. C. G., and Vilar, O. M. (2008). Use of recycled construction and demolition wastes (RCDW) as backfill of reinforced soil structures. In Proceedings of the 4th European Conference on Geosynthetics–EUROGEO, **4**.

Santos, E. C. G., Palmeira, E. M., and Bathurst, R. J. (2010). Construction of a full-scale wrapped face geogrid reinforced wall using recycled construction and demolition waste as backfill material. In 9th International Conference on Geosynthetics, Guarujá, Brazil, **4**, 17.

Santos, E. C., Palmeira, E. M., and Bathurst, R. J. (2013). Behaviour of a geogrid reinforced wall built with recycled construction and demolition waste backfill on a collapsible foundation, *Geotextiles and Geomembranes*, **39**, 9-19.

Santos, E. C. G., Palmeira, E. M., and Bathurst, R. J. (2014). Performance of two geosynthetic reinforced walls with recycled construction waste backfill and constructed on collapsible ground, *Geosynthetics International*, **21**, 4, 256-269.

Saride, S., Puppala, A. J., and Williammee, R. (2010). Assessing recycled/secondary materials as pavement bases, *Proceedings of the ICE-Ground Improvement*, **163**, 1, 3-12.

Schmertmann, J. H. (1991). The mechanical aging of soils, *Journal of Geotechnical Engineering*, **117**, 9, 1288-1330.

Seed, H. B., Mitchell, J. K. and Chan, C. K. (1960). The strength of compacted cohesive soils. Proceedings, ASCE Research Conference on Cohesive soils, Boulder, American Society of Civil Engineers, New York, 877-964.

Sharma, H. D., and Reddy, K. R. (2004). Geoenvironmental Engineering. Hoboken. John Willy & Sons Inc.

Shibuya, S., and Tanaka, H. (1996). Estimate of elastic shear modulus of Holocene soil deposits, *Soils and Foundations*, **36**, 4, 45-55.

Shibuya, S., Hwang, S. C., and Mitachi, T. (1997). Elastic shear modulus of soft clays from shear wave velocity measurement, *Ge'otechnique*, **47**, 3, 593-601.

Sirigiripet, S. K. (2007). Experimental and field studies on recycled materials as pavement bases. ProQuest. MSc thesis, Faculty of the Graduate School, The University of Texas at Arlington

Sivakumar, V., McKinley, J. D., and Ferguson, D. (2004). Reuse of construction waste: performance under repeated loading. Proceedings of the Institution of Civil Engineers, *Geotechnical Engineering*, **157**, 2, 91-96.

Sivapullaiah, P. V., Sridharan, A., and Stalin, V. K. (2000). Hydraulic conductivity of bentonite-sand mixtures, *Canadian Geotechnical Journal*, **37**, 2, 406-413.

Soleimanbeigi, A., Edil, T. B., and Benson, C. H. (2011). Recycled asphalt shingles mixed with granular byproducts as structural fills, *Journal of ASTM International*, **9**, 1, 1-19.

Soleimanbeigi, A., and Edil, T. B. (2015). Compressibility of recycled materials for use as highway embankment fills, *Journal of Geotechnical and Geoenvironmental Engineering*, **141**, 5.

Spencer, R. (1989). Recycling opportunities for demolition debris, *Biocycle*, **30**, 11, 42-44.

Spencer, R. (1990). Opportunities for recycling C & D debris, *Biocycle*.

Suebsuk, J., Suksan, A., and Horpibulsuk, S. (2014). Strength assessment of cement treated soil-reclaimed asphalt pavement (RAP) mixture, *International Journal of Geomate*, **6**, 2,878-884.

Sustainability Victoria. (2010). Victorian recycling industries annual report 2008-2009., Melbourne, VIC, Australia.

State Planning Organization. (2001) Eighth Development Plan: Report on Solid Waste Control. Ankara, Turkey, http://ekutup.dpt.gov.tr/ icmesuyu/oik524.pdf (in Turkish).

Taha, R., Al-Harthy, A., Al-Shamsi, K., and Al-Zubeidi, M. (2002). Cement stabilization of reclaimed asphalt pavement aggregate for road bases and subbases, *Journal of Materials in Civil Engineering*, **14**, 3, 239-245.

Tam, V.W.Y., and Tam, C. M. (2007). Crushed aggregate production from centralized combined and individual waste sources in Hong Kong, *Construction and Building Materials*, **21**, 4, 879-886.

Terzaghi, K., and Peck, R. B. (1967). Soil mechanics in engineering practice, 2nd edition, Wiley, New York.

Terzaghi, K. (1925). Erdbaumechanik auf bodenphysikalischer Grundlage, Vienna, Deuticke, Leipzig.

Thakur, J. K., and Han, J. (2015). Recent development of recycled asphalt pavement (RAP) bases treated for roadway applications, *Transportation Infrastructure Geotechnology*, **2**, 2, 68-86.

Van Der Merwe, D. H. (1964). The prediction of heave from the plasticity index and percentage clay fraction of soil, *The Civil Engineer in South Africa*, **6**, 12,103-107.

Vieira, C. S., and Pereira, P. M. (2015). Use of recycled construction and demolition materials in geotechnical applications: A review. Resources, *Conservation and Recycling*, **103**, 192-204.

Warner, J.D. (2007). The Beneficial reuse of asphalt shingles in roadway construction. MSc. thesis, Dept. of Civil and Environmental Engineering, Univ. of Wisconsin-Madison, Madison, WI.

Warner, J. D. and Edil, T. B. (2012). An Evaluation of Reclaimed Asphalt Shingles for Beneficial Reuse in Roadway Construction, Testing and Specification of Recycled Materials for Sustainable Geotechnical Construction, *Journal of ASTM International*, STP154020120008, T. Edil, Ed., West Conshohocken, PA, 146-167

Watabe, Y., Yamada, K., and Saitoh, K., (2011). Hydraulic conductivity and mixtures of compressibility of Nagoya clay with sand or bentonite, *Geotechnique*, **61**, 3, 211-219.

Wei, M. L., Du, Y. J., and Jiang, N. J. (2012). Compression behavior of zinc contaminated clays solidified with cement. Proceedings of Geo Congress, 4042-4049.

Wilson, P. R. (2009). Large-scale passive force-displacement and dynamic earth pressure experiments and simulations, PhD Thesis, university of California, San Diego.

YEŞİLBAŞ, G. (2004). Stabilization of expansive soils using aggregate waste, rock powder and lime, PhD Thesis, Middle East Technical University.

Young, M. H., Moran, E. A., Yu, Z., Zhu, J., and Smith, D. M. (2009). Reducing saturated hydraulic conductivity of sandy soils with polyacrylamide, *Soil Science Society of America Journal*, **73**, 1, 13-20.

Yeung, A. T., Mok, K. Y., Tham, L. G., Lee, P. K. K., and Pei, G. (2006). Use of inert CDMS materials for seawall foundation: A field-scale pilot test, *Resources, Conservation and Recycling*, **47**, 4, 375-393.

Zaman, M., Laguros, J. G., and Sayah, A. (1992). Soil stabilization using cement kiln dust. Proceedings of the 7th International Conference on Expansive Soils, Dallas, TX, **1**, 347–351.

Zhu, J., Wu, S., Zhong, J., and Wang, D. (2012). Investigation of asphalt mixture containing demolition waste obtained from earthquake-damaged buildings, *Construction and Building Materials*, **29**, 466–475.

## CURRICULUM VITAE

**PERSONAL INFORMATION**

Name and Surname: Muhamd Dafer Abdulnafaa AL YAHYA BAG

Nationality: Iraqi

Birth place and date: Mosul-Iraq / 29-10-1979

Marital status: Married-3 child

Phone number: 05342439543

E-mail: mohammed_al_heyaly@yahoo.com

**EDUCATION**

| Degree | Graduate School | Year |
|---|---|---|
| MS | University of Mosul | 2004 |
| BS | University of Mosul | 2001 |
| High School | Al mutameezen High School | 1997 |

WORK EXPERIENCE

| Year | Place | Enrollment |
|---|---|---|
| 2005-2010 | Mosul University | Assistant lecturer |
| 2010- present | Mosul University | Lecturer |

**PUBLICATIONS**

**A. Journals**

1- Cabalar, A. F., Zardikawi, O. A. A., and **Abdulnafaa**, M. D. (2017). Utilisation of construction and demolition materials with clay for road pavement subgrade. *Road Materials and Pavement Design*, **1-13**.

2- Cabalar, A. F., Hassan, D. I., and **Abdulnafaa**, M. D. (2017). Use of waste ceramic tiles for road pavement subgrade. *Road Materials and Pavement Design*, 18(**4**), 882-896.

3- Cabalar, A. F., **Abdulnafaa**, M. D., and Karabash, Z. (2016). Influences of various construction and demolition materials on the behavior of a clay. *Environmental Earth Sciences*, 75(**9**), 841.

4- Al-Khashab, M. N., and **Al-Hayalee**, M. T. (2010). The Effect of Organic Matter's Content on the Engineering Properties of Expansive Soils. *Eng. & Technology*, 28(**8**).

5- Al-Khashab, M. N., and **Al-Hayalee**, M. T. (2008). Treatment of Expansive Clayey Soil with Crushed Limestone. *Eng. & Technology*.

6- Al-Khashab, M. N., and **Al-Hayalee**, M. T. (2008). Stabilization of expansive clayey soil modified by lime with an emulsified asphalt addition. *Eng. & Technology*, 26(**10**).

7- Cabalar, A. F., **Abdulnafaa**, M. D., (2018). The role of construction and demolition materials in swelling of a clay. *Arabian Journal of Geosciences*, (under review).

8- Cabalar, A. F., G Hayder, and **Abdulnafaa**, M. D., (2018). Use of spiral aluminum CNC milling waste in road pavement subgrade. *Journal of Transportation Engineering, Part B: Pavements,* (under review).